

South Dakota
Department of Transportation
Office of Research



U.S. Department
of Transportation
**Federal Highway
Administration**

SD1998-18-F



The Determination of the Permeability, Density, and Bond Strength of Non-Metallic Fiber Reinforced Concrete in Bridge Deck Overlay Applications

Study SD1998-18 Final Report

Prepared by
Dr. V. Ramakrishnan, Distinguished Professor
Kumar R. Santhosh, Research Associate
Department of Civil and Environmental Engineering, SDSM&T,
501 East St. Joseph Street
Rapid City, SD 57701-3995

July 2000

DISCLAIMER

The contents of this report reflect the views of the authors who are responsible for the facts and accuracy of the data presented herein. The contents do not necessarily reflect the official views or policies of the South Dakota Department of Transportation, the State Transportation Commission, or the Federal Highway Administration. This report does not constitute a standard, specification, or regulation.

ACKNOWLEDGEMENTS

This work was performed under the supervision of the SD1998-18 Technical Panel:

Bill Brinkmann, P.E.....	SD ACPA	Paul Nelson.....	Pierre Region
Mark Clausen	FHWA	Hal Rumpca.....	Office of Research
Tom Gilsrud	Office of Bridge Design	Daniel Strand.....	Office of Research
Ron McMahon	Off. of Mat. & Testing		

The work was performed in cooperation with the United States Department of Transportation Federal Highway Administration.

TECHNICAL REPORT STANDARD TITLE PAGE

1 Report No. SD1998-18-F		2 Government Accession No.		3 Recipient's Catalog No.	
4 Title and Subtitle The Determination of the Permeability, Density, and Bond Strength of Non-Metallic Fiber Reinforced Concrete in Bridge Deck Overlay Applications				5 Report Date July 30, 2000	
				6 Performing Organization Code	
7 Author(s) Dr. V. Ramakrishnan				8 Performing Organization Report No.	
9 Performing Organization Name and Address Department of Civil and Environmental Engineering South Dakota School of Mines and Technology 501, East St. Joseph Street Rapid City, SD 57701-3995				10 Work Unit No.	
				11 Contract or Grant No. 310652	
12 Sponsoring Agency Name and Address South Dakota Department of Transportation Office of Research 700 East Broadway Avenue Pierre, SD 57501-2586				13 Type of Report and Period Covered Final Report July 2000	
				14 Sponsoring Agency Code	
15 Supplementary Notes Project Monitor: Mr. Daniel Strand An executive summary is published separately as SD1998-18-X.					
16 Abstract <p>This final report presents the procedures and results of the rapid chloride permeability, density, and bond strengths of cores taken from non-metallic fiber reinforced concrete (NMFRC) and plain low slump dense concrete (LSDC) bridge deck overlays constructed earlier on the bridge at Exit 212 over I-90 (I-90/US 83), and Exit 32 on I-90 (I-90/SD-79).</p> <p>Both the field in-place and laboratory bond tests were done for the cores drilled in the field. The density and chloride permeability were also determined for the concrete specimens cast in the laboratory with 5 different compacting efforts, for each different concrete used in the construction of the above referred bridge decks.</p> <p>A comparison of the results from the field and laboratory mixes had shown that there was good bond between the overlay concrete and the old concrete and the bond strength was greater than the tensile strength of the old concrete, because in all cores the failure was in the old concrete. The chloride permeability and density values of NMFRC were found to be almost similar to the values of the plain LSDC. This was true in both field and laboratory tests. The chloride permeability mainly depended on the cement content and compacting effort used in making the cylinders. The addition of fibers did not influence the chloride permeability and density of the concrete. Recommendations were made regarding the equipment and testing procedures necessary for designing the NMFRC mix, and equipment and testing procedures required for quality control in the field.</p>					
17 Keywords Bond, Chloride permeability, Density, Low Slump Dense Concrete (LSDC), Non-Metallic Fiber Reinforced Concrete (NMFRC).			18 Distribution Statement No restrictions. This document is available to the public from the sponsoring agency.		
19 Security Classification (of this report) Unclassified		20 Security Classification (of this page) Unclassified		21 No. of Pages 101	
				22 Price	

EXECUTIVE SUMMARY

The South Dakota Department of Transportation (SDDOT) used Low Slump Dense Concrete (LSDC) overlay over older bridge decks to either protect the black steel in older decks and/or as a form of maintenance to extend the life of the deck to the service life of the bridge. The LSDC created an almost impermeable barrier between the surface of the overlay and the deck steel. The feasibility of using Non-Metallic Fiber Reinforced Concrete (NMFRC) in the construction of highway structures had been established in many previous studies. The new NMFRC with enhanced fatigue, impact resistance, modulus of rupture, ductility and toughness properties was particularly suitable for the construction of thin bridge deck overlays and whitetopping.

In 1994 a research project was initiated to study the use of 3M's Polyolefin Fibers (non-metallic fiber reinforced concrete (NMFRC)) in several applications. One application incorporated these fibers in the bridge deck overlay concrete for the structure at Exit 212 over I-90 (I-90/US83). A comparison of SDDOT's LSDC was made with the fiber overlay concrete. As a result of the 1994 study, it was found that the fiber deck overlay performed favorably. Therefore, because of the fibers ability to greatly enhance the concretes structural properties, the department decided to include these fibers in the deck overlay concrete for the two severely deteriorated bridge decks at Exit 32 on I-90 (I-90/SD-79). The Department hopes that these overlays would extend the life of those decks for seven years from the time of construction (to about 2004).

As a result of the study of the fiber concrete bridge deck overlays, which were constructed in 1997, it was recommended that fiber concrete overlays be considered not only on badly deteriorated bridge decks, but also on a case by case basis for all the bridges. Although the performance of the fiber concrete deck overlays appeared to be acceptable, some questions remained unanswered. How do the permeability, density, and bond strength of the NMFRC deck overlays compare to the plain LSDC? Does the higher initial slump, prior to the addition of fiber, adversely affect the compactive effort of the deck overlay machine? What equipment and testing procedures are necessary for designing the NMFRC mix? Also what equipment and testing procedures are necessary for quality control in the field? Therefore the proposed research was undertaken to find answers for these questions.

The research objectives were

- To determine the permeability, density, and bond strength of bridge deck overlay NMFRC as compared to South Dakota's plain LSDC.
- To develop standard mix design and field testing procedures for bridge deck NMFRC.

Literature relevant to chloride permeability test and field and laboratory bond testing was reviewed. Cores were taken from the following sections and tested for chloride permeability (ASTM C1202), bond and density.

- Plain LSDC from the northbound lane of the exit 212 interchange bridge over I-90 (I-90/US83) at Vivian.
- NMFRC Bridge deck overlay with fibers added at a rate of 14.8 kg/m^3 (25lbs./cu.yd.) from the southbound lane of Vivian interchange bridge.
- NMFRC Bridge deck overlay with fibers added at a rate of 11.9 kg/m^3 (20lbs./cu.yd.) from the southbound lane of Vivian interchange bridge.
- NMFRC White topping with fibers added at a rate of 14.8 kg/m^3 (25 lbs./cu.yd.) from the approach to the Vivian interchange bridge.
- NMFRC Bridge deck overlay from the eastbound lanes of the Exit 32 interchange on I-90 (I-90/SD79) at Sturgis, with fibers added at a rate of 14.8 kg/m^3 (25lbs./cu.yd.).
- NMFRC Bridge deck overlay from the westbound lanes of the Exit 32 Sturgis Interchange Bridge, with fibers added at a rate of 14.8 kg/m^3 (25lbs./cu.yd.).

Both the field and laboratory bond testing of the cores were done. The density and permeability of specimens cast in the laboratory, with different compaction efforts, and with the same mix proportions used in the construction of the above-referred bridge decks were determined. The field and laboratory tests results were compared.

The test program on fresh concrete included slump, concrete temperature, air content and unit weight. The hardened concrete properties included compressive strength, static modulus, modulus of rupture, load-deflection curves, first crack toughness and post crack behavior, ASTM toughness indices, Japanese toughness indices and equivalent flexural strength. The results from the rapid chloride permeability test (RCPT) showed that the approach concrete was the most permeable in both the East and the West bound lanes at

Exit 32, I 90 (Sturgis). The driving lane in the West bound lane and the passing lane in the East bound lane were found to be more permeable than the other lanes.

The RCPT results from the cores obtained from the different parts of the bridge at Exit 212 I 90 (Vivian) again showed that the concrete in the approach was the most permeable.

For the cores from Exit 32, I 90 (Sturgis), the density of the sample from the approach (average of 3 readings) was less than that from the bridge (average of 8 readings). The average density obtained from the samples from the bridge, from all the four lanes, was 2194.74 Kg/m^3 (137 lbs/ft^3) and the average density obtained from the approaches was 2082.6 Kg/m^3 (130 lbs/ft^3).

At the Exit 212 I 90 (Vivian), the density values obtained were 2178.72, 2266.83, 2229.98 and 2193.14 Kg/m^3 (136.0 , 141.5 , 139.2 and 136.9 lbs/ft^3) from the approach. North half of the South bound lane, South half of the South bound lane and the North bound lane respectively. The concrete at the section of the bridge with fiber at 11.9 Kg/m^3 (20 lbs/ft^3) was the densest of all concretes.

The determination of bond strength of the bridge deck overlay concrete included two phases. First, the bond test on 50.8 mm (2 in.) cores drilled into the bridge deck in the field using a pull out tester and second the bond strength of 101.6 mm (4 in.) core samples obtained from the bridge deck in the laboratory. The bond test results from both the bridges at Exit 32, I90 (Sturgis) and Exit 212, I90 (Vivian) indicated that the in-place underlying concrete was weaker than both the bond and the overlying fiber reinforced concrete. All the cores from both the West and East bound lanes of the bridge at Exit 32, I90 (Sturgis), failed in the underlying concrete below and within 6 to 12 mm (0.25 to 0.5 in.) from the interface. This might be attributed to the fact that the milling and/or sand blasting operations during the overlay surface preparation might have damaged the surface of the underlying concrete. Two types of causes for failure were noticed when the fractured cores were examined after the bond test. One was due to the lack of good bond between the coarse aggregates and the cement mortar in the underlying concrete and the other due to the failure of the coarse aggregates in the underlying concrete.

Similar results were obtained from all the parts of the bridge at Exit 212, I90 (Vivian). No difference was observed in the tension stress results from the North and

South halves of the bridge with different fiber contents. This may be explained by the fact that the failure was mostly in the underlying concrete and the variation in the fiber content on the overlay did not have any effect on it. It was observed that the FRC overlay was not properly consolidated which was evident by the presence of voids (minor honey-combing) in all the cores. Comparable results were obtained from the laboratory bond test of the cores from various locations. The difference between the field and lab tests varied from 4 to 28 psi.

The quality control tests on specimens cast in lab with same mix proportions as that of the actual concrete used for the construction of the bridge decks revealed that, both the fresh concrete and hardened concrete properties were not very much different from the values recorded for the corresponding mixes in the field. All the values were found to be within the tolerance allowed in concrete testing.

CONCLUSIONS

1. The chloride permeability and density values of NMFRC were found to be similar to the values of the plain LSDC. This was true in both field and laboratory tests. The addition of fibers did not seem to have much influence on the chloride permeability and the density of the concrete.
2. The chloride permeability of the field cores was similar to the permeability values obtained for the specimens made in the laboratory with 30 sec. vibration. The higher initial slump, prior to the addition of fiber, did not affect the compactive effort of the deck overlay machine. The NMFRC cores taken from the field had small voids indicating that NMFRC possibly needed more consolidation. With more consolidation NMFRC would have higher impermeability than LSDC.
3. Truck delivered concrete was needed for NMFRC. Initially higher slump and reduced angle on tining fork were needed for NMFRC. The same operations for consolidation, and finishing, used for plain concrete were adequate for NMFRC.
4. Visual inspection of the cores from the bridge deck showed that many major cracks in the underlying old concrete did not propagate to the overlay concrete. Therefore it could be concluded that the NMFRC would improve the performance of the overlay

by minimizing large cracks, spalling and loss of material from the top of the deck and thus reduce the potential for hazards to the public.

5. The field and the laboratory bond strength test showed that the NMFRC was adequately bonded with the underlying concrete on the bridge deck which strengthens the acceptability of NMFRC for its usage in bridge decks overlays.
6. Both types of bond tests (field and laboratory) indicated that the failure was always due to the tensile failure of the old concrete. The bond between the old and new concrete was stronger than the tensile strength of the old concrete.

RECOMMENDATIONS

1. It is recommended that NMFRC be used for deck overlays when an overlay would be placed over badly deteriorated bridge decks. Bonded overlay is desirable to provide a composite action for the slab, which would reduce the potential tensile stresses and cracking in concrete overlays. A thin layer of cement-slurry bonding agent should be used.
2. It is recommended that the NMFRC should have the same specifications and mixture proportions as that for SDDOT's plain LSDC with the exception of the inclusions of 3M's polyolefin fibers (type 50/63) at a rate of 14.8 Kg/m^3 (25 lbs/yd³). The LSDC specification is in SDDOT's *Standard Specifications for Roads and Bridges*. A higher slump can be permitted for NMFRC overlays. The initial slump before the addition of fibers should be high enough to accommodate these fibers such that when they are added, the slump comes down to the specified amount.
3. The same construction procedures for transporting, placing, consolidating, finishing, and curing used for construction with plain concrete be used for construction of NMFRC. For tining a reduced angle on tining fork should be used for NMFRC. The mixing should be done in a ready-mix truck or in a batch plant.
4. When NMFRC is used the following quality control tests according to ASTM procedures be conducted for the fresh concrete: slump (ASTM C143), unit weight (ASTM C138), and air content (ASTM C231). The fiber content should be determined as per the procedure given in this report. The concrete temperature, the ambient temperature, humidity and the wind velocity be recorded during placing of

the concrete. The following hardened concrete tests be conducted on field samples collected and cured according to ASTM standard procedures for NMFRC at 28 days: compressive strength (ASTM C39), elastic modulus (ASTM C469), flexural strength (ASTM C78), fatigue strength (ACI Committee 544) and toughness values (ASTM and Japanese standards). Additionally it is recommended that the test for the average residual strength (ASTM C 1399) be conducted on the hardened NMFRC. SDDOT should establish minimum specifications for each of these above tests for acceptable testing.

5. It is recommended that either the field or the laboratory bond test or both tests should be specified, depending on the time available for closing of the highway for traffic. If the longer closing time (2 hours additional) is permissible then the field bond test could be specified. If longer closing of highways was not permissible, then the lab bond test is recommended. These tests are not yet adopted as ASTM standards. Therefore the same procedure as developed and used in this research project (Research Task 5) could be specified for conducting the bond tests. Both tests are simple tests and they gave reliable results. A minimum bond strength of 0.69Mpa (100 psi) should be specified.
6. The ASTM C1202 test should be used for the determination of rapid chloride permeability. SDDOT should establish a minimum value for acceptance testing.

CONTENTS

Cover Page.....	
Title Page.....	
Executive Summary.....	
Contents.....	iii
List of Tables.....	v
List of Figures.....	vii
Glossary.....	x
Background.....	1
Research objectives.....	3
Research Task 1: Review and summarize literature related to equipment and testing requirements necessary for NMFRC.....	3
Research Task 2: Attend SDDOT's coring operation of the selected sites to ensure that the samples obtained are acceptable for the testing to be conducted.....	15
Research Task 3: Perform permeability testing on the 3 or 4 cores taken from each of the following test sections:	
• Plain LSD concrete from the northbound lane of the exit 212 interchange bridge over I-90 (I-90/US83) at Vivian.	
• Bridge deck overlay NMFRC with fibers added at a rate of 25 lbs./cu.yd. from the southbound lane of Vivian interchange bridge.	
• Bridge deck overlay NMFRC with fibers added at a rate of 20 lbs./cu.yd. from the southbound lane of Vivian interchange bridge.	
• White topping with fibers added at a rate of 25 lbs./cu.yd. from the approach to the Vivian interchange bridge.	
• Bridge deck overlay NMFRC from the eastbound lanes of the Exit 32 interchange on I-90 (I-90/SD79) at Sturgis.	
• Bridge deck overlay NMFRC from the westbound lanes of the Exit 32 Sturgis Interchange Bridge.....	18

Research Task 4: Determine the density of whitetopping and deck overlay concrete from the cores provided by the SDDOT.....	25
Research Task 5: Determine the bond strength of the bridge deck overlay concrete to the original deck from the cores provided.....	28
Research Task 6: Using NMFRC laboratory mixes, make specimens and determine their density and permeability. The specimens should be made using different levels of compactive effort. The laboratory mixes should be similar to that used for the Vivian and Sturgis NMFRC bridge deck overlays. NOTE: This task may give an indication whether a bridge deck paving machine will provide the desired density and permeability even though it does not apply any compactive effort unlike a bridge deck overlay machine.....	55
Research Task 7: Compare the permeabilities and densities of the samples taken for Task 3 with those of Task 6.....	72
Research Task 8: Identify and recommend equipment and testing requirements necessary for the development of bridge deck overlay NMFRC mix designs.....	94
Research Task 9: Identify and recommend necessary equipment, tests, and procedures required for quality control testing in the field.....	94
Research Task 10: Submit a final report summarizing relevant literature, research methodology, test results, NMFRC mix design specifications, required testing equipment, laboratory and field testing procedures, conclusions and recommendations.....	96
Research Task 11: Make an executive presentation to the SDDOT Research Review Board summarizing the findings and conclusions.....	96
Conclusion.....	96
Recommendations.....	97
References.....	99
Appendix A: Core Location for Field and Laboratory Bond Tests.....	A1
Appendix B: Tables and Figures.....	B1
Appendix C: Photographs of the Field and Laboratory Bond Test.....	C1

LIST OF TABLES

Research Task 3

Table 3.1: Average Permeability Values of Cores from Exit 32, I90 (Sturgis).....	22
--	----

Table 3.2: Average Permeability Values of Cores from Exit 212, I90 (Vivian).....	22
--	----

Research Task 4

Table 4.1: Density of Overlying FRC at Exit 32, I90 (Sturgis).....	26
--	----

Table 4.2: Density of Overlying FRC at Exit 212, I90 (Vivian).....	27
--	----

Research Task 5

Table 5.1: Details of the Core Numbering at Exit 32, I90 (Sturgis).....	39
---	----

Table 5.2: Results of the Field Bond Test on the West Bound Passing Lane at Exit 32, I90 (Sturgis).....	40
--	----

Table 5.3: Results of the Field Bond Test on the East Bound Passing Lane at Exit 32, I90 (Sturgis).....	41
--	----

Table 5.4: Cores from the West Bound Lane at Exit 32, I90 (Sturgis) for Lab Tests.....	42
--	----

Table 5.5: Cores from the East Bound Lane at Exit 32, I90 (Sturgis) for Lab Tests.....	43
--	----

Table 5.6: Details of the Core Numbering at Exit 212, I90 (Vivian).....	44
---	----

Table 5.7: Results of Field Bond Test on the South Bound Lane at Exit 212, I90 (Vivian).....	45
---	----

Table 5.8: Results of Field Bond Test on the North Bound Lane at Exit 212, I90 (Vivian).....	47
---	----

Table 5.9: Cores from the South Bound Lane at Exit 212, I90 (Vivian) for Lab Tests....	48
--	----

Table 5.10: Cores from the North Bound Lane at Exit 212, I90 (Vivian) for Lab Tests.....	49
---	----

Table 5.11: Results of the Lab Bond Test on the Cores from West Bound Lane at Exit 32, I90 (Sturgis).....	50
--	----

Table 5.12: Results of the Lab Bond Test on the Cores from East Bound Lane at Exit 32, I90 (Sturgis).....	51
--	----

Table 5.13: Results of the lab Bond Test on the Cores from the Bridge at Exit 212, I90 (Vivian).....	52
---	----

Table 5.14: Comparison of Lab and Field Bond Test Results at Exit 32, I90 (Sturgis).....	53
---	----

Table 5.15: Comparison of Lab and Field Bond Test Results at Exit 212, I90 (Vivian).....	54
---	----

Research Task 6

Table 6.1: Details of Lab Mixes.....	59
--------------------------------------	----

Table 6.2: Properties of Fresh Concrete.....	59
--	----

Table 6.3: Details of Specimen Designation.....	60
---	----

Table 6.4: Cylinder Compressive Strength and Static Modulus.....	61
--	----

Table 6.5: Plain Flexure Test.....	62
------------------------------------	----

Table 6.6: First Crack Strength and Maximum Flexural Strength.....	62
--	----

Table 6.7: Japanese Standard – Toughness and Equivalent Strength.....	63
---	----

Table 6.8: ASTM Toughness Indices.....	64
--	----

Table 6.9: Dry Density of Concrete with Different Compactive Efforts – Mix 1.....	65
---	----

Table 6.10: Dry Density of Concrete with Different Compactive Efforts – Mix 2.....	66
--	----

Table 6.11: Dry Density of Concrete with Different Compactive Efforts – Mix 3.....	67
--	----

Table 6.12: Dry Density of Concrete with Different Compactive Efforts – Mix 4.....	68
--	----

Table 6.13: Dry Density of Concrete with Different Compactive Efforts – Mix 5.....	69
Table 6.14: Rapid Chloride Permeability Test Results for the Specimens Cast in the Lab.....	70

Research Task 7

Table 7.1: Comparison of Permeabilities of Cores from Field and Cylinders Cast in Lab.....	76
Table 7.2: Comparison of Dry Densities of Cores from Field and Cylinders Cast in Lab.....	77
Table 7.3: Comparison of Properties of Fresh Concrete from Record and Lab Mixes.....	78
Table 7.4: Comparison of Properties of Hardened Concrete from Record and Lab Mixes.....	79
Table 7.5: Comparison of Properties of Hardened Concrete from Record and Lab Mixes (ASTM Toughness Indices).....	80

Appendix B: Tables

Table B1: RCPT Results of Specimens from the West Bound Lane at Exit 32, I90 (Sturgis).....	B1
Table B2: RCPT Results of Specimens from the East Bound Lane at Exit 32, I90 (Sturgis).....	B2
Table B3: RCPT Results of Specimens from the Approach and the Plain Concrete Section at Exit 212, I90 (Vivian).....	B3
Table B4: RCPT Results of Specimens from the South Bound Lane at Exit 212, I90 (Vivian).....	B4

LIST OF FIGURES

Research Task 1

Figure 1.1: Applied Voltage Apparatus used on Slab.....	5
Figure 1.2: General Arrangement of the Tank and Diffusion Cell.....	6
Figure 1.3: Detail of the Diffusion Cell for the Potential Difference Test.....	7
Figure 1.4: Detail of the Assembled Rapid Chloride Permeability Cell.....	8
Figure 1.5: Test Setup for Uniaxial Tensile Bond Strength using Friction-grips.....	10
Figure 1.6: Test Setup for Uniaxial Tensile Bond Strength using Pipe-nipple grips.....	11
Figure 1.7: Slant Shear Specimen Being Compressed.....	12
Figure 1.8: Schematic Diagram of the Setup for Bond Test as per ASTM C1245-93.....	13
Figure 1.9: Setup of the Bond Test Conducted in Lab as Described in Task 5.....	14
Figure 1.10: Schematic Diagram Showing the Setup for the Tensile Strength Test As per British Standard 1881-Part 207.....	14

Research Task 3

Figure 3.1: Comparison of the Charge Passed Through Cores from West and East Bound Lanes at Exit 32, I90 (Sturgis).....	23
Figure 3.2: Comparison of the Charge Passed Through Cores from Various Locations on the Bridge at Exit 212, I90 (Vivian).....	24

Research Task 7

Figure 7.1: Comparison of Permeabilities of Cores from Field on the North Bound Lane of the Bridge at Exit 212, I90 (Vivian) and Cylinders cast in Lab.....	81
Figure 7.2: Comparison of Permeabilities of Cores from Field on the North Half of the South Bound Lane of the Bridge at Exit 212, I90 (Vivian) and Cylinders cast in Lab.....	81
Figure 7.3: Comparison of Permeabilities of Cores from Field on the South Half of the South Bound Lane of the Bridge at Exit 212, I90 (Vivian) and Cylinders cast in Lab.....	82
Figure 7.4: Comparison of Permeabilities of Cores from Field on the Approach to the Bridge at Exit 212, I90 (Vivian) and Cylinders cast in Lab.....	82
Figure 7.5: Comparison of Permeabilities of Cores from Field on the Bridge at Exit 32, I90 (Sturgis) and Cylinders cast in Lab.....	83
Figure 7.6: Comparison of Densities of Cylinders cast in Lab (North Bound Lane of the Bridge at Exit 212, I90 (Vivian)).....	83
Figure 7.7: Comparison of Densities of Cylinders cast in Lab (North Half of the South Bound Lane of the Bridge at Exit 212, I90 (Vivian)).....	84
Figure 7.8: Comparison of Densities of Cylinders cast in Lab (South Half of the South Bound Lane of the Bridge at Exit 212, I90 (Vivian)).....	84
Figure 7.9: Comparison of Densities of Cylinders cast in Lab (Approach to the Bridge at Exit 212, I90 (Vivian)).....	85
Figure 7.10: Comparison of Densities of Cylinders cast in Lab (Bridge at Exit 32, I90 (Sturgis)).....	85
Figure 7.11: Comparison of Concrete temperature from Record and Lab Mixes.....	86
Figure 7.12: Comparison of Fresh Concrete Unit Weight from Record and Lab Mixes.....	86

Figure 7.13: Comparison of Slump from Record and Lab Mixes.....	87
Figure 7.14: Comparison of Air Content from Record and Lab Mixes.....	87
Figure 7.15: Comparison of Compressive Strength from Record and Lab Mixes.....	88
Figure 7.16: Comparison of Static Modulus from Record and Lab Mixes.....	88
Figure 7.17: Comparison of First crack Strength from Record and Lab Mixes.....	89
Figure 7.18: Comparison of Maximum Flexural Strength from Record and Lab Mixes.....	89
Figure 7.19: Comparison of Japanese Standard Toughness from Record and Lab Mixes.....	90
Figure 7.20: Comparison of Japanese Standard Equivalent Strength from Record and Lab Mixes.....	90
Figure 7.21: Comparison of First Crack Toughness from Record and Lab Mixes.....	91
Figure 7.22: Comparison of Toughness Index I5 from Record and Lab Mixes.....	91
Figure 7.23: Comparison of Toughness Index I10 from Record and Lab Mixes.....	92
Figure 7.24: Comparison of Toughness Index I20 from Record and Lab Mixes.....	92
Figure 7.25: Comparison of Toughness Ratio I10/I5 from Record and Lab Mixes.....	93
Figure 7.26: Comparison of Toughness Ratio I20/I10 from Record and Lab Mixes.....	93

Appendix A

Figure A1: Location of Field Bond Test on West Bound Lane of the Interchange Bridge at Exit 32, I90 (Sturgis).....	A1
Figure A2: Location of 4" Cores for the Laboratory Tests on West Bound Lane of the Interchange Bridge at Exit 32, I90 (Sturgis).....	A2
Figure A3: Location of Field Bond Test on East Bound Lane of the Interchange Bridge at Exit 32, I90 (Sturgis).....	A3
Figure A4: Location of 4" Cores for the Laboratory Tests on East Bound Lane of the Interchange Bridge at Exit 32, I90 (Sturgis).....	A4
Figure A5: Details of the Number of Cores of Different Diameters in Different Parts of the Bridge and its Naming at Exit 32, I90 (Sturgis).....	A5
Figure A6: Location of Field Bond Test on the North and South Bound Lanes of the Interchange Bridge at Exit 212, I90 (Vivian).....	A6
Figure A7: Location of 4" Cores for the Laboratory Tests on the North and South Bound Lanes of the Interchange Bridge at Exit 212, I90 (Vivian).....	A7
Figure A8: Details of the Number of Cores of Different Diameters in Different Parts of the Bridge and its Naming at Exit 212, I90 (Vivian).....	A8

Appendix B: Figures

Figure B1: RCPT Results of Specimens from West Bound Lane at Exit 32, I90 (Sturgis).....	B5
Figure B2: RCPT Results of Specimens from East Bound Lane at Exit 32, I90 (Sturgis).....	B5
Figure B3: RCPT Results of Specimens from North Half of the South Bound Lane of the Bridge at Exit 212, I90 (Vivian).....	B6
Figure B4: RCPT Results of Specimens from South Half of the South Bound Lane of the Bridge at Exit 212, I90 (Vivian).....	B6
Figure B5: RCPT Results of Specimens from North Bound Lane of the Bridge at Exit 212, I90 (Vivian).....	B7
Figure B6: RCPT Results of Specimens from Approach to the Bridge at	

Exit 212, I90 (Vivian).....	B7
Figure B7: Load Deflection Curve (ASTM C 1018) Specimen 2G1.....	B8
Figure B8: Load Deflection Curve (ASTM C 1018) Specimen 2G2.....	B8
Figure B9: Load Deflection Curve (ASTM C 1018) Specimen 2G3.....	B9
Figure B10: Load Deflection Curve (ASTM C 1018) Specimen 2G4.....	B9
Figure B11: Load Deflection Curve (ASTM C 1018) Specimen 3G1.....	B10
Figure B12: Load Deflection Curve (ASTM C 1018) Specimen 3G2.....	B10
Figure B13: Load Deflection Curve (ASTM C 1018) Specimen 3G3.....	B11
Figure B14: Load Deflection Curve (ASTM C 1018) Specimen 3G4.....	B11
Figure B15: Load Deflection Curve (ASTM C 1018) Specimen 4G1.....	B12
Figure B16: Load Deflection Curve (ASTM C 1018) Specimen 4G2.....	B12
Figure B17: Load Deflection Curve (ASTM C 1018) Specimen 4G3.....	B13
Figure B18: Load Deflection Curve (ASTM C 1018) Specimen 4G4.....	B13
Figure B19: Load Deflection Curve (ASTM C 1018) Specimen 5G1.....	B14
Figure B20: Load Deflection Curve (ASTM C 1018) Specimen 5G2.....	B14
Figure B21: Load Deflection Curve (ASTM C 1018) Specimen 5G3.....	B15
Figure B22: Load Deflection Curve (ASTM C 1018) Specimen 5G4.....	B15

Appendix C:

Photographs of Laboratory and Field Bond Test Procedure.....	C1
--	----

GLOSSARY

The following is a glossary of terms used in this report.

0.1 General Terms

Bond Strength - Tensile Strength of the joint between overlay concrete and underlying old concrete.

Balling - When fibers entangle into large clumps or balls in a mixture.

Equivalent Flexural Strength (JCI) - It is defined by

$$F_c = T_b \times s / \delta_{tb} \times b \times d^2$$

where

F_c = equivalent flexural strength, psi

T_b = flexural toughness, inch-lb

s = span, inches

δ_{tb} = deflection of 1/150 of the span, inches

b = breadth at the failed cross-section, inches

d = depth at the failed cross-section, inches

Flexural Toughness Factor (JCI) - The energy required to deflect the fiber reinforced concrete beam to a mid point deflection of 1/150 of its span.

Fiber content - The weight of fibers in a unit volume of concrete.

First Crack - The point on the flexural load-deflection or tensile load-extension curve at which the form of the curve first becomes nonlinear.

First Crack Deflection - The deflection value on the load deflection curve at the first crack.

First Crack Strength - The stress obtained when the load corresponding to first crack is inserted in the formula for modulus of rupture given in ASTM Test Method C 78.

First Crack Toughness - The energy equivalent to the area of the load deflection curve up to the first crack.

Flexural Toughness - The area under the flexural load-deflection curve obtained from a static test of a specimen up to a specified deflection. It is an indication of the energy absorption capability of a material.

High Performance Concrete - In this report, High Performance Concrete is defined as a concrete with highly enhanced (or improved) desirable properties for the specific purpose and function for which it is used. It need not necessarily be high-strength concrete. High performance concrete for the bridge deck overlay (pavement and whitetopping) will have highly enhanced ductility, fatigue strength, durability, impact resistance, toughness, impermeability and wear resistance.

Overlay - Thin layer of concrete provided over existing old concrete.

Rapid Chloride Permeability - Total amount of charge passed (in coulombs) through a concrete specimen of standard size as per ASTM C1202-97 test.

Residual Strength Factor $R_{5,10}$ - The number obtained by calculating the value of $20(I_{10}-I_5)$, as given in ASTM C 1018.

Residual Strength Factor $R_{10,20}$ - The number obtained by calculating the value of $10(I_{20}-I_{10})$, as given in ASTM C 1018.

Static Modulus - The value of Young's modulus of elasticity obtained from measuring stress-strain relationships derived from other than dynamic loading.

Toughness Indices - The numbers obtained by dividing the area under the load-deflection curve up to a specified deflection by the area under the load-deflection curve up to "First Crack" as given in ASTM C 1018.

Toughness Index, I_5 - The number obtained by dividing the area up to 3.0 times the first crack deflection by the area up to the first crack of the load deflection curve, as given in ASTM C 1018.

Toughness Index, I_{10} - The number obtained by dividing the area up to 5.5 times the first crack deflection by the area up to the first crack of the load deflection curve, as given in ASTM C 1018

Toughness Index, I_{20} - The number obtained by dividing the area up to 10.5 times the first crack deflection by the area up to the first crack of the load deflection curve, as given in ASTM C 1018

Whitetopping - Whitetopping is concrete placed over asphalt where the concrete thickness is 101 mm (4 in.) or more.

0.2 Acronyms Used

ACI - American Concrete Institute

FRC - Fiber Reinforced Concrete

HMA - Hot Mixed Asphalt

LSDC - Low Slump Dense Concrete (used for bridge deck overlays).

NMFRC - Non-Metallic Fiber Reinforced Concrete. This acronym refers only to Polyolefin Fiber Reinforced Concrete. These fibers were "supplied" by 3M for the purpose of this study.

PCC - Portland Cement Concrete

SFRC - Steel Fiber Reinforced Concrete.

RCPT - Rapid Chloride Permeability Test

0.3 ASTM Specifications

A 820 - Specification for Steel Fibers for Fiber Reinforced Concrete

C 31 - Practices for Making and Curing Concrete Test Specimens in the Field

C 39 - Test Method for Compressive Strength of Cylindrical Concrete Specimens

C 78 - Test Method for Flexural Strength of Concrete (Using Simple Beam with Third-point Loading)

C 94 - Specification for Ready-Mixed Concrete

C138 - Test for Unit Weight, Yield and Air Content (gravimetric) of concrete

C 143 - Test Method for Slump of Portland Cement Concrete

C 172 - Method of Sampling Freshly Mixed Concrete

- C 173 - Test Method of Air Content of Freshly Mixed Concrete by the Volumetric Method
- C 231 - Test Method for Air Content of Freshly Mixed Concrete by the Pressure Method
- C 469 - Test Method for Static Modulus of Elasticity and Poisson's Ratio of Concrete in Compression
- C 882 - Standard Test Method for Bond Strength of Epoxy-Resin Systems Used with Concrete by Slant Shear
- C 995 - Test Method for Time of Flow of Fiber-Reinforced Concrete Through Inverted Slump cone
- C1018 - Test Method for Flexural Toughness and First Crack Strength of Fiber Reinforced Concrete (Using beam with Third-point Loading)
- C 1116 - Specification for Fiber Reinforced Concrete and Shotcrete
- C 1202 - Test Method for Electrical Indication of Concrete's Ability to Resist Chloride Ion Penetration.
- C 1245 - Test method for Determining Bond Strength Between Hardened Roller-Compacted Concrete and Other Hardened Cementitious Mixtures (Point Load Test).

0.4 International Standards

- A - American Concrete Institute Committee 544 Fiber Reinforced Concrete
 - ACI 544.2R.89 Flexural Fatigue Endurance
 - Impact Resistance
 - Toughness
- B - British Standards Institute
 - BS1881: Part 2, Methods of Testing Concrete-Vebe Test
- C - Japanese Society of Civil Engineers
 - JSCE Standard III-1, Specification of Steel Fibers for Concrete, Concrete Library.
 - No. 50, March 1983,

- JSCE-SF4 Standard for Flexural Strength and Flexural Toughness, "Method of Tests for Steel Fiber Reinforced Concrete," *Concrete Library of JSCE*, No. 3, June 1984, Japan Concrete Institute (JCI), pp. 58-66.
- "Standard Test Method for Flexural Strength and Flexural Toughness of Fiber Reinforced Concrete, (Standard SF4)," *JCI Standards for Test Methods of Fiber Reinforced Concrete*, Japan Concrete Institute, 1983, pp. 45-51.
- D** - British Standard Institution, *Guide to the Use of Non-Destructive Methods of Test for Hardened concrete*, BS 1881, 1986, Part 201.

BACKGROUND

The feasibility of using Non-Metallic Fiber Reinforced Concrete (NMFRC) in the construction of highway structures had been established in many of our previous studies (1,2,3,4,5). The NMFRC which enhanced fatigue, impact resistance, modulus of rupture, ductility and toughness properties was particularly suitable for the construction of thin bridge deck overlays and whitetopping.

Polyolefin fiber reinforced concrete is one material that promises to provide many advantages over steel and polypropylene fibers while providing a practical approach to enhanced durability and cost-effectiveness in concrete construction. Currently, polypropylene fibers are typically used at 0.1% to 0.3% by volume in concrete to reduce plastic shrinkage cracking. These fibers provide only minimal benefit to the mechanical properties of hardened concrete. Steel fiber, used more extensively in Europe, is typically incorporated in quantities up to 0.5 to 1.0% by volume, and while it does enhance the structural performance of hardened concrete, it poses other problems such as staining, inherent corrosion and potentially harmful protrusions.

Polyolefin fiber reinforced concrete incorporates 50 mm x 0.64mm (2 in. x 0.025 in.) fibers into the concrete mix. These fibers are longer and larger than polypropylene fibers previously used to reinforce concrete, and a proprietary packaging technology enables rapid and uniform mixing into the concrete matrix at quantities up to 2% by volume. These volumes of fiber significantly alter the concrete's physical properties, especially toughness, ductility and resistance to shrinkage cracking. The improved properties make polyolefin fiber reinforced concrete an attractive material for bridge deck overlays.

To be successful and long-lived, a deck overlay must be durable and resistant to fatigue, and must have only thin cracks (less than 0.178mm(0.007in)) and these cracks must be held tightly to resist intrusion of chlorides (5). In the past, transportation agencies throughout the nation have found these requirements (especially low cracking) were difficult to achieve. Several research projects have been undertaken to solve these problems, but with limited success. However, these challenges may be overcome by NMFRC'S enhanced properties.

The South Dakota Department of Transportation had sponsored research to investigate the properties of polyolefin fiber reinforced concrete (1,2,3,4,5). Through laboratory tests at the South Dakota School of Mines and Technology and construction of a segment of pavement, a bridge deck overlay, concrete barrier replacement, and a thin unbonded overlay of asphalt bridge approaches, the material proved to be workable and significantly more resistant to early cracking than ordinary concrete. Previous research results demonstrated increased fatigue capacity and crack width reductions below American Concrete Institute (ACI) recommendations for chloride intrusion. The favorable research results warrant more widespread use of polyolefin fiber reinforced concrete in other applications, including bridge deck overlays.

The South Dakota Department of Transportation (SDDOT) used concrete overlay over older bridge decks to either protect the black steel in older decks and/or as a form of maintenance to extend the life of the deck to the service life of the bridge. The concrete used was low-slump dense concrete (LSDC), which created an almost impermeable barrier between the surface of the overlay and the deck steel. When the LSDC was placed, the low slump bridge deck overlay machines are designed to apply some compactive effort into the fresh concrete to increase the concrete density.

In 1994 a research project (SD94-04) was initiated to study the use of 3M's Polyolefine Fibers (non-metallic fiber reinforced concrete (NMFRC)) in several applications. One application incorporated these fibers in the bridge deck overlay concrete for the structure at Exit 212 over I-90 (I-90/US83). A comparison of SDDOT's LSDC was made to the fiber overlay concrete. As a result of the 1994 study, it was found that the fiber deck overlay performed favorably. Therefore, because of the fibers' ability to greatly enhance the concrete's structural properties, the department decided to include these fibers in the deck overlay concrete for the two severely deteriorated bridge decks at Exit 32 on I-90 (I-90/SD-79) (Research Project SD97-11). The Department hopes that these overlays would extend the life of those decks for seven years from the time of construction (to about 2004).

As a result of the study of the NMFRC bridge deck overlays, which were constructed in 1997, it was recommended that fiber concrete overlays be considered not only on badly deteriorated bridge decks, but on a case by case basis for all the bridges. Although the performance of the fiber concrete deck overlays appears to be acceptable,

some questions continue to be unanswered. How does the permeability, density, and bond strength of the NMFRC deck overlays compare to the plain LSDC? Does the higher initial slump, prior to the addition of fiber, adversely affect the compactive effort of the deck overlay machine? What equipment and testing procedures are necessary for designing the NMFRC mix? Also what equipment and testing procedures are necessary for quality control in the field? Therefore, research needed to be conducted to determine these properties and determine how they compare to South Dakota's (SD) plain LSDC. In addition, equipment and testing requirements need to be identified and recommended for mix design development and field-testing.

RESEARCH OBJECTIVES

- To determine the permeability, density, and bond strength of bridge deck overlay NMFRC as compared to South Dakota's plain LSDC.
- To develop standard mix design and field testing procedures for bridge deck NMFRC.

Research Task 1: Review and summarize literature related to equipment and testing requirements necessary for NMFRC.

Considerable amount of research and developmental testing had been done at the South Dakota School of Mines and Technology (SDSM&T), Rapid City, SD, for the past 25 years. The testing methodology, equipment and the interpretation of results were in par with the present day methods and principles used by various agencies and organizations for the testing of NMFRC. In addition to the review of our own research, attempts had been made to find out whether any different testing requirements were specified and/or used by others for evaluating NMFRC in this research task.

Chloride permeability

Significant damage to concrete results from the intrusion of corrosive solutions. Any treatment that effectively blocks the penetration of corrosive solutions would greatly reduce the damage and lead to increased durability improving economic benefits. Considerable research had been done in this area including the evaluation of special

coatings, pore-blocking admixtures, and special concretes such as polymer impregnated concrete, dense Portland cement concrete (Iowa method), internally sealed concrete, and polymer concrete applied as overlays (6). One successful system for overlays had been latex-modified concrete (7). In addition to the added cost of materials for such overlays, special equipment and expertise were needed for field applications, consequently such concretes were considerably more expensive than commercially prepared ready-mixed concretes (8).

There were different methods for determining the chloride permeability in concrete like the ponding with chloride solutions (9), or accelerated weathering exposure (10), or the in situ method (11). Work by Betelle, Columbus laboratories (12) as well as Kansas DOT (13) had shown that it was possible to remove significant amounts of chloride ions from concrete by application of an electric field between the surface of the concrete and the reinforcing steel. It was hypothesized that this technique could be utilized as a chloride permeability test method if the polarity was reversed. That is, by making the reinforcing steel anodic (+); chloride ion, having a negative charge, would migrate into the concrete. As the electrical resistivity of concrete decreased with increasing chloride ion concentration, a measure of the increase in current, with time, could be correlated with the amount of chloride entering the concrete. Also at the end of the test, samples could be taken to verify the ingress of chloride by subsequent wet chemical analysis.

The applied voltage technique (11), which was developed on the basis of "electrophoresis" (14), was an in-situ method which would allow the assessment of protective system performance to be made shortly after, or even during, the construction period. The field test procedure could be conveniently broken down into four separate stages.

1. Location of reinforcing steel and bonding of test dike
2. Vacuum saturation and heating of test area
3. Applied voltage test
4. Chloride sampling (optional)

Each test took two full working days, by the use of two dikes, four tests could be completed in one working week. Stage 2 required overnight operations; however, the unit could be left unattended during this period. A complete description of the test procedure could be found in Reference 15. Figure 1.1 shows the set up used for this test. The method was found to give good correlation with long-term ponding data on companion slabs. It could be used as a quality control tool for new construction or as a means of monitoring permeability of structures.

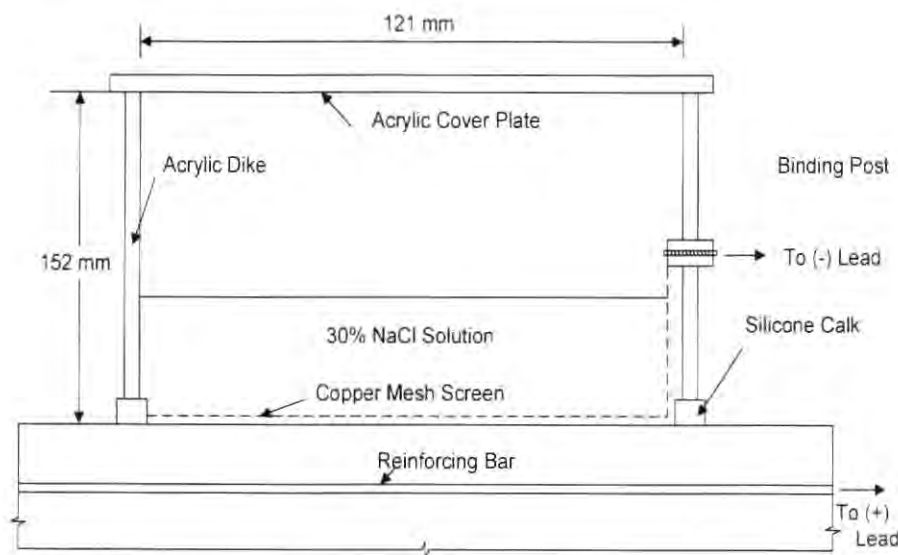


Figure 1.1: Applied Voltage Apparatus used on Slab (Reference 15)

Previous attempts to determine coefficient of diffusion of chloride ions in concrete more rapidly had met with limited success. Goto and Roy (16) applied a potential difference of up to 2 V (dc) across thin paste specimens (<5 mm thick), assuming that the small perturbation did not change the diffusion of chloride ions significantly. The results of accelerated chloride ingress tests on bridge deck concrete, in laboratory and in situ, obtained by Whiting (11) were not correlated with the coefficient of diffusion of chloride ions in concrete. It was recognized that the transportation of chlorides during the tests was not by diffusion.

A simple rapid test that greatly accelerated the transportation of chlorides through concrete was developed by R. K. Dhir et al (17). This method also gave a mathematical solution of Fick's First Law to evaluate the results of both the rapid and conventional non-perturbative diffusion tests. The rapid test utilized a perturbative application of a

small potential difference at a low current across a concrete specimen in a diffusion cell with an electrode and an electrical supply to the diffusion cell. The assembled diffusion cell (Figure 1.3) was placed in an immersion tank in which chloride solution was continuously recirculated through a heater, to avoid any local rise in temperature. The tank was filled with a 5M sodium chloride solution (Figure 1.2). Graphite was used as anode and a 3 mm stainless steel plate was used as cathode. A potential difference of 10 V was applied during the test period of 7-12 days and the current was measured. The detail of this process and the mathematical model of the diffusion process could be found in Reference 17.

The AASHTO Test Method T 277-83I, "Rapid Determination of Chloride Permeability of Concrete" was adopted in 1983. Virtually the same test procedure was designated by ASTM as C1202 (18), "Electrical Indication of Concretes Ability to Resist Chloride Ion Penetration". In this ASTM test, one surface of a water saturated concrete specimen was exposed to sodium chloride solution and the other surface to sodium hydroxide solution. A 60-volt DC electrical potential was placed across the specimen for a period of six hours. The electrical charge (in coulombs) passed through the concrete specimen represented its "rapid chloride permeability". The ease and speed of this test method had made it more popular compared to the other methods (19).

The rapid test method ASTM C 1202 was now commonly required by construction project specification for both precast and cast-in-place concrete. The rating

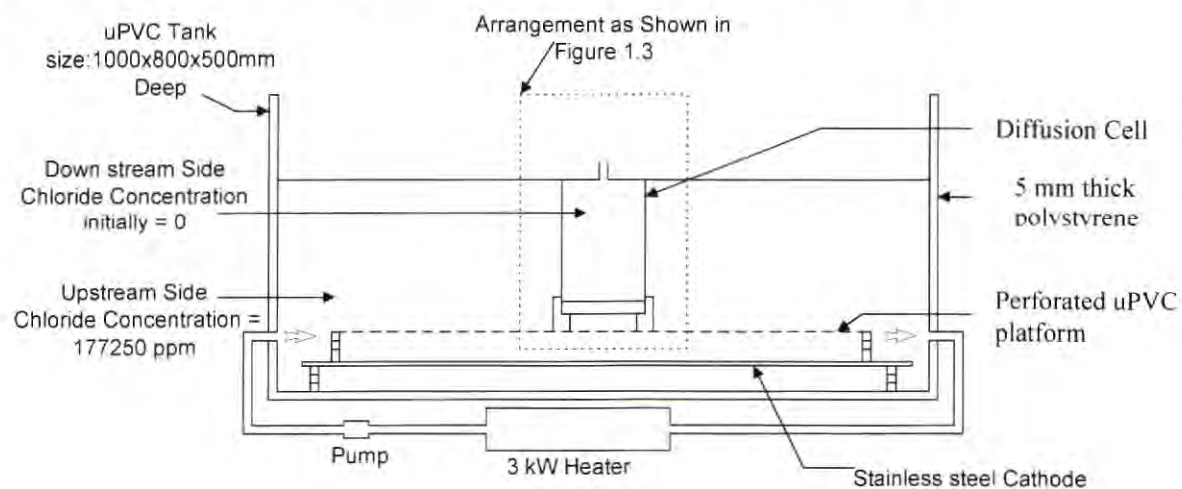
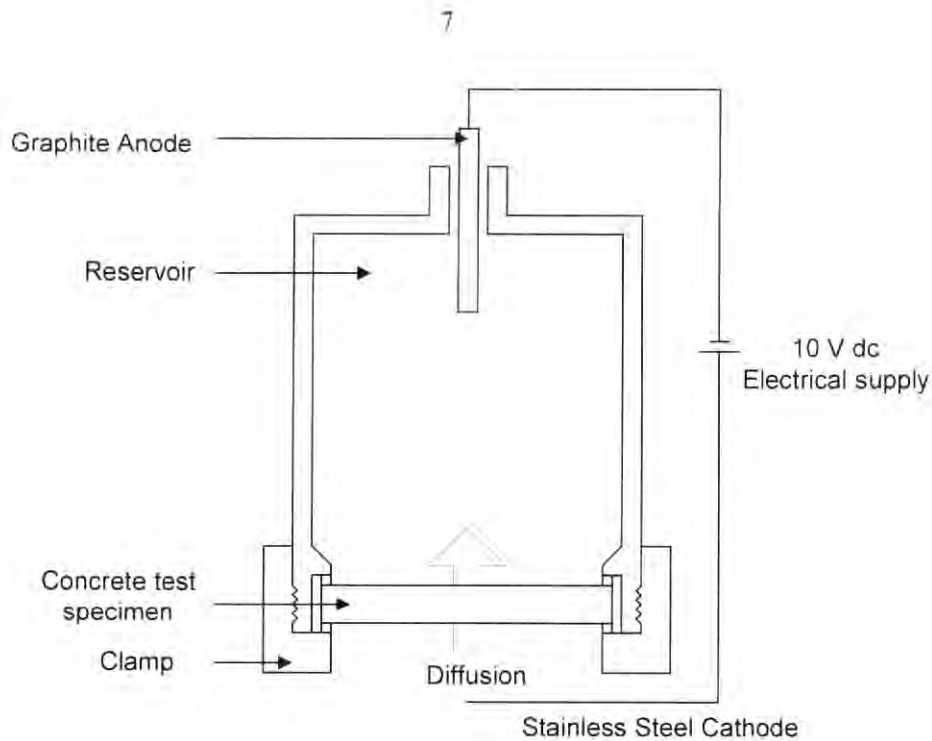


Figure 1.2: General Arrangement of the Tank and Diffusion Cell (Reference 17).



**Figure 1.3: Detail of the Diffusion Cell for the Potential Difference test
(Reference 17).**

of the charge passed was usually chosen from the scale shown below by the engineer or owner as per their requirements:

<u>Charge Passed</u> (Coulombs)	<u>Chloride Permeability</u> (ASTM C 1202)
> 4000	High
2000 – 4000	Moderate
1000 – 2000	Low
100 – 1000	Very low
< 100	Negligible

The detailed description of the process is discussed in Research Task 3. Figure 1.4 shows the details of an assembled RCPT cell.

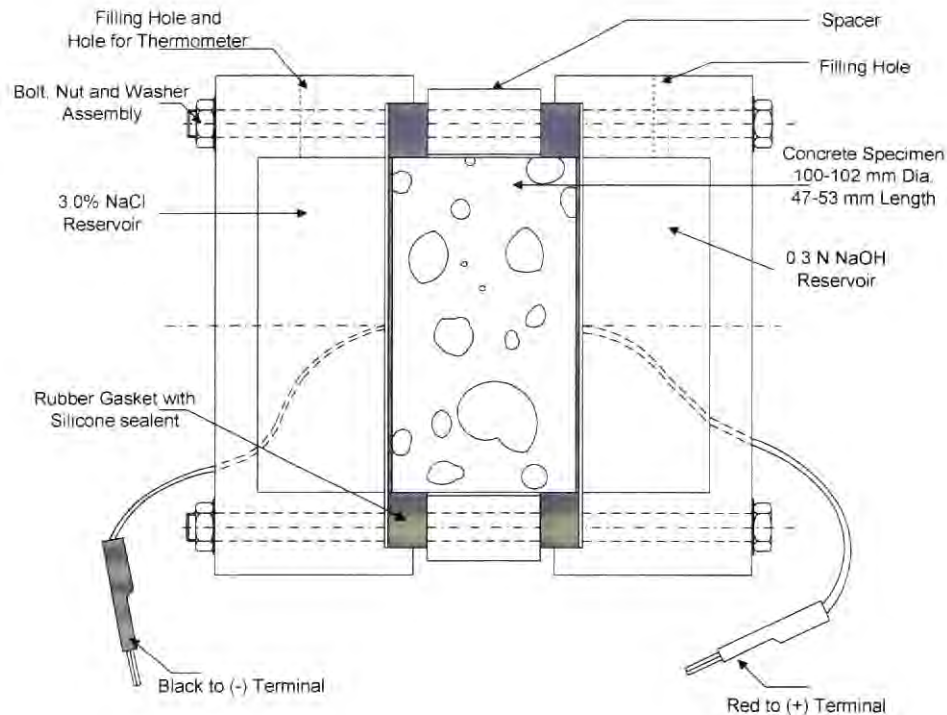


Figure 1.4: Detail of the Assembled Rapid Chloride Permeability Cell (ASTM C 1202)

Bond tensile strength tests between the overlay and the underlying old concrete

The rehabilitation of pavement concrete commonly requires the removal of deteriorated concrete and repair with a patch material and/or an overlay. To ensure long service of the rehabilitated concrete, it was imperative that the repair material was well bonded to the underlying concrete. Proper surface preparation of the substrate was an important factor for the success of any repair. The field tensile bond strength was a quick, simple and accurate method for determining how well the repair material was bonded to the underlying concrete (20).

In 1984, A. E. Long and A. M. Murray had reported about a pulloff test in which a metal disk was bonded to the concrete surface and a tensile load was applied causing a tensile failure in the concrete. The slant shear method used concrete samples which contained a layer of the overlay concrete and a layer of the underlying concrete, which

had been prepared, cured, and tested under ideal conditions in the laboratory (21). The slant shear test was developed to determine the quality of a bonding agent, not the bond strength of an overlay in the field. This test was not suited to measure the in-place bond strength of cores containing an overlay.

In a study of the interface shear strength between the thin bonded concrete overlay (TBCO) and continuously reinforced concrete pavement (CRCP) (22), cores of 101.6 mm (4 in.) diameter were taken through the overlay and the CRCP. Since the effective bonding between the CRCP and TBCO was critical, the interface was tested in shear. A sliding two-part shear collar similar to the one used in Iowa (23) was used with the shear force induced in compression instead of tension. It was observed that the interface shear strength varied from 79 to 377 psi with a mean of 201 psi and a standard deviation of 100 psi under the worst scenario. Researchers at the Texas A&M University at Austin concluded that a shear stress of 64 psi could be expected for a bridge deck overlaid with 50.8 mm (2 in.) bonded concrete subjected to impact loading (24). The calculations using elastic-layered theory showed that a maximum shear of 24 psi could be expected under a standard 18 kips single-axle load on dual tires at the interface of a 50.8 mm (2 in.) TBCO and a highway CRCP on weak foundation. This led to the conclusion that once the bonding was achieved, the bonding capacity was usually not a problem (22).

A previous study (25) developed a test method to determine the uniaxial tensile bond strength. That study concentrated primarily on the bond strength of new Portland cement paste to old Portland cement paste. As an extension to that study, another study was done to investigate the uniaxial tensile bond strength of concrete instead of cement paste (26). In this study, two methods of gripping uniaxial tensile specimens were investigated. Also, a modified ASTM C 882 (21) slant shear bond strength test method was conducted.

Uniaxial tensile bond strength using friction grips

The required friction around the lateral surface area of the bond strength specimen was developed by closing together the sides of a 76 mm (3 in.) long steel pipe which had been split along its longitudinal axis (26). Two identical split pipe pieces were used: one to grip the repair material and the other to grip the base concrete. A rubber "O" ring provided a 4.8 mm (3/16 in.) spacing between the split pipe pieces at the bond plane.

Universal ball and socket connections were used to eliminate any eccentricities during loading. Figure 1.5 shows the test set up.

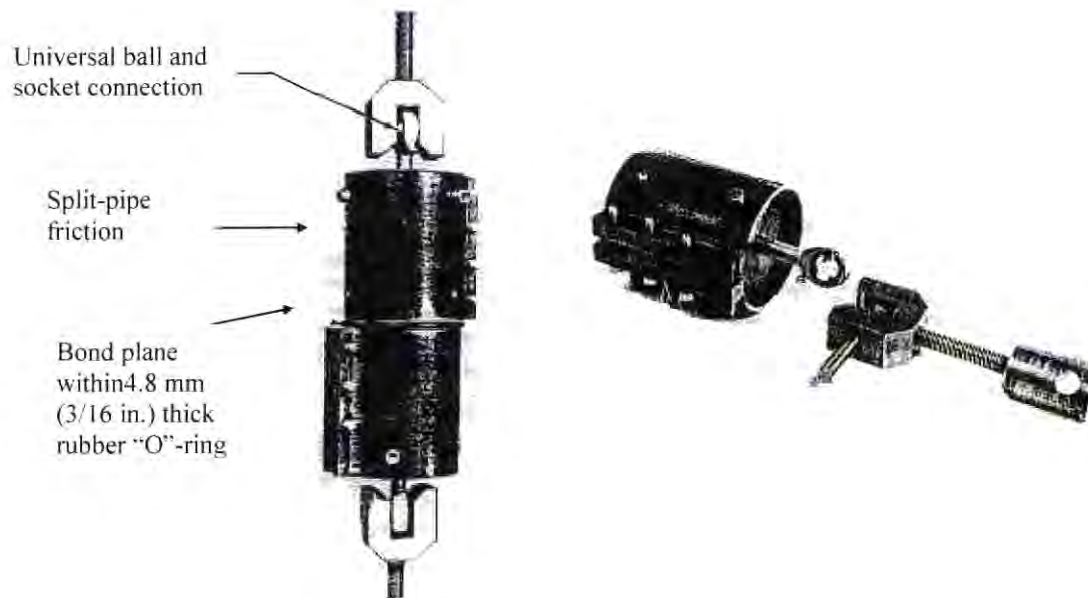


**Figure 1.5: Test Setup for Uniaxial Tensile Bond Strength using Friction-grips
(Reference 26)**

Uniaxial tensile bond strength using pipe nipple grips

The lateral circumference of a 76 mm (3 in.) diameter by approximately 76 mm (3 in.) long base PCC cylinder with a sawn surface on one side and an "O" ring on the other side was bonded with epoxy inside of a nominal 76 mm (3 in.) inside diameter, black steel pipe nipple (26). The "O" ring provided about 4.8 mm (3/16 in.) spacing. After the epoxy had cured, the specimen was inverted and a black steel pipe nipple of the same dimensions was mounted on top of the base concrete-pipe nipple "O" ring assembly and the repair material was cast into the empty steel pipe nipple. After curing, the repair material had bonded to the sawn surface of the base concrete and to the inside of the pipe nipple into which it had been poured. Pipe caps with special arrangements as shown in Figure 1.6, including universal ball and socket connections, were screwed on the pipe nipples at both ends, in order to attach the specimen to the testing machine.

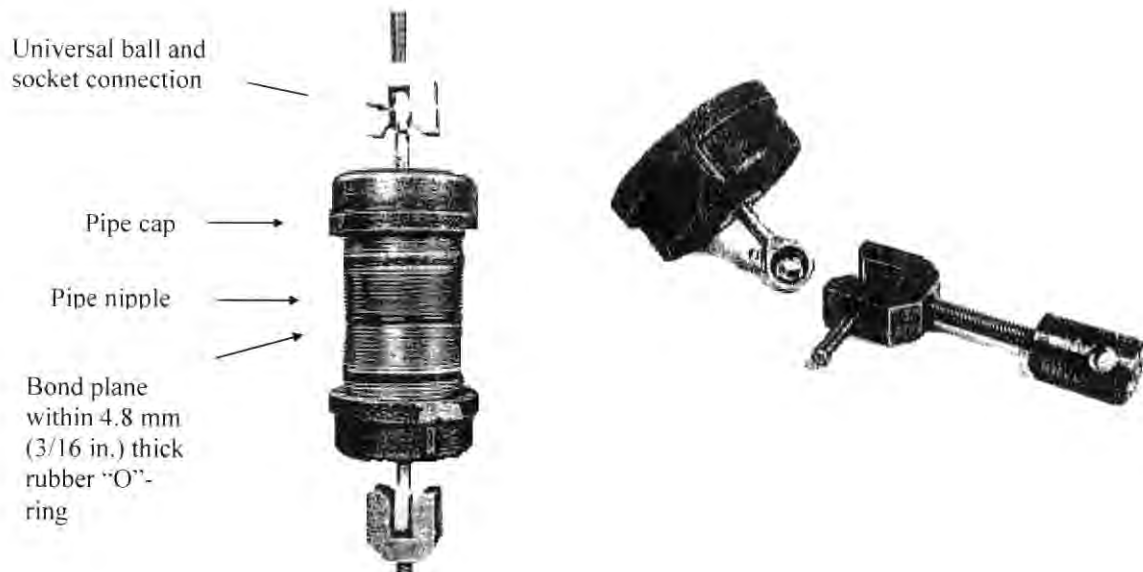


Figure 1.6: Test Setup for Uniaxial Tensile Bond Strength Test using Pipe-nipple grips (Reference 26)

Modified slant shear bond strength test method

The modification of ASTM C 882 (21) slant shear bond test consisted of replacing one-half of the slant shear specimens with repair material. That is, one-half of the specimen was repair material bonded to the other half, which was base concrete. The angle of the shear plane was approximately 30° with respect to the longitudinal axis of the cylinder. Figure 1.7 shows a slant shear specimen being compressed.

For the two higher strength repair materials investigated, the relative precision of the slant shear and the uniaxial tensile strength method using the pipe nipple grips were comparable and relatively good with a coefficient of variation of about 5%. It was concluded that both the slant shear test method and the pipe nipple grips uniaxial tensile test method were promising methods for screening and selecting repair materials, for overlaying or patching Portland cement concrete (26).



Figure 1.7: Slant Shear Specimen Being Compressed. One half of the Specimen was Base Portland Cement Concrete and the other half was the Repair Material.
(Reference 26)

The ASTM C 1245-93 (27) gives another method to test the relative bond between layers of hardened concrete in multiple-lift forms of construction. This test method was intended to test roller-compacted concrete. However, it could be applied for all types of layered concrete construction, which involved an upper layer of concrete or mortar bonded on an underlying layer of concrete or mortar. Figure 1.8 shows the schematic diagram of the test setup. Bond strength of drilled cores or cast cylindrical specimens in which the bond surface was essentially normal to the longitudinal axis at approximately the mid-length of the specimen were determined. A splitting tensile stress normal to the bond surface was produced by point-loading the specimen across its diameter at that surface.

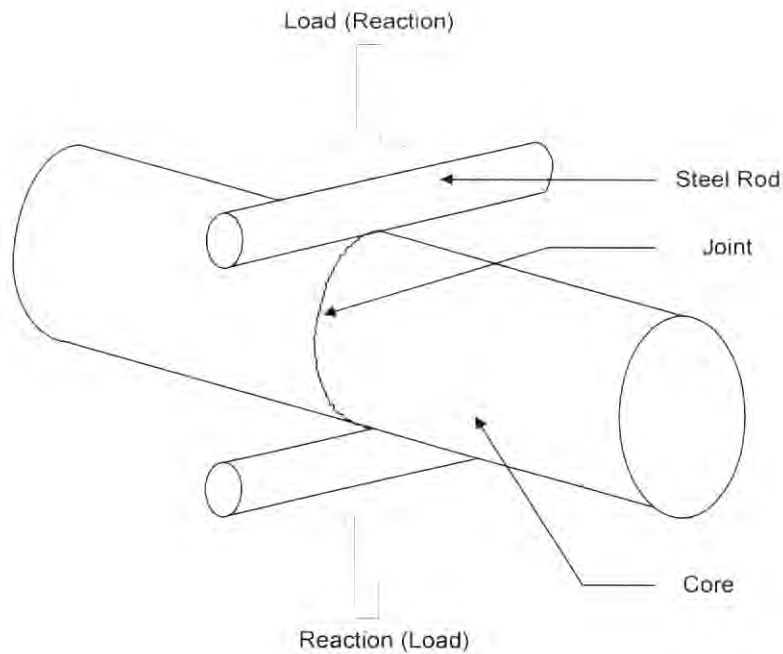


Figure 1.8: Schematic Diagram of the set up for Bond Test as per ASTM C 1245-93

In our present investigation, bond strength tests of cores from the bridge deck were carried out to determine the tensile bond strength of the overlying NMFRC with the underlying old concrete. The field tests were done on 50.8 mm (2 in.) partially cut cores and the laboratory tests were done on 101.6 mm (4 in.) cores from the bridge deck under test. The Research task 5 explains in detail, the field and the laboratory bond test methods and its results and the Figure 1.9 shows the set up for the test.

Another method, described in the British Standard 1881-Part 207 (28) for testing the tensile strength of concrete, could also be used to determine the bond strength between the overlay and the underlying concrete. In this method, a 50 mm (1.96 in.) diameter metal disk (Figure 1.10) is glued to the concrete surface using an epoxy adhesive. The disk is then pulled in tension until fracture occurs in the concrete. The tensile strength is determined by dividing the maximum load by the area of the disk. This method is similar to the method used for the determination of bond strength in the field as described in the Research Task.

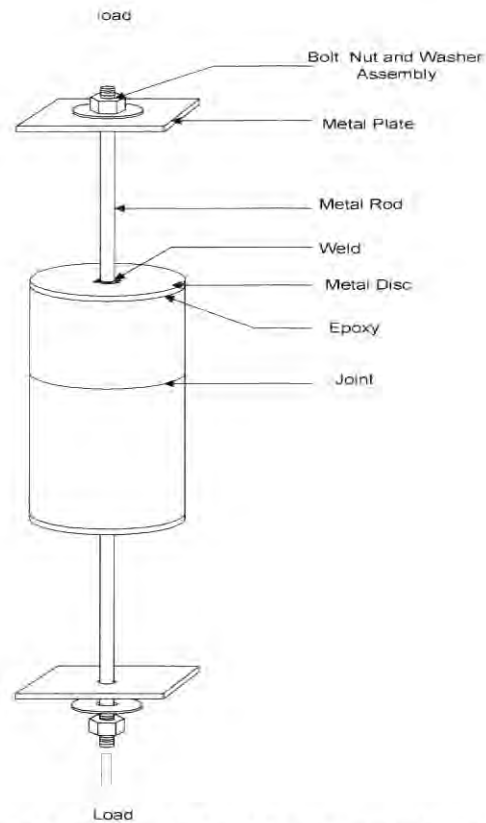


Figure 1.9: Set up of the Bond Test Conducted in Lab as Described in Research Task 5

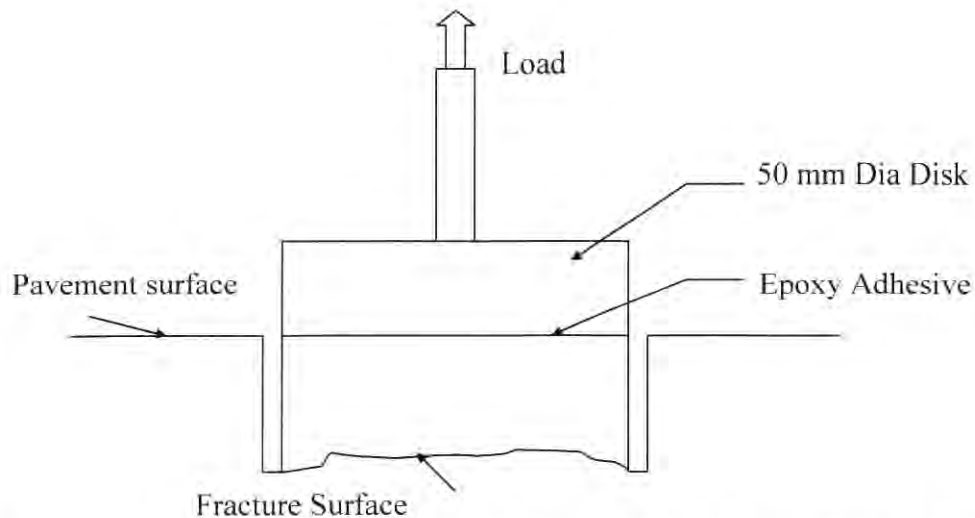


Figure 1.10: Schematic Diagram showing the Setup for the Tensile Strength Test as per British Standard 1881-Part 207

Most of the recent research orient towards nondestructive methods to evaluate the bond quality at interfaces in layered sections and also to evaluate the overall performance of highway bridge deck and girder concretes. The methods like sonic methods (Impact-Echo and Spectral Analysis of Surface Waves), Ground Penetrating Radar, and Infrared Thermography were being investigated. Various recent case studies indicated the use of the impact echo method for different purposes such as: detection of horizontal cracking in a 1 m thick reinforced deck of a railway bridge in Denmark; voids detection in grouted tendon ducts of a post-tensioned highway bridge in Northeastern USA and detection of the delaminations in concrete bridge girders with asphalt overlay in New York state.

Research Task 2: Attend SDDOT's coring operation of the selected sites to ensure that the samples obtained are acceptable for the testing to be conducted.

Coring and Bond Test on Bridge at Exit 32, I 90 (Sturgis)

The coring and bond tests at Exit 32 on I 90 were carried out on July 8, 1999. The research team from SDSM&T comprising of Dr. V. Ramakrishnan and two graduate students accompanied the engineers from the Federal Highway Administration Mr. Leif G. Wathne and Mr. Gene Clark to the site and met Mr. Anselem H. Rumpca and Mr. Frank Droz with their assistants from the SD-DOT.

The passing lanes of both East and West bound lanes were closed to traffic first and the coring operations were started on the West bound passing lane. Eight 50.8 mm (2 in.) cores were drilled approximately to a depth of 88.9 mm (3.5 in.) for the field bond test. Five were on the bridge and one on each approach. One of the six cores (W2) on the bridge was a duplicate because of the steel encountered during coring. Six 101.6 mm (4 in.) cores, four on the bridge and one each on both approaches were also taken for the laboratory bond test, rapid chloride permeability test and the determination of density. Similarly six 50.8 mm (2 in.) cores were drilled on the East bound passing lane with four on the bridge and two on the approach for the field bond test, also six 101.6 mm (4 in.) cores were taken for the laboratory tests. After the coring operations were completed, the

location of the cores were marked and noted down and the holes were filled back with cement mortar. Then the driving lanes of both the East and West bound lanes were closed for traffic and six 101.6 mm (4 in.) cores were taken from each lane for the laboratory tests.

The locations of both the 50.8 mm (2 in.) cores and the 101.6 mm (4 in.) cores were marked with respect to the permanent reference points on the bridge. The system of triangular plotting was used to locate the cores on the map. The joint between the bridge and the approach was taken as the benchmark and all the other dimensions were taken with respect to the benchmark. Only linear measurements were taken and the distances were measured to an accuracy of 25.4 mm (1 in.).

The locations of both the 50.8 and 101.6 mm (2 and 4 in.) cores were first marked on the deck slab with the help of a cover meter to avoid the cutting of steel during the coring operation. The cores and their locations were immediately marked after they were removed and recorded. The details of the names and locations of both 50.8 and 101.6 mm (2 and 4 in.) cores on the East and West bound lanes are given in the Figures A1 to A4 and the summary is given in Figure A5 in Appendix A. The bond test was carried out on the 50.8 mm (2 in.) cores as per the procedure described in Research task 5.

Coring and Bond Test on Bridge at Exit 212, I 90 (Vivian)

The coring and bond test on the bridge at Exit 212 on I 90 near Vivian was done on July 21, 1999. The research team from SDSM&T met Mr. Dan Strand and Mr. Frank Droz with his assistant from the SDDOT at the site.

The bridge consisted of four parts, the North approach (whitetopping), the North half (FRC, with fibers at the rate of 11.9 Kg/m^3 - 20 lbs/yd^3) and the South half (FRC, with fibers at the rate of 14.8 Kg/m^3 - 25 lbs/yd^3) of the South bound lane, and the North Bound lane (plain cement concrete). It was decided to conduct four field bond tests on each part and to take six 101.6 mm (4in.) cores from each part of the bridge for the laboratory tests. The details of the names and locations of both 50.8 and 101.6 mm (2 and 4 in.) cores on the North and South bound lanes are given in the Figures A6 and A7 in

Appendix A. The details about the naming and the number of cores from each part of the bridge is shown in the Figure A8 in Appendix A.

The South bound lane was first closed to traffic. It was decided to drill the 101.6 mm (4 in.) cores first so that the vehicle with the coring equipment could easily maneuver on the bridge for drilling the 50.8 mm (2 in.) cores. The core locations were marked; a cover meter was used to detect the reinforcement under the concrete so that it was not damaged during the coring operation. The 101.6 mm (4 in) cores on the North approach to the bridge, with whitetopping were drilled to a depth of about 254 mm (10 in.) to obtain the full depth of the underlying asphalt and the cores on the deck slab were drilled to a depth of about 165 to 177.8 mm (6.5 in. to 7 in.). All the cores and their locations were marked immediately as the cores were removed. The distance of the cores from temporary bench marks were measured and recorded. The system of triangular plotting was used to locate the positions of the cores. The expansion joints at either end of the bridge were taken as permanent bench marks. All linear measurements were taken to an accuracy of 25.4 mm (1in.) After the 101.6 mm (4 in.) cores were completed, the 50.8 mm (2 in.) cores were drilled and care was taken to retain the core intact to conduct the field bond test. The locations of the 50.8 mm (2 in.) cores were marked with the help of a cover meter and the linear distance of these locations with respect to the temporary bench marks set up earlier during the marking of the 101.6 mm (4 in.) cores were measured and recorded. The locations of the 50.8 mm (2 in.) cores were cleaned and scarified as described in the procedure for the field bond test in Research Task 5. First the field bond test was conducted on drilled cores in the South bound lane and the results were recorded. A 16 KN (3595.5 lbs.) bond tester with a least count of 0.1 KN (22.47 lbs.) was used on all the cores except BS10, for which a 50 KN (11235.95 lbs.) tester with least of 0.5 KN (112.36 lbs.) was used.

Once all the coring operations and bond tests were completed in the South Bound Lane, the holes were filled with rich cement mortar and the lane was opened to traffic. The North bound lane was then closed to traffic.

Similarly the coring and bond test operations were carried out on the North bound lane and all the locations of both the 50.8 mm (2 in.) and 101.6 mm (4 in.) cores were marked and recorded. The holes were closed after all the bond tests were conducted. The

tests were conducted using a 50 KN (11235.95 lbs.) bond tester with a least count of 0.5 KN (112.36 lbs.).

Research Task 3: Perform permeability testing on the 3 or 4 cores taken from each of the following test sections:

- Plain LSD concrete from the northbound lane of the exit 212 interchange bridge over I-90 (I-90/US83) at Vivian.
- NMFRC Bridge deck overlay with fibers added at a rate of 25 lbs./cu.yd. from the southbound lane of Vivian interchange bridge.
- NMFRC Bridge deck overlay with fibers added at a rate of 20 lbs./cu.yd. from the southbound lane of Vivian interchange bridge.
- NMFRC White topping with fibers added at a rate of 25 lbs./cu.yd. from the approach to the Vivian interchange bridge.
- NMFRC Bridge deck overlay with fibers added at a rate of 25 lbs./cu.yd. from the eastbound lanes of the Exit 32 interchange on I-90 (I-90/SD79) at Sturgis.
- NMFRC Bridge deck overlay with fibers added at a rate of 25 lbs./cu.yd. from the westbound lanes of the Exit 32 Sturgis Interchange Bridge.

The Rapid Chloride Permeability Test (RCPT) was conducted on the core samples from the bridge at Exit 32, I 90 (Sturgis) and Exit 212, I 90 (Vivian).

The following cores were selected for the RCPT:

Bridge at Exit 32, I 90 (Sturgis)

Two specimens each from the approach (ED1 and ED6), driving lane (ED2 and ED4) and passing lane (EP2 and EP5) were tested from the East bound lane.

One specimen (WD1) from the approach and two each from the driving lane (WD2 and WD5) and passing lane (WP2 and WP4) were tested from the West bound lanes.

Bridge at Exit 212, I 90 (Vivian)

VS1, VS3 and VS9 from the North approach (whitetopping)

VN1, VN2 and VN6 from the North bound lane (plain concrete)

VS4, VS5 and VS7 from the North half (FRC, with fibers @ 20 lbs/cu.yd.) of the South bound lane

VS11, VS12 and VS13 from the South half (FRC, with fibers @ 25 lbs/cu.yd.) of the South bound lane

Rapid Chloride Permeability Test

The RCPT was conducted in accordance with the procedure given in ASTM C 1202. A brief summary of the procedure followed is given below:

Test Specimen

- The 100 mm x 200 mm (4 in. x 8 in.) cylinders were cut to a thickness of 50 mm (2 in.) from the top (finished) surface by using a Hillquist rock saw. This slice was used as the test specimen.

Conditioning

- Two liters of tap water was boiled vigorously and then allowed to cool to the room temperature.
- The specimens were allowed to dry for one hour. A sufficient amount of two-part epoxy was mixed in a plastic container. This epoxy was then coated on the circumferential sides of the specimens using a brush. The epoxy used was DEVCON High Strength (5-minute fast drying) containing Epoxy Resin, 2,4,6-TRI (Dimethylaminomethyl) Phenol and Amine/Mercaptan hardener. The epoxy was allowed to dry thoroughly.
- The specimens were then placed in the vacuum desiccator (PR-1070-L for humidifying 8 samples bought from Germann Instruments) bowl such that both ends of each specimen were exposed. The ledges of the lid were cleaned and lightly oiled. The lid was then placed on the desiccator and the vacuum pump was turned on. The vacuum was maintained at -0.8 BAR (-13 psi) for 3 hours.
- After three hours, the separatory funnel was filled with deaerated water. With the vacuum pump still running, the water stopcock was opened and sufficient water was

let into the desiccator to completely submerge the specimens. The stopcock was then closed and the vacuum pump was run for one additional hour.

- At the end of the additional hour the vacuum pump was turned off and the vacuum line stopcock was opened to let in the air and the specimens were allowed to soak under water for 18 ± 2 hours.

Test Procedure for Rapid Chloride Permeability Testing

- The vacuum saturated specimens were removed from the desiccator and then they were placed in a plastic bag filled with water in order to prevent them from drying.
- The inside surface of the vulcanized rubber gaskets 100 mm [4 in.] outside diameter and 75 mm [3 in.] inside diameter and 6mm [0.5 in.] thick were coated with a cell sealant. The sealant used was SILICONE (Dow Corning Brand) available in 82.8 ml (2.8 fl.oz.) tubes.
- One of the gaskets (PR-1010M sealing rings bought from Germann Instruments) was placed in the space above the mesh. Then the specimen was governed into the gasket. The spacer was placed over the specimen and the other gasket was positioned at the end of the specimen. Finally, the second cell half was positioned over the gasket with bolts going through the attachment holes. The washers and the nuts were attached to the bolts and tightened.
- The specimen was positioned in the measuring cell (PR-1000 Measuring Cell, complete with two connecting cables and temperature probe bought from Germann Instruments) containing a fluid reservoir at each end of the specimen. One reservoir was filled with 3% sodium chloride (NaCl) solution and the other with 0.3 N (Normality) oxide (NaOH) solution. The specimen was positioned such that the finished surface of the specimen was facing the NaCl reservoir and the cut surface facing the NaOH reservoir. The reservoir containing NaCl is connected to the negative terminal; the NaOH reservoir is connected to the positive terminal of the power supply.
- The lead wires were attached to cell electrical connectors and the cells were connected to the power supply. The equipment used was a PROOVE it (PR-1050 bought from Germann Instruments, Inc.) power supply with microprocessor and circuits for measuring the voltage and the current on each attached cell. The voltage

supplied to the power supply unit was 115VAC, frequency 60 Hz. The voltage output from the power supply unit was 10/20/30/60 VDC, selected by the microprocessor (we used 60 VDC). The power supply can test a maximum of 8 cells at a time. The built-in A/D converter was controlled by the microprocessor, which in turn transferred the data to the computer, where the data was processed and stored for a later printout. Figure B1 shows the assembled cell for the RCPT.

- The power supply was turned on and the voltage value was set to 60 VDC. The computer program used (PR-1040 Software supplied by Germann Instruments) recorded the current (in mA) and temperature (in °C) values every 5 minutes.
- The test was terminated after six hours. The specimen was removed and the cells were rinsed thoroughly in tap water and the residual sealant was stripped out and discarded.

The results of the RCPT conducted on the above mentioned cores are tabulated in Tables B1 to B4 in Appendix B and the plot between the amount of current passed with time for each specimen is given in Figures B1 to B6 in Appendix B. The average permeability values for both the bridges at Exit 32 and Exit 212 are given in the Tables 1 and 2 respectively. The comparison of these values is given in Figures 1 and 2 respectively.

It was observed that the approach concrete was the most permeable in both the East and the West bound lanes at Exit 32 (Sturgis). The driving lane in the West bound lane and the passing lane in the East bound lane were found to be more permeable than the other lanes.

The results from the cores obtained from the different parts of the bridge at Exit 212 (Vivian) again showed that the concrete in the approach was the most permeable and that the concrete in the South half of the bridge with fibers at the rate of 14.8 Kg/m^3 (25 lbs/yd^3) was more permeable than the concrete in the North half of the bridge with fibers at the rate of 11.9 Kg/m^3 (20 lbs/yd^3), which was slightly more permeable than the concrete from the plain concrete section of the North bound lane of the bridge.

Table 3.1: Average Permeability Values of Cores from Exit 32, I 90 (Sturgis)

Location of Cores	West bound lane		East bound lane	
	Specimen #	Total Charge Passed (coulombs)	Specimen #	Total Charge Passed (coulombs)
Approach	WD1	5730.8	ED1	2088
			ED6	6131.2
			Average	4109.6
Driving Lane	WD2	3049.7	ED2	1659.9
		2277.5	ED4	1012.6
		Average	Average	1336.3
Passing Lane	WP2 WP4	1832.1	EP2	4062.1
		1476.5	EP5	1327.6
		Average	Average	2694.9

Table 3.2: Average Permeability Values of Cores from Exit 212, I 90 (Vivian)

Location of Cores	Specimen #	Total Charge Passed (coulombs)
Approach (Whitetopping)	VS1	7112
	VS3	3634
	VN9	3310.6
	Average	4685.5
North Bound Lane (Plain Concrete)		1491.3
		2984.5
		1624.1
	Average	2033.3
North Half of South Bound Lane FRC (20 lbs/cft)		3239.6
		2719.5
		1595.6
	Average	2518.2
South Half of South Bound Lane FRC (25 lbs/cft)		3307.2
		2309.1
		2772.2
	Average	2796.2

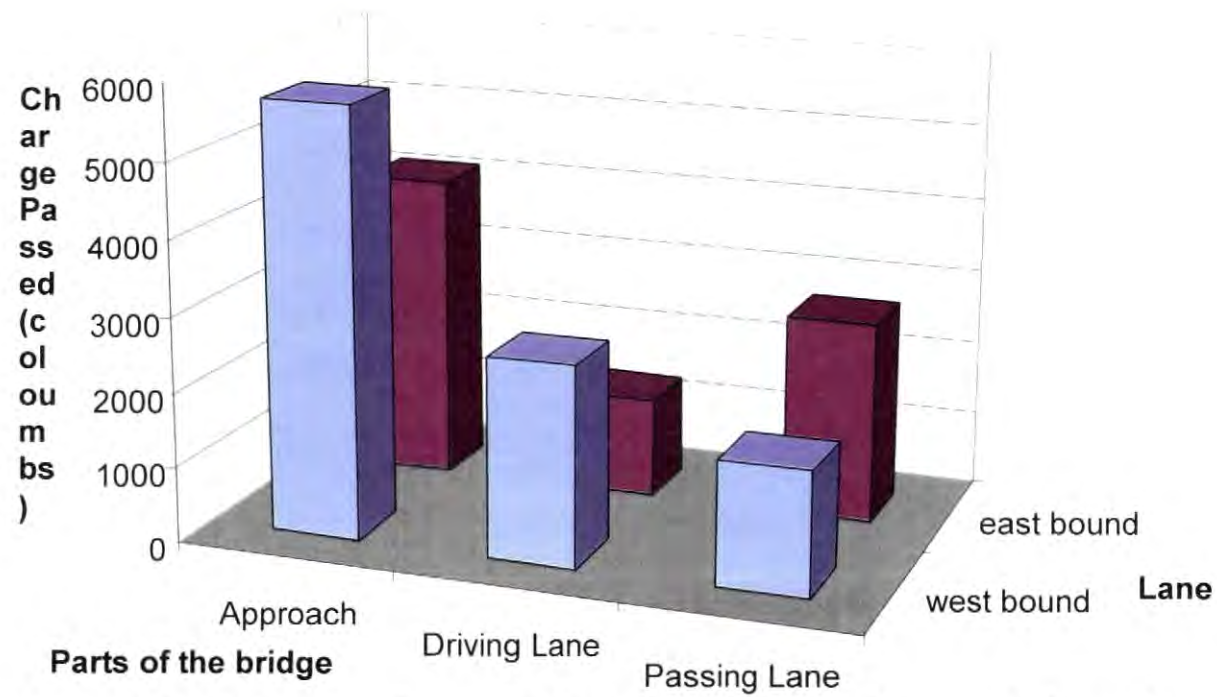


Figure 3.1: Comparison of the Total Charge Passes Through Cores from West and East Bound Lanes at Exit 32, I 90 (Sturgis)

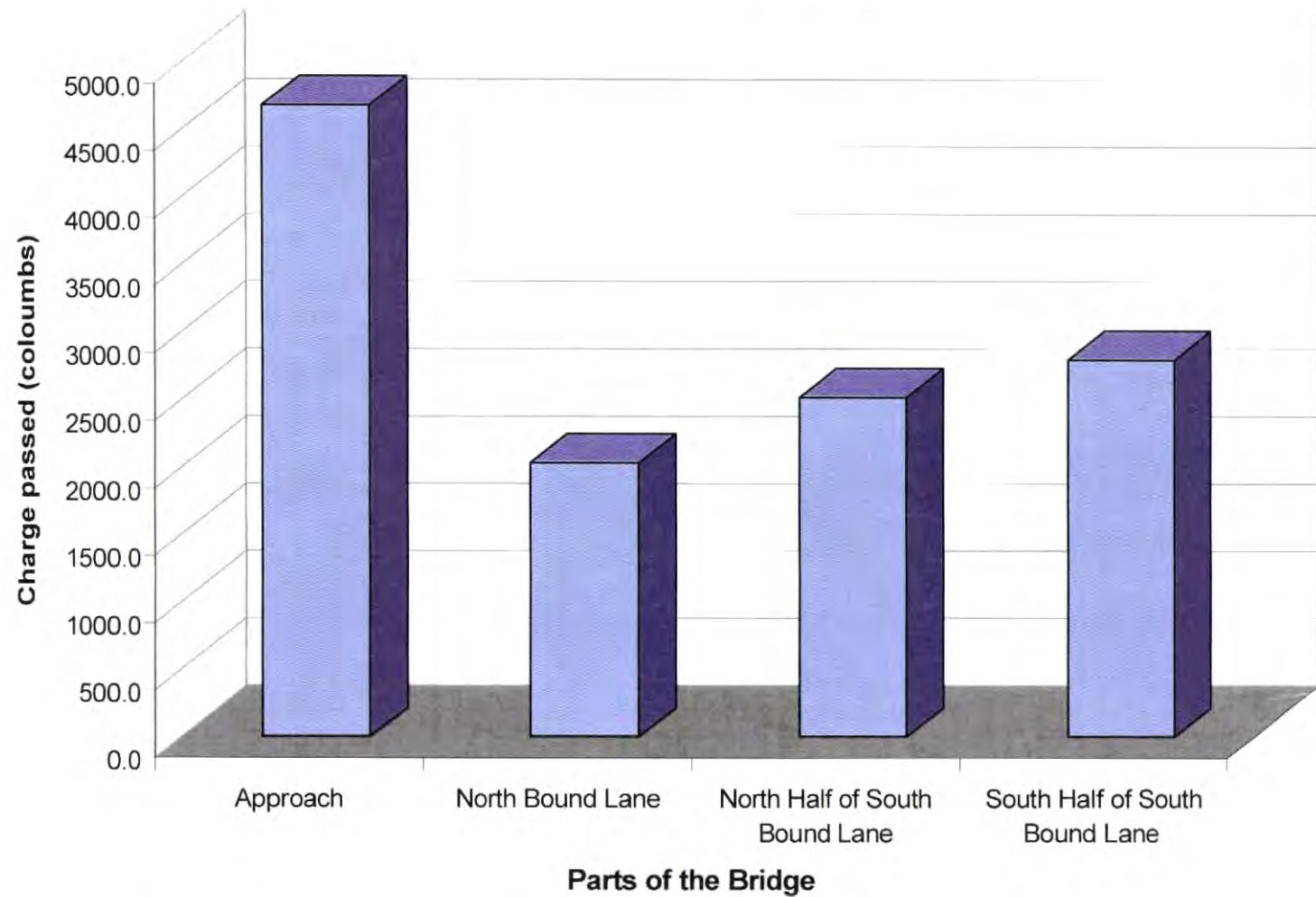


Fig 3.2: Comparison of the Total Charge Passed Through Cores from Various Locations on the Bridge at Exit 212, I 90 (Vivian)

Research Task 4: Determine the density of whitetopping and deck overlay concrete from the cores provided by the SDDOT.

All the core samples obtained from the field used for the rapid chloride permeability test were also used to determine the density. A 50.8 mm (2 in.) portion of the cores was cut using a Hillquist rock saw. This portion was marked with the same number as that on the parent core sample immediately after cutting. The 50.8 mm (2 in.) portion of the core was carefully washed and air dried. The dimensions of the core specimen were taken using a vernier caliper with a least count of 0.025 mm (0.001 in.). The average of three readings for the diameter and three readings for the height were obtained. The weight of these specimens was recorded to the nearest 0.01 lb. The density of these samples was then determined by the ratio of the weight to the volume. Table 4.1 gives the values of the densities for the core samples tested from the Exit 32, I 90 (Sturgis) and the Table 4.2 gives the densities of the core samples from Exit 212, I 90 (Vivian).

Density of overlying NMFRC at Exit 32, I 90 (Sturgis)

The density of the following cores were determined: WD1 (approach), WD2 and WD5 from the West bound driving lane; WP2 and WP4 from the West bound passing lane; ED1 (approach), ED2, ED4 and ED6 (approach) from the East bound driving lane and EP2 and EP5 from the East bound passing lane.

The density of the sample from the approach (average of 3 readings) was found to be less than that from the bridge (average of 8 readings). The average density obtained from the samples from the bridge, from all the four lanes, was 2194.74 Kg/m^3 (137 lbs/ft^3) and the average density obtained from the approaches was 2082.6 Kg/m^3 (134 lbs/ft^3).

Density of overlying NMFRC at Exit 212, I 90 (Vivian)

The density of the following cores were determined: VS1, VS3 and VN9 from the Whitetopping Approach; VS4, VS5 and VS7 from the North half of the South bound lane with fibers at the rate of 11.9 Kg/m^3 (20 lbs/yd^3); VS11, VS12 and VS13 from the South

Table 4.1: Density of Overlying NMFC at Exit 32,I 90 (Sturgis)

Core No.	Diamater			Avg.	Height			Avg.	Vol. (in ³)	Wt. (lbs)	Density (lbs/ft ³)
	Dia 1	Dia 2	Dia 3	Dia.	Ht 1	Ht 2	Ht 3	Height			
	(in)	(in)	(in)	(in)	(in)	(in)	(in)	(in)			
West Bound Driving Lane- Fiber Content=25lbs/cu.yd											
WD1*	3.999	4.007	3.997	4.001	2.016	2.038	2.012	2.022	25.422	1.95	132.6
WD2	3.998	3.998	3.997	3.998	2.067	2.095	2.061	2.074	26.036	2.02	134.3
WD5	3.999	3.998	3.993	3.997	2.002	2.003	2.027	2.011	25.225	2.01	137.6
										Average	134.8
										SD	2.5
West Bound Passing Lane- Fiber Content=25lbs/cu.yd											
WP2	3.998	3.996	4.018	4.004	2.075	2.117	2.037	2.076	26.144	2.07	136.9
WP4	3.999	4.005	4.000	4.001	1.999	1.950	1.990	1.980	24.894	1.98	137.4
										Average	137.1
										SD	0.3
East Bound Driving Lane- Fiber Content=25lbs/cu.yd											
ED1*	3.998	3.999	4.007	4.001	2.006	2.000	2.004	2.003	25.191	2.04	139.7
ED2	3.998	3.995	3.996	3.996	1.994	1.996	1.998	1.996	25.037	2.03	140.2
ED4	4.000	3.999	3.999	3.999	1.997	1.996	1.983	1.992	25.024	2.00	137.9
ED6*	4.003	4.002	4.005	4.003	1.999	1.965	1.998	1.987	25.015	1.88	129.6
										Average	135.9
										SD	5.6
East Bound Passing Lane- Fiber Content=25lbs/cu.yd											
EP2	4.010	3.999	3.998	4.002	2.000	1.981	2.037	2.006	25.238	1.94	132.7
EP5	3.999	3.996	4.005	4.000	1.932	1.900	1.945	1.926	24.199	1.94	138.7
										Average	135.7
										SD	4.3

*Cores from Approach

Average Density Value for the samples from the bridge deck 137.0 (lbs/ft³)Average Density Value for the samples from the approach 134.0 (lbs/ft³)

Table 4.2: Density of Overlying NMFRC at Exit 212, I 90 (Vivian)

Core No.	Diameter			Avg.	Height			Avg.	Vol. (in ³)	Wt. (lbs)	Density (lbs/ft ³)
	Dia 1	Dia 2	Dia 3	Dia.	Ht 1	Ht 2	Ht 3	Height			
	(in)	(in)	(in)	(in)	(in)	(in)	(in)	(in)			
Approach- Fiber Content=25lbs/cu.yd											
VS1	3.996	3.999	4.000	3.998	2.000	1.990	1.965	1.985	24.924	1.89	131.0
VS3	4.005	3.999	4.000	4.001	1.950	1.974	1.948	1.957	24.613	1.96	137.7
VN9	3.997	3.985	3.990	3.991	2.020	1.999	2.025	2.015	25.199	2.03	139.3
										Average	136.0
										SD	4.4
South Bound Lane - Fiber Content = 20lbs/cu.yd.											
VS4	3.990	3.995	3.999	3.995	1.995	2.024	2.043	2.021	25.325	2.07	140.9
VS5	3.996	3.990	3.990	3.992	2.060	2.095	2.060	2.072	25.929	2.12	141.4
VS7	3.990	3.995	3.993	3.993	2.095	2.115	2.165	2.125	26.606	2.19	142.1
										Average	141.5
										SD	0.6
South Bound Lane - Fiber Content = 25lbs/cu.yd.											
VS11	4.000	3.998	3.996	3.998	2.120	2.123	2.125	2.123	26.648	2.14	139.0
VS12	3.999	4.000	4.000	4.000	2.040	2.045	2.095	2.060	25.882	2.10	140.1
VS13	4.000	3.998	4.000	3.999	2.035	2.075	2.035	2.048	25.732	2.06	138.6
										Average	139.2
										SD	0.8
North Bound Lane LSDC											
VN1	3.999	3.990	3.995	3.995	2.015	1.998	2.000	2.004	25.120	2.02	139.2
VN2	4.006	3.992	3.994	3.997	1.995	1.981	1.974	1.983	24.890	1.90	131.8
VN6	4.040	4.035	4.035	4.037	1.899	1.925	1.937	1.920	24.576	1.99	139.6
										Average	136.9
										SD	4.4

half of the South bound lane with fibers at the rate of 14.8 Kg/m^3 (25 lbs/yd³); and VN1, VN2 and VN6 form the North bound lane comprising of plain concrete only.

The average density values obtained were 2178.72, 2266.83, 2229.98 and 2193.14 Kg/m^3 (136.0, 141.5, 139.2 and 136.9 lbs/ft³) from the approach, North half of the South bound lane, South half of the South bound lane and the North bound lane respectively. The concrete at the section of the bridge with fiber at 11.9 Kg/m^3 (20 lbs/yd³) was the densest of all concretes.

Research Task 5: Determine the bond strength of the bridge deck overlay concrete to the original deck from the cores provided.

The determination of bond strength of the bridge deck overlay concrete included two methods: 1) field bond tests on 50.8 mm (2 in.) cores using FHWA's bond test equipment, and 2) laboratory bond tests on 101.6 mm (4 in.) core samples obtained from the bridge deck.

Determination of field bond strength using the pull-off tester.

Bond test procedure

The following test procedure was used in the determination of the bond strength of bridge deck overlays in the field:

1. The core locations were identified such that they represent samples of the bridge deck and the approach road concretes. Care was taken to avoid selecting core locations on any overlay cracks and depressed areas. Also a cover meter was used to locate the core locations such that they did not cut into the underlying reinforcement.
2. The surface of the pavement was scarified, (chipped with a hammer, smoothed with a concrete carbide abrasive and cleaned with a wire brush) prior to the coring. This was done to ensure that all the surface defects like swelling, carbonation etc. were removed which in turn aids in the good bonding of the surface with epoxy.
3. A mark was made on the core bit which was about 0.5 to 1 in. greater than the actual depth of coring required. This mark allowed the coring operator to know when he had

reached the required depth of coring. Care was taken during the coring operations to keep the core bit exactly vertical and also not to apply any sort of lateral pressure on the cores, which may result in the breakage of the cores.

4. After the coring operation, the core location was thoroughly cleaned with compressed air. All the concrete dust, pieces of rock and moisture was removed from the core rim.
5. The core location was marked on the pavement and its position with respect to a permanent benchmark was measured and recorded.
6. The cored locations were allowed to dry for about half-hour. During this time, the bond disks were cleaned to ensure that no oil content was present on the disks.
7. The bond disks were placed close to the core locations and the epoxy was also placed in the open to allow them to reach the same ambient temperature.
8. A small quantity of epoxy was discarded initially because it may not be mixed properly.
9. Before applying epoxy on the cores, a small test lump of epoxy was placed next to the core on the bridge deck. This allowed us to determine when the epoxy was cured.
10. The core locations were cleaned very gently immediately before applying the epoxy with a wire brush and the epoxy was placed. A sufficient quantity of epoxy was placed on the core such that it would adequately cover the top of the core/disk interface when the aluminum disk was placed on it.
11. The bond disk was placed on the core such that the hole for the pull-pin face up and was gently pressed onto the core until it was finally seated and centered.
12. The epoxy was allowed to cure for 2 hours. The engineers from the Federal Highway Administration supplied the epoxy. The properties of the epoxy are give below:

Pot life : 7-9 mins.

Initial set : 30-60 mins.

Intial cure : 2-3 hrs.

Final cure : 12-24 hrs.

Shelf life : 2 years

Requires dry surface, 45°F and above temperature

13. After the curing time had elapsed, the test lump of epoxy was checked for its hardness to ensure the epoxy had cured.
14. The pull-pin was screwed into the disk. The bond test equipment was positioned on the disk. By adjusting the notched wheel on the top, the head of the pull-pin was fixed into the socket at the base of the central axis of the equipment. It was ensured that the crank was fully turned in the counter-clockwise direction till it stops. The equipment was leveled by adjusting the three legs. Once it was leveled, the legs were locked by tightening the black screw on top of each leg, so that no further disturbances occur in the leveling. It was very important that the jig was exactly perpendicular to the pavement surface, so that it pulled the core axially with out any significant eccentricities.
15. The gage was set to zero by pushing the button located on the left of the gage and turning the little knob on the upper part of the gage simultaneously.
16. All the play between the head of the pull-pin and the jack was removed by rotating the notched wheel on the top of the equipment clockwise until the pointer in the gage started moving.
17. The core was loaded by turning the crank clockwise at a rate of 1 KN per 25 seconds and the maximum load was recorded at the failure of the core.
18. The crank was rotated back until it stopped.
19. The core diameter was measured and all the details about the failure surface and the qualities of both overlying and underlying concretes were recorded.
20. The bond tensile strength is the load applied divided by the cross sectional area of the fractured plane.

The photographs in Appendix C clearly show each step discussed in the above bond testing procedure.

Field bond testing on the Exit 32, I 90 (Sturgis)

The bond testing on the Exit 32, I 90 (Sturgis) was carried out on the July 8, 1999.

The procedure described above was followed to determine the bond strength. The Figures A1 and A3 in Appendix A, show the details of the location of the cores for the bond test in the West bound and the East bound lanes respectively. Tables 5.2 and 5.3 show the results of the field bond test on the West and the East bound lanes respectively.

Observations for Field Bond Tests at Exit 32

The bond test results from the West bound passing lane indicated that the in-place underlying concrete was weaker than both the bond and the overlying fiber reinforced concrete. All the eight cores, which were tested, had failed in the underlying concrete below and within 6mm (0.25 in.) from the interface. This might be attributed to the fact that the milling and/or sand blasting operations during the overlay surface preparation might have damaged the surface of the underlying concrete. It is also possible that enough material may not have been removed when it was scarified. Two types of causes for failure were noticed when the fractured cores were examined after the bond test. One was due to the lack of bond between the coarse aggregates and the cement mortar in the underlying concrete and the other due to the failure of the coarse aggregates. Three out of the 8 cores tested showed the lack of bond between the coarse aggregate and the cement mortar (W2, W3 and W5), another 3 showed the failure of the coarse aggregates (W1, W4 and W8) and the remaining 2 cores showed a mixed failure (W6 and W7). The bond between the NMFRC overlay and the underlying old concrete never failed. It was the underlying concrete that failed.

On further analysis of the test results, it was found that the strength of the bond between the coarse aggregates and the cement mortar was less than the strength of the coarse aggregates. This was evident from the low tensile strength obtained for the cores, which failed due to the lack of bond between the coarse aggregates and the cement mortar in the underlying concrete. It was also observed that the bond strengths on the bridge were consistently lower than the bond strength on the approach, though the failure types of all the cores were similar.

The results from the East bound passing lane also indicated that the weakest portions of the concrete cores were the portions immediately below the surface of the underlying old concrete. All the cores failed in the underlying concrete within about

19mm (0.5 in.) from the interface. The causes for failure were again found to be the lack of bond between coarse aggregates and cement mortar and the failure of the coarse aggregates in the existing concrete. It was also found that the cement mortar of the underlying concrete was weak and could be removed with a fingernail.

Another observation made from the investigation of both the 50.8mm (2 in.) and the 101.6 mm (4 in.) cores was that the fiber reinforced overlay was not consolidated properly. This was evident from the numerous voids of various sizes present in all the cores. NMFRC apparently required more consolidation.

Sample Calculation

Core no. W1

Max load measured on field = 1.5 KN

Average diameter = $(2.200 + 2.199 + 2.212) / 3 = 2.204$ in.

Cross section area = $3.14 \times (\text{Avg. dia.})^2 / 4 = 3.14 \times (2.204)^2 / 4 = 3.812 \text{ in}^2$.

Max load = $(1.5 \times 1000) / 4.45 = 337.08 \text{ lb}$

Tensile stress = $337.08 / 3.812 = \underline{\underline{88 \text{ psi}}}$

Field bond testing on the Exit 212, I 90 (Vivian)

The bond testing on the Exit 212, I 90 (Vivian) was carried out on July 21, 1999. The procedure described above was followed to determine the bond strength. Figure A6 in Appendix A, shows the details of the location of the cores for the bond test in the North and South bound lanes. Tables 5.7 and 5.8 show the results of the bond test on the South and the North bound lanes respectively.

Observations for Field Bond Tests at Exit 212

The observations of the bond test results from this bridge were similar to those recorded in the bridge at Sturgis. The underlying old concrete was found to be weaker than both the bond between the old concrete and the NMFRC overlay and the NMFRC overlay itself. The cores in the approach road with whitetopping failed at the asphalt layer

due to asphalt failure and it can be seen that the bond tensile stresses of these cores are much lesser than the rest as expected.

All but two cores on the South bound lane failed in the underlying old concrete below and within 4.8 mm (0.19 in.) from the interface. This might be attributed to the fact that the milling and/or sand blasting operations during the surface preparation might have damaged the surface of the underlying concrete. The reasons for the failure of the cores were found to be due to 1) the failure of the bond between the coarse aggregates and the cement mortar in the old concrete, 2) the failure of the coarse aggregates, 3) the failure of the asphalt (in the approach), and 4) due to some percentage of bond failure between the underlying old concrete and the NMFRC overlay (in two cores). The lack of bond between the coarse aggregates and the cement mortar in the old concrete was found to be a predominant reason for the failure. Out of the 8 (BS 3-10) cores tested on the bridge deck, 2 cores (BS3, BS9) failed due to lack of bond, 1 core (BS4) failed due to the failure in the coarse aggregates, 3 cores (BS5, BS6, BS8) failed due to both the lack of bond between the coarse aggregates and the cement mortar and due to the failure of the coarse aggregates. In the remaining 2 cores (BS7, BS10) it was observed that less than 50% of the failure was due to the failure of the bond between the old underlying concrete and the NMFRC overlay with the remainder of the failure due to the lack of bond between the coarse aggregates and the cement mortar in the underlying concrete.

Not much of a difference was observed in the tension stress results from the North and South halves of the bridge with different fiber contents. This may be explained by the fact that the failure was mostly in the underlying concrete and the variation in the fiber content on the overlay did not have any effect on it.

It was observed that the NMFRC overlay was not properly consolidated which was evident by the presence of voids (minor honey-combing) in all the cores. Obviously NMFRC needed more consolidation than LSDC. The surface was not fully leveled before the pouring of the overlay concrete. This was evident by the varying depths of the overlay seen on the surface of the cores.

Similar results were obtained from the bond tests conducted on the North bound lane. Seven 50.8 mm (2 in) cores were drilled with 2 located on the approach and 5 on the plain concrete in the bridge deck. Two cores (BN5, BN6) on the approach failed during

the removal of the coring jig. The results of the tests were comparable with the results obtained from the South bound lane. All the five cores tested on the deck failed due to the lack of bond between the coarse aggregates and the cement mortar in the old concrete. The core on the approach (BN6) failed due to the failure in the asphalt. The lack of proper consolidation of the whitetopping was again evident from the presence of voids on the surface of the cores.

Determination of laboratory bond strength

The 101.6 mm (4 in.) cores from the bridge deck were packed, labeled and transported to the lab. The cores were cleaned and its dimensions were measured. The average of 3 readings was taken for the diameter, average depth of overlay and the total depth of core. Tables 5.4 and 5.5 give the details of the measurements of the cores from the West and East bound lanes of the bridge at Exit 32, I 90 (Sturgis), respectively. Tables 5.9 and 5.10 give the details of dimensions for cores from the South and North bound lanes of the bridge at Exit 212, I 90 (Vivian), respectively.

The following cores were selected for the bond test in the lab:

Bridge at Exit 32, I 90 (Sturgis)

WD3, WD4 and WD6 form the West bound driving lane and WP3, WP5 and WP6 from the West bound passing lane.

ED3 and ED5 from the East bound driving lane and EP1, EP3, EP4 and EP6 from the East bound passing lane.

Bridge at Exit 212, I 90 (Vivian)

VS2, VN7 and VN8 from the North approach (whitetopping).

VS6, VS8 and VS9 form the North half (NMFRC, with fibers at the rate of 11.9 Kg/m³ - 20 lbs/yd³) of the South bound lane.

VS10, VS14 and VS15 from the South half (NMFRC, with fibers at the rate of 14.8 Kg/m³ -25 lbs/yd³) of the South bound lane.

Bond test procedure

The following test procedure was used to determine the bond strength in the lab:

1. The designated cores for the bond testing were marked very clearly and its location and dimensions were recorded.
2. Thin layers from the top and bottom surfaces of the core were cut, to make the surface level and smooth for the plate to stick on it. Care was taken to cut the minimum thickness from both ends of the core and also to maintain the cut surface parallel and at right angles to the core length. The cutting was done using a Hillquist rock saw.
3. The cores were washed with clean water to remove all the dust particles and air-dried.
4. The apparatus used for the bond test was a pair of plate and rod assemblies with a nut and a washer at the end of each threaded rod. A mild steel plate was used with a thickness 6.35 mm (0.25 in.) and diameter 101.6 mm (4 in.). A mild steel rod of diameter 19.05 mm (0.75 in.) and 304.8 mm (12 in.) long with one end threaded was welded to the center of the plate. The length of thread was 76.2 mm (3 in.). The angle between the plate and rod was maintained at 90° exactly so that there was no eccentricity in the loading.
5. The concrete surface and the metal plate surface were scarified with a concrete carbide abrasive to make the surface rough for the epoxy to hold well. The surfaces were then dusted with a jet of compressed air and cleaned with acetone to remove any oil or grease particles.
6. The epoxy used was POLY CARB, Mark-198, fast setting moisture insensitive epoxy grout. A sufficient amount of epoxy was placed on the core such that it would coat the entire surface between the core and the plate.
7. The metal plate was placed on the core and was gently pressed onto the core until it was finally seated and centered. The epoxy was allowed to cure for 24 hours.
8. The core was supported on a bench vise with the metal rod of the already epoxied assembly in the vise and the top of the concrete surface exposed. The concrete surface was maintained horizontal with a level and the same procedure was followed to stick the metal plate. The assembly was left undisturbed for 24 hours.

9. After the epoxy had cured, the assembly was loaded on a Tinius Olsen machine, on the tension side. Two plates with a central hole of 25.4mm (1in.) diameter were fixed on both the loading and stationary ends of the machine. The assembled specimen was held in between the loading and stationary ends with a nut and washer arrangement, with the metal rod on both ends passing through the central holes in the plate. The system of plates was used instead of a chuck to grip the rods, so as to allow any misalignment of the assembled specimen such that the loading was axial instead of eccentric.
10. The specimen was loaded until failure and the maximum load was recorded. All the observations regarding the type and cause for failure and the cross sectional dimension were recorded. An average of three readings was found for the diameter and the cross sectional area was calculated.
11. The bond tensile strength was determined by dividing the load by the cross sectional area of the fractured plane.

Laboratory Bond testing of cores from the bridge at Exit 32, I 90 (Sturgis)

The laboratory bond test on the above-mentioned cores was done following the above-mentioned procedure. Eight cores were tested in the lab which were obtained from the West bound lanes of the bridge at Exit 32, I 90 (Sturgis). Out of the 8 cores, 2 cores (WD3 and WP5) exhibited failure of coarse aggregates and the fracture in the remaining 4 cores (WD4, WD6, WP3 and WP6) was due to the lack of bond between the cement mortar and the coarse aggregates. The cores from the approach (WD6 and WP6) showed higher tensile strength similar to the trend of results obtained from the field bond test.

The Laboratory bond test of the specimens from the East bound lanes also showed similar results. Out of the 6 cores tested, 4 (ED3, ED5, EP1 and EP4) showed that the lack of sufficient bond between the coarse aggregates and cement mortar was the main reason for the fracture of the underlying concrete, 1 core (EP6) failed due to the failure of coarse aggregate in the underlying concrete and the remaining specimen (EP3) failed due to the failure of the old cement mortar in the underlying concrete. None of the cores failed in the overlay region nor at the bond between the overlay concrete and the

underlying concrete. The cores from the approach (EP1 and EP6) again showed higher bond strength.

Laboratory Bond testing of cores from the bridge at Exit 212, I 90 (Vivian)

The laboratory bond test of the cores from the bridge at Exit 212, I 90 (Vivian) was done as per the procedure discussed above. Three specimens each were tested from each part of the bridge. All 3 cores (VS2, VN7 and VN8) from the North approach to the bridge failed due to the failure of the asphalt. Out of the 3 cores tested from the North half of the South bound lane, 2 cores (VS8 and VS9) failed due to the failure of coarse aggregates in the old concrete and 1 (VS6) failed due to the failure of the old cement mortar. All the cores tested from the South half of the South bound lane and the North Bound lane failed due to the failure of the coarse aggregates in the old concrete. The overlay concrete never failed and neither did the bond between the overlay and the underlying concrete fail. These results indicate that the underlying concrete was weaker than the bond strength between the two layers of concrete and the strength of the overlay itself.

Comparison of lab and field bond test results

The results obtained from the field and the lab bond testing from both the bridges on I 90 at Exit 32 (Sturgis) and at Exit 212 (Vivian) are shown in Table 5.15 and Table 5.16 respectively. It can be seen that the results were comparable, keeping in mind the fact that the number of specimens for the lab test was less than that of the field test. The results are expected to converge much more, with more number of specimens. The difference between the field and lab tests varied from a minimum of 4 to a maximum of 28 psi, except for the result from the North approach, which varied up to 77 psi. Since the failure criterion for all the cores from the North Approach (both field and lab) to the bridge at Exit 212 was the failure of the asphalt, the difference in the result could be explained. In these cores the tensile strength of the asphalt was the governing factor, which could change with temperature and moisture content. The tensile bond strength

obtained from the field (16 psi) was found to be much less than the strength obtained from the laboratory (93 psi). It is therefore inferred that the field result was less due to the higher ambient temperature during the test. The pavement was exposed to direct sunlight throughout the day, which might have caused melting of a few inches of asphalt from the surface. This might explain the less tensile stress obtained in the field test.

Table 5.1: Details of the Core Numbering at Exit 32, I 90 (Sturgis)

Core Number	Diameter and Location
W 1-8	2" cores on West bound Passing lane for field Bond Test
E 1-6	2" cores on East bound Passing lane for field Bond Test
WD 1-6	4" cores on West bound Driving Lane
WP 1-6	4" cores on West bound Passing Lane
ED 1-6	4" cores on East bound Driving Lane
EP 1-6	4" cores on East bound Passing Lane

Table 5.2: Results of Field Bond Test on the West bound Passing Lane at Exit 32, I 90 (Sturgis)

Core No.	Max. Load (KN)	Diameter			Avg. Dia (in)	C/S Area (in ²)	Avg. Depth of Overlay (in)	Max. Load (lb)	Tensile Stress (psi)	Remarks
		Dia 1 (in)	Dia 2 (in)	Dia 3 (in)						
W1	1.50	2.200	2.199	2.21	2.204	3.812	2.750	337.08	88	The fracture was at an average depth of 0.187 in. below the overlay, the failure of the coarse aggregate was very evident with about 5 large pieces of broken aggregates in the cross section
W2	1.00	2.298	2.200	2.21	2.234	3.919	2.875	224.72	57	The fracture was at an average depth of 0.125 in. below the overlay, the lack of bond between the coarse aggregates and the cement mortar in the old concrete was evident
W3	1.00	2.195	2.198	2.19	2.195	3.783	2.813	224.72	59	The fracture was at an average depth of 0.312 in. below the overlay, the lack of bond between the coarse aggregates and the cement mortar in the old concrete was evident
W4	1.25	2.192	2.199	2.2	2.198	3.794	2.000	280.90	74	The fracture was at an average depth of 0.187 in. below the overlay, almost all the aggregate in the cross-section had failed
W5		2.206	2.207	2.200	2.204	3.814	2.562			The core broke during the coring operation and therefore the bond test was not conducted, however it was found that the bond between the coarse aggregates and the cement mortar in the old concrete had failed
W6	2.00	2.199	2.202	2.2	2.202	3.805	3.125	449.44	118	The fracture was at an average depth of 0.125 in. below the overlay, it was a mixed failure, both due to the failure of coarse aggregate and the lack of bond between the cement mortar and the coarse aggregate
W7	2.25	2.205	2.203	2.210	2.206	3.820	2.187	505.62	132	The fracture was at an average depth of 0.125 in. below the overlay, this was again a mixed failure
W8	2.00	2.205	2.197	2.2	2.202	3.806	1.625	449.44	118	The fracture was at an average depth of 0.187 in. below the overlay, the failure of the coarse aggregate was very evident in the cross section with large pieces of broken aggregates

Note: 1. There were voids in all the cores, which indicated the lack of consolidation of the fiber reinforced concrete overlay.

2. The depth of overlay is the average of three readings.

3. A 50 KN pull-off tester with a least count of 0.5 KN was used.

4. It was evident that the weakest portion in the concrete cores were the portion immediately below the overlay surface, this might be due to the fact that the milling or sand blasting operations during the surface preparation might have damaged the surface of the existing concrete.

5. W8 and W7 are the cores from the west and the east approach to the bridge respectively.

6. The locations of the cores can be seen in Figure A1.

Table 5.3: Results of Field Bond Test on the East bound Passing Lane at Exit 32, I 90 (Sturgis)

Core No.	Max. Load (KN)	Diameter			Avg. Dia (in)	C/S Area (in ²)	Avg. Depth of Overlay (in)	Max. Load (lb)	Tensile Stress (psi)	Remarks
		Dia 1 (in)	Dia 2 (in)	Dia 3 (in)						
E1	2.70	2.218	2.209	2.21	2.211	3.839	2.750	606.74	158	The fracture was at an average depth of 0.125 in. below the overlay, the lack of bond between the coarse aggregates and the cement mortar in the old concrete was evident
E2	1.30	2.219	2.216	2.21	2.214	3.847	2.312	292.13	76	The fracture was at an average depth of 0.25 in. below the overlay, the lack of bond between the coarse aggregates and the cement mortar in the old concrete was evident
E3	1.70	2.210	2.212	2.21	2.212	3.841	1.937	382.02	99	The fracture was at an average depth of 0.187 in. below the overlay, the failure of the coarse aggregate was evident and was through its plane of formation, a vertical crack was seen in the underlying concrete, but was not present in the FRC overlay
E4	1.20	2.221	2.217	2.21	2.216	3.856	2.250	269.66	70	The fracture was at an average depth of 0.250 in. below the overlay, it was a mixed failure, both due to the failure of coarse aggregate and the lack of bond between the cement mortar and the coarse aggregate
E5	0.70	2.213	2.204	2.200	2.206	3.819	2.625	157.30	41	The fracture was at an average depth of 0.125 in. below the overlay, it was a mixed failure, both due to the failure of coarse aggregate and the lack of bond between the cement mortar and the coarse aggregate
E6	0.70	2.204	2.195	2.17	2.191	3.768	2.937	157.30	42	The fracture was at an average depth of 1in. below the overlay, the failure was mainly due to the lack of bond between the coarse aggregate and the cement mortar, it was evident from the void in the bottom portion of the core just above the reinforcement, that the underlying concrete was poorly consolidated around the dowel bars

Note: 1. There were voids in all the cores, which indicated the lack of consolidation of the fiber reinforced concrete overlay.

2. The depth of overlay is the average of three readings.

3. A 16 KN pull-off tester with a least count of 0.1 KN was used.

4. It was evident that the weakest portion in the concrete cores were the portion immediately below the overlay surface, this might be due to the fact that the milling or sand blasting operations during the surface preparation might have damaged the surface of the existing concrete.

5. E1 and E6 are the cores from the east and the west approach to the bridge respectively.

6. The locations of the cores can be seen in the Figure A3.

Table 5.4: Cores from the West Bound lane at Exit 32, I 90 (Sturgis) for Lab Tests

Lane	Core no.	Diameter			Avg. Dia (in)	Avg. Depth of Overlay (in)	Total Depth of Core (in)	Remarks
		Dia 1 (in)	Dia 2 (in)	Dia 3 (in)				
Driving Lane	WD1	4.004	4.002	4.006	4.004	3.250	11.375	Core location - on the East approach to the bridge, the average full depth of the underlying concrete was found to be 8.125 in.
	WD2	4.003	4.012	4.014	4.010	3.000	3.750	Core location - on the bridge deck
	WD3	3.998	4.002	4.004	4.001	3.000	6.375	Core location - on the bridge deck
	WD4	4.005	4.002	4.006	4.004	3.000	6.750	Core location - on the bridge deck
	WD5	3.998	4.005	3.993	3.999	3.500	6.125	Core location - on the bridge deck
	WD6	4.005	4.011	4.008	4.008	2.250	10.625	Core location - on the West approach to the bridge, the average full depth of the underlying concrete was found to be 8.400 in.
Passing lane	WP1	4.008	4.006	3.998	4.004	2.250	3.375	Core location - on the West approach to the bridge
	WP2	4.000	3.998	3.999	3.999	2.875	3.312	Core location - on the bridge deck
	WP3	4.033	4.007	3.999	4.013	2.000	3.250	Core location - on the bridge deck
	WP4	4.000	4.002	4.004	4.002	2.375	6.125	Core location - on the bridge deck
	WP5	4.004	4.004	4.006	4.005	2.875	6.375	Core location - on the bridge deck
	WP6	4.002	4.001	4.006	4.003	1.500	9.937	Core location - on the East approach to the bridge, the average full depth of the underlying concrete was found to be 8.437 in.

- Note: 1. All the cores had voids in the overlay concrete which indicates the lack of good consolidation.
 2. The Average Depth of Overlay and the Total Depth of Core is the average of 3 readings.
 3. The locations of the cores can be seen in Figure A2.

Table 5.5: Cores from the East Bound lane at Exit 32, I 90 (Sturgis) for Lab Tests

Lane	Core no.	Diameter			Avg. Dia (in)	Avg. Depth of Overlay (in)	Total Depth of Core (in)	Remarks
		Dia 1 (in)	Dia 2 (in)	Dia 3 (in)				
Driving Lane	ED1	4.010	4.009	4.014	4.011	2.500	10.750	Core location - on the West approach to the bridge, the average full depth of the underlying concrete was found to be 8.250 in.
	ED2	4.002	4.009	4.006	4.006	2.750	4.875	Core location - on the bridge deck
	ED3	4.002	4.003	4.006	4.004	3.000	7.250	Core location - on the bridge deck
	ED4	4.005	3.999	4.008	4.004	2.250	6.500	Core location - on the bridge deck
	ED5	4.006	4.010	4.011	4.009	2.250	6.375	Core location - on the bridge deck
	ED6	4.005	4.006	4.006	4.006	2.562	11.375	Core location - on the East approach to the bridge, the average full depth of the underlying concrete was found to be 8.813 in.
Passing lane	EP1	4.002	4.008	4.007	4.006	1.750	8.875	Core location - on the East approach to the bridge
	EP2	3.997	4.008	4.009	4.005	2.375	8.875	Core location - on the bridge deck, the average full depth of the underlying concrete was found to be 6.500 in., a hole was left on the bridge deck after coring
	EP3	4.004	3.998	4.006	4.003	2.125	6.750	Core location - on the bridge deck, a piece of reinforcement bar was seen
	EP4	4.011	4.012	4.007	4.010	2.250	8.187	Core location - on the bridge deck, the average full depth of the underlying concrete was found to be 5.937 in., a hole was left on the bridge deck after coring
	EP5	4.004	4.004	4.006	4.005	2.750	5.875	Core location - on the bridge deck, a piece of reinforcement bar was seen
	EP6	3.999	3.999	4.004	4.001	2.000	11.062	Core location - on the West approach to the bridge, the average full depth of the underlying concrete was found to be 9.062 in.

Note: 1. All the cores had voids in the overlay concrete which indicates the lack of good consolidation.

2. The Average Depth of Overlay and the Total Depth of Core is the average of 3 readings.

3. The locations of the cores can be seen in Figure A4.

Table 5.6: Details of the Core Numbering at Exit 212, I 90 (Vivian)

Core Number	Diameter and Location
BS 1-10	2" cores on the South Bound lane
BN 1-7	2" cores on the North Bound lane
VS 1-15	4" cores on the South bound lane
VN 1-9	4" cores on the North bound lane

Table 5.7: Results of Field Bond Test on the South Bound Lane at Exit 212, I 90 (Vivian)

Core No.	Max. Load (KN)	Diameter			Avg. Dia (in)	C/S Area (in ²)	Avg. Depth of Overlay (in)	Max. Load (lb)	Tensile Stress (psi)	Remarks
		Dia 1 (in)	Dia 2 (in)	Dia 3 (in)						
BS1	0.50	2.211	2.217	2.207	2.212	3.840	2.687	112.36	29	The fracture was at an average depth of 3.75 in. below the interface, the asphalt failure was evident, the core was taken from the North approach to the bridge
BS2	0.10	2.208	2.209	2.215	2.211	3.836	3.125	22.47	6	The fracture was at an average depth of 0.125 in. below the interface, though the fracture was just near the interface of the whitetopping and the asphalt, the asphalt failure was evident, the core was taken from the North approach to the bridge
BS3	2.60	2.222	2.224	2.235	2.227	3.893	2.625	584.27	150	The fracture was at an average depth of 1.687 in. below the interface, in the old concrete, the fracture was mainly due to the lack of bond between the coarse aggregates and the cement mortar
BS4	2.20	2.217	2.213	2.219	2.216	3.856	2.625	494.38	128	The fracture was at an average depth of 0.062 in. below the interface in the old concrete, the reason for the fracture was the failure of the coarse aggregates, lack of proper consolidation of the overlay was evident from the void of about 0.75 in. on the surface
BS5	1.30	2.224	2.215	2.224	2.221	3.872	3.750	292.13	75	The fracture was at an average depth of 0.75 in. below the interface, the lack of bond between the coarse aggregates and the cement mortar and the failure of the coarse aggregates were the reason for the fracture, the lack of proper surface preparation was evident by the varying depth of the underlying concrete, lack of proper consolidation of the overlay was evident from the void of about 2 in. long and 0.5 in. wide in which the fibers were not bonded with the concrete
BS6	1.80	2.220	2.224	2.224	2.223	3.878	2.250	404.49	104	The fracture was at an average depth of 0.125 in. below the interface, in the old concrete, both the failure of the coarse aggregates and the lack of bond between the coarse aggregates and the cement mortar can be attributed to the reasons for fracture
BS7	0.80	2.232	2.231	2.225	2.229	3.901	2.500	179.78	46	The fracture was at an average depth of 0.062 in. below the interface, the fracture was mainly due to the lack of bond between the coarse aggregates and the cement mortar in the old concrete, about 20% of the failure was at the interface

Contd..

Table 5.7: Results of Field Bond Test on the South Bound Lane on I 90, Exit 212, Contd..

Core No.	Max. Load (KN)	Diameter			Avg. Dia (in)	C/S Area (in ²)	Avg. Depth of Overlay (in)	Max. Load (lb)	Tensile Stress (psi)	Remarks
		Dia 1 (in)	Dia 2 (in)	Dia 3 (in)						
BS8	1.60	2.230	2.224	2.228	2.227	3.894	4.500	359.55	92	The fracture was at an average depth of 0.125 in. below the interface, a mixed failure due to both lack of bond between coarse aggregates and the cement mortar and the failure of coarse aggregates in the old concrete were the reasons for the fracture, considerable amount of blow holes on the core showed the lack of proper consolidation of the overlay
BS9	1.90	2.224	2.230	2.223	2.226	3.889	2.500	426.97	110	The fracture was at an average depth of 0.187 in. below the interface, the failure was mainly due to the lack of bond between the coarse aggregates and the cement mortar in the old concrete
BS10	3.00	2.224	2.230	2.225	2.226	3.891	4.750	674.16	173	Though the fracture was at the interface of the NMFRC and the old concrete, half of the cross section of the core appeared to have a bond failure between the NMFRC and the old concrete and the other half had a failure in the old concrete and it appeared that the lack of bond between coarse aggregates and the cement mortar was the reason for the failure, considerable amount of blow holes were present on the surface of the core which showed the lack of proper consolidation of the fiber reinforced concrete

- Note: 1. The depth of overlay and the depth of fracture is the average of three readings.
2. A 16KN pull-off tester with an least count of 0.1KN was used for all the cores except for the core no. BS10, for which a 50 KN pull-off tester with a least count of 0.5 KN was used.
3. It was evident that the weakest portion in the concrete cores was the portion immediately below the overlay surface, this might be due to the fact that the milling or sand blasting operations during the surface preparation might have damaged the surface of the existing concrete.
4. The locations of the cores can be seen in Figure A6.

Table 5.8: Results of Field Bond Test on the North Bound Lane at Exit 212, I 90 (Vivian)

Core No.	Max. Load (KN)	Diameter			Avg. Dia (in)	C/S Area (in ²)	Avg. Depth of Overlay (in)	Max. Load (lb)	Tensile Stress (psi)	Remarks
		Dia 1 (in)	Dia 2 (in)	Dia 3 (in)						
BN1	2.00	2.223	2.224	2.220	2.222	3.877	2.500	449.44	116	The fracture was at an average depth of 0.125 in. from the interface in the old concrete, the fracture was mainly due to the lack of bond between the coarse aggregates and the cement mortar, even though one piece of coarse aggregate was broken in the cross section of the core
BN2	2.00	2.312	2.218	2.223	2.251	3.978	2.375	449.44	113	The fracture was at an average depth of 0.187 in. from the interface the fracture was mainly due to the lack of bond between the coarse aggregates and the cement mortar in the old concrete
BN3	2.25	2.222	2.226	2.235	2.228	3.896	1.875	505.62	130	The fracture was at an average depth of 2.0 in. from the interface in the old concrete, the fracture was mainly due to the lack of bond between the coarse aggregates and the cement mortar
BN4	2.75	2.223	2.224	2.231	2.226	3.890	2.250	617.98	159	The fracture was at an average depth of 1.75 in. from the interface in the old concrete, the fracture was mainly due to the lack of bond between the coarse aggregates and the cement mortar
BN5		2.235	2.223	2.233	2.230	3.905	4.250			The core was fractured during the removal of the coring jig, the failure was at about 0.125 in. from the interface in the asphalt, the core was taken from the North approach to the bridge
BN6	0.25	2.225	2.231	2.236	2.231	3.906	4.000	56.18	14	The fracture was at an average depth of 1.75 in. from the interface in the asphalt, failure of the asphalt was the main reason for the fracture, the core was taken from the North approach to the bridge
BN7		2.228	2.232	2.231	2.230	3.905	4.125			The core was fractured during the removal of the coring jig, the failure was at about 2.5 in. from the interface in the asphalt, the core was taken from the North approach to the bridge

- Note:
1. The depth of overlay and the depth of fracture is the average of three readings.
 2. A 50 KN pull-off tester with a least count of 0.5 KN was used.
 3. It was evident that the weakest portion in the concrete cores was the portion immediately below the overlay surface, this might be due to the fact that the milling or sand blasting operations during the surface preparation might have damaged the surface of the existing concrete.
 4. The locations of the cores can be seen in Figure A6.

Table 5.9: Cores from the South Bound lane at Exit 212, I 90 (Vivian) for Lab Bond Test

Core Location	Core no.	Diameter			Avg. Dia (in)	Avg. Depth of Overlay (in)	Total Depth of Core (in)	Remarks
		Dia 1 (in)	Dia 2 (in)	Dia 3 (in)				
North Approach	VS1	3.995	3.997	3.995	3.996	2.750	10.625	The full depth of the asphalt was found to be 7.875 in.
	VS2	3.995	4.005	4.003	4.001	2.875	9.687	The full depth of the asphalt was found to be 6.812 in.
	VS3	4.004	3.996	4.003	4.001	3.000	9.437	The full depth of the asphalt was found to be 6.437 in.
North half of the Bridge	VS4	4.014	4.005	4.012	4.010	2.750	3.000	
	VS5	4.012	4.006	4.003	4.007	2.625	4.125	
	VS6	4.004	4.008	4.007	4.006	2.625	5.500	
	VS7	4.002	4.002	4.004	4.003	2.500	4.375	
	VS8	3.975	3.993	3.993	3.987	2.000	5.250	
	VS9	4.003	4.002	4.003	4.003	2.000	4.500	
South half of the Bridge	VS10	4.002	4.003	4.005	4.003	2.500	4.250	
	VS11	3.999	4.003	4.002	4.001	3.000	3.500	About 30% of the failure was in the overlay and the rest in the underlying concrete, the impression of reinforcement was also seen on the cut surface
	VS12	4.004	4.002	4.003	4.003	2.625	4.125	
	VS13	4.006	4.017	4.018	4.014	2.500	2.625	The fracture was not at the interface but in the underlying concrete
	VS14	4.002	3.998	3.997	3.999	4.500	6.000	Reinforcement was visible on the surface of the core and also the overlay was of varying thickness which showed the lack of proper surface preparation
	VS15	3.999	4.002	4.003	4.001	2.000	5.500	

Note: 1. All the cores had voids in the overlay concrete which indicated the lack of good consolidation.

2. The Average Depth of Overlay and the Total Depth of Core is the average of 3 readings.

3. The locations of the cores can be seen in Figure A7.

Table 5.10: Cores from the North Bound lane at Exit 212, I 90 (Vivian) for Lab Bond Test

Core Location	Core no.	Diameter			Avg. Dia (in)	Avg. Depth of Overlay (in)	Total Depth of Core (in)	Remarks
		Dia 1 (in)	Dia 2 (in)	Dia 3 (in)				
On the Bridge	VN1	3.998	4.002	4.004	4.001	2.625	5.625	
	VN2	4.006	4.009	4.011	4.009	3.750	6.250	
	VN3	4.003	4.002	4.009	4.005	2.500	6.500	
	VN4	4.003	4.006	3.995	4.001	2.500	6.750	
	VN5	4.004	4.008	4.010	4.007	1.750	7.250	
	VN6	4.010	4.008	4.007	4.008	2.325	6.750	
North Approach	VN7	4.008	4.009	4.008	4.008	5.250	8.825	The full depth of the asphalt was found to be 3.575 in.
	VN8	3.998	4.008	4.009	4.005	3.875	8.750	The full depth of the asphalt was found to be 4.875 in.
	VN9	4.002	4.008	4.006	4.005	4.125	10.125	The full depth of the asphalt was found to be 6.000 in.

- Note: 1. All the cores had voids in the overlay concrete which indicated the lack of good consolidation.
 2. The Average Depth of Overlay and the Total Depth of Core is the average of 3 readings.
 3. The locations of the cores can be seen in Figure A7.

Table 5.11: Results of Lab Bond Test on the Cores from West bound Lane at Exit 32, I 90 (Sturgis)

Core No.	Diameter			Avg. Dia (in)	C/S Area (in ²)	Max. Load (lb)	Tensile Stress (psi)	Remarks
	Dia 1 (in)	Dia 2 (in)	Dia 3 (in)					
Driving Lane								
WD3	4.010	4.008	4.002	4.007	12.602	681	54	The fracture was due to the failure in the underlying concrete, the failure of the coarse aggregate was evident form large pieces of broken aggregates in the cross section, mortar failure was also evident at some places
WD4	4.017	4.002	4.012	4.010	12.625	638	51	The underlying concrete failed and the failure was mainly due to the lack of bond between the coarse aggregates and the cement mortar in the old concrete, few small coarse aggregates also broke
WD6	4.002	4.011	4.006	4.006	12.600	1214	96	The underlying concrete failed and the failure was mainly due to the lack of bond between the coarse aggregates and the cement mortar in the old concrete, this core was obtained from approach
Passing Lane								
WP3	4.005	4.003	4.004	4.004	12.585	542	43	The underlying concrete failed and failure was mainly due to the lack of bond between the coarse aggregates and the cement mortar.
WP5	4.006	4.002	4.004	4.004	12.585	1099	87	The underlying concrete failed and failure was mainly due to the failure of coarse aggregates, large pieces of broken coarse aggregates were visible on the fractured surface
WP6	4.006	4.012	4.008	4.009	12.614	1659	132	The underlying concrete failed and failure was mainly due to the lack of bond between the coarse aggregate and the cement mortar in the underlying concrete, some pieces of broken coarse aggregate was also seen in the fracture surface, but not of much importance

- Note: 1. There were voids in all the cores, which indicated the lack of consolidation of the fiber reinforced concrete overlay.
 2. WD6 and WP6 were the cores from the west approach to the bridge.
 3. The locations of the cores can be seen in Figure A2.

Table 5.12: Results of Lab Bond Test on the Cores from East bound Lane at Exit 32, I 90 (Sturgis)

Core No.	Diameter			Avg. Dia (in)	C/S Area (in ²)	Max. Load (lb)	Tensile Stress (psi)	Remarks
	Dia 1 (in)	Dia 2 (in)	Dia 3 (in)					
Driving Lane								
ED3	4.008	4.006	4.012	4.009	12.614	654	52	The underlying concrete failed and failure was mainly due to the lack of bond between the coarse aggregate and the cement mortar in the underlying concrete, although some pieces of broken coarse aggregate was also seen in the fracture surface
ED5	4.003	4.002	3.999	4.001	12.568	875	70	The underlying concrete failed and failure was mainly due to the lack of bond between the coarse aggregate and the cement mortar in the underlying concrete
Passing Lane								
EP1	4.002	4.006	4.008	4.005	12.594	1373	109	The underlying concrete failed and failure was mainly due to the lack of bond between the coarse aggregates and the cement mortar.
EP3	4.003	4.005	3.999	4.002	12.575	551	44	The underlying concrete failed and failure was mainly due to the mortar failure, although 2 small pieces of broken coarse aggregates were also found in the fracture surface
EP4	4.011	4.009	4.012	4.011	12.627	1458	115	The underlying concrete failed and failure was mainly due to the lack of bond between the coarse aggregates and the cement mortar.
EP6	4.002	3.998	4.002	4.001	12.564	1242	99	The underlying concrete failed and failure was mainly due to the failure of the coarse aggregates since large pieces of broken coarse aggregates were found in the fracture surface

Note: 1. There were voids in all the cores, which indicated the lack of consolidation of the fiber reinforced concrete overlay.

2. EP1 and EP6 are the cores from the east and the west approach to the bridge respectively.

3. The locations of the cores can be seen in the Figure A4.

Table 5.13: Results of Lab Bond Test of the Cores from the Bridge at Exit 212, I 90 (Vivian)

Lane	Core Location	Core no.	Diameter			Avg. Dia (in)	C/S Area (in ²)	Max. Load (lb)	Tensile Stress (psi)	Remarks
			Dia 1 (in)	Dia 2 (in)	Dia 3 (in)					
South Bound	North Approach	VS2	3.985	3.897	4.005	3.962	12.325	1336	108	Asphalt failure
		VN7	3.994	4.003	4.003	4.000	12.560	1225	98	Asphalt failure
		VN8	4.005	3.986	4.002	3.998	12.545	900	72	Asphalt failure
	North half of the Bridge	VS6	4.003	4.006	4.008	4.006	12.596	1819	144	The underlying concrete failed and the failure was mainly due to the mortar failure, many pieces of coarse aggregates were exposed indicating a lack of bond between the coarse aggregate and the cement mortar
		VS8	3.995	4.003	3.998	3.999	12.552	1723	137	The underlying concrete failed and the failure was mainly due to the failure of coarse aggregates
		VS9	4.005	4.004	4.002	4.004	12.583	1680	134	The underlying concrete failed and the failure was mainly due to the failure of coarse aggregates
	South half of the Bridge	VS10	4.003	3.999	4.002	4.001	12.568	986	78	The underlying concrete failed and the failure was mainly due to the failure of coarse aggregates
		VS14	4.005	3.998	3.987	3.997	12.539	1041	83	The underlying concrete failed and the failure was mainly due to the failure of coarse aggregates, although 3 small pieces of coarse aggregates were seen exposed, slipped from the cement mortar
		VS15	3.999	4.004	4.003	4.002	12.579	977	78	The underlying concrete failed and the failure was mainly due to the failure of coarse aggregates
	North Bound	Plain concrete section	VN3	3.989	4.005	4.003	3.999	12.579	1326	105
VN4			4.006	4.003	3.897	3.969	11.921	1107	93	Failure mainly due to failure of coarse aggregates.
VN5			4.005	4.006	3.998	4.003	12.547	1340	107	Failure mainly due to failure of coarse aggregates, although a few small pieces of aggregates was seen exposed due to the lack of bond between aggregates and cement mortar

Note: 1. All the cores had voids in the overlay concrete which indicated the lack of good consolidation.

2. The locations of the cores can be seen in Figure A7.

Table 5.14: Comparison of Lab and Field Bond Test Results at Exit 32, I 90 (Sturgis)

Location	West Bound Passing Lane				East Bound Driving Lane			
	Lab Test		Field Test		Lab Test		Field Test	
	Core No.	Tensile bond	Core No.	Tensile bond	Core No.	Tensile bond	Core No.	Tensile bond
		Strength (psi)		Strength(psi)		Strength(psi)		Strength (psi)
Bridge Deck	WP3	43	W1	88	EP3	44	E2	76
	WP5	87	W2	57	EP4	115	E3	99
			W3	59			E4	70
			W4	74			E5	41
			W6	118				
	Average	65	Average	79	Average	80	Average	72
Approach								
	WP6	132	W7	132	EP1	109	E1	158
			W8	118	EP6	99	E6	42
		132	Average	125	Average	104	Average	100

**Table 5.15: Comparison of Lab and Field Bond Test Results
at Exit 212, I 90 (Vivian)**

North Approach (Whitetopping)				North Bound Lane (Plain Concrete)			
Lab Test		Field Test		Lab Test		Field Test	
Core No.	Tensile bond	Core No.	Tensile bond	Core No.	Tensile bond	Core No.	Tensile bond
	Strength (psi)		Strength(psi)		Strength(psi)		Strength (psi)
VS2	108	BS1	29	VN3	105	BN1	116
VN7	98	BS2	6	VN4	93	BN2	113
VN8	72	BN6	14	VN5	107	BN3	132
						BN4	159
Average	93	Average	16	Average	102	Average	130

North Half (FRC @ 20 lbs/cu.yd.)				South Half (FRC @ 25 lbs/cu.yd.)			
Lab Test		Field Test		Lab Test		Field Test	
Core No.	Tensile bond	Core No.	Tensile bond	Core No.	Tensile bond	Core No.	Tensile bond
	Strength (psi)		Strength(psi)		Strength(psi)		Strength (psi)
VS6	144	BS3	150	VS10	78	BS7	46
VS8	137	BS4	128	VS14	83	BS8	92
VS9	134	BS5	75	VS15	78	BS9	110
		BS6	104			BS10	173
Average	138	Average	114	Average	80	Average	105

Research Task 6: Using NMFRC laboratory mixes, make specimens and determine their density and permeability. The specimens should be made using different levels of compactive effort. The laboratory mixes should be similar to that used for the Vivian and Sturgis NMFRC bridge deck overlays. NOTE: This task may give an indication whether a bridge deck paving machine will provide the desired density and permeability even though it does not apply any compactive effort unlike a bridge deck overlay machine.

The materials used in the Vivian (1) and Sturgis (4) NMFRC Bridge deck overlays, were obtained and using the same mixture proportions, the following laboratory mixes were made:

- Mix 1.** Plain low-slump dense concrete with the same mix proportions used in the North bound lane at the Exit 212-interchange bridge over I-90 in Vivian.
- Mix 2.** NMFRC with fiber added at the rate 11.9 Kg/m^3 (20 lbs/yd^3) with same mix proportions used in the North half of the South bound lane of the Vivian interchange bridge.
- Mix 3.** NMFRC with fiber added at the rate 14.8 Kg/m^3 (25 lbs/yd^3) with same mix proportions used in the South half of the South bound lane of the Vivian interchange bridge.
- Mix 4.** NMFRC mix similar to the mix used for whitetopping with fibers added at a rate 14.8 Kg/m^3 (25 lbs/yd^3) at Exit 212 interchange bridge over I-90 in Vivian.
- Mix 5.** NMFRC mix similar to the mix used in the bridge deck overlay at Exit 32 interchange Bridge on I-90 in Sturgis.

Table 6.1 gives the details of the mix proportions used for each mix and also the locations of the actual bridge where these mix proportions were used before.

Test Specimens

A total of 24 cylinder specimens of dimension 101.6 mm (4 in.) diameter and 203.2 mm (8 in.) height were made for each mix. Out of these 24 cylinder specimens, 4 were cast with no vibration (series-A), 4 were cast in 2 lifts with each lift being rodded 25

times (series-B), 4 were cast with 10 seconds of vibration for both layers (series-C), 4 were cast with 20 seconds of vibration for both layers (series-D), 4 were cast with 30 seconds of vibration for both layers (series-E) and the last four (series-F) were cast as per standard procedure following the ASTM C1018 7.2.1. Four beams of dimensions 101.6 x 101.6 x 355.6 mm (4 x 4 x 14 in.) were also cast (series-G).

All the mixing, placing and compacting of concrete was done in identical conditions. The ambient temperature and humidity conditions were maintained constant through out the mixing, placing and compacting periods and also for 24 hours after casting. The beams were cast in steel molds and the cylinders in plastic molds. All the molds were oiled prior to the casting. A digital stopwatch was used during the casting of the specimens to time the duration of vibration. After casting, the specimens were covered with plastic sheets for 24 hours and kept at room temperature. They were then demolded and placed in lime saturated water tank for curing. The beams and cylinders remained in the curing tanks until testing at 28 days. The specimens in the series A to E were used to determine the density and permeability and the specimens in the series F and G were used to determine the 28 day hardened concrete properties. The details of the specimen designations are given in the Tables 5.11 and 5.12.

Each mix was made in a batch of 0.07 m^3 (2.5 cu.ft.). All mixing was done in a drum mixer of 0.25 m^3 (9 cu.ft.) capacity. The weighing of the materials was done one day prior to the mixing and stored in the lab at constant humidity and temperature conditions. The moisture contents of fine and coarse aggregates were determined. The mixing water was adjusted to saturated surface dry (SSD) condition of the coarse and fine aggregates based on the calculated moisture contents of the aggregates. The concrete was thoroughly mixed to ensure uniform mixing and the mixing was done according to ASTM C192.

Specimen Designation

Four specimens each were made for each of the 7 (series A to G) different series of specimens. Each specimen designation had 3 parts: mix #, series # and specimen # respectively. Table 6.3 gives the details of the specimen designation.

Quality control tests

Tests on fresh concrete

The fresh concrete was tested for slump (ASTM C143), air content (ASTM C231), fresh concrete unit weight (ASTM C138) and concrete temperature. The ambient temperature and humidity were also recorded. Table 6.2 gives the details of the fresh concrete properties.

Tests on hardened concrete

Compressive strength and static modulus

Cylinders were tested for static modulus (ASTM C469) and compressive strength (ASTM C39) after 28 days of curing. Prior to the test, the dimensions of the cylinders were measured and their weights were also recorded. The dry unit weight was obtained by dividing the weight of the specimen by the measured volume of the specimen. Table 6.4 gives the compressive strength and static modulus for all the mixes.

Modulus of rupture test (Static flexural strength)

Beams were tested at 28 days for the flexural strength in accordance with the ASTM C78, which was a load-control test. The beams were tested over a simply supported span of 300 mm (12 in.) and third point loading was applied to the beams. The dimensions and the weight of the beams were also measured before the test. Table 6.5 gives the results of the static flexural strength test.

The beams were also tested for the flexural toughness and first crack strength properties in accordance with the ASTM C1018. Table 6.6 gives the first crack strength and Maximum flexural strength, Table 6.7 gives the Japanese standard Toughness and equivalent strength and Table 6.8 gives the ASTM toughness indices for the fiber reinforced concrete mixes.

Dry density

The dry density of the specimens prepared for the RCPT were determined. The cylinders cast in lab were cut into a slice of 50.8 mm (2 in.) height from the finished surface and its dimensions and weight were recorded. The averages of three readings were taken to obtain the average diameter and height. The dimensions were recorded to an accuracy of 0.025 mm (0.001 in.) with a vernier caliper. The weight was recorded to an accuracy of 4.5 gm (0.01 lbs.) and the dry density was calculated as the ratio of weight to volume. Tables 6.9 to 6.13 gives the density values for different compactive efforts of all the 5 mixes.

Rapid chloride permeability test (RCPT)

The RCPT was conducted in accordance with the procedure given in ASTM C1202. A brief summary of the procedure followed is given in Research Task 3. Table 6.14 gives the RCPT results for the specimens cast in the laboratory.

Table 6.1: Details of Lab Mixes

Mix #	Mixture Proportions (lbs/cu.yd.)							Remarks
	Cement	Fly Ash	Coarse Aggregate	Fine Aggregate	Fiber (%)	Water	AEA (oz)	Similar to Mix Proportions of
1	823	nil	1394	1394	0	270	17	North Bound Lane of Bridge at Vivian, Exit 212, I 90
2	823	nil	1394	1394	20	270	17	North Half of South Bound Lane of Bridge at Vivian, Exit 212, I 90
3	823	nil	1394	1394	25	270	17	South Half of South Bound lane of Bridge at Vivian, Exit 212, I 90
4	575	115	1400	1400	25	291	6	The Approach to Bridge at Vivian, Exit 212, I 90
5	823	nil	1394	1394	25	270	17	Interchange Bridge at Sturgis, Exit 32, I 90

Table 6.2: Properties of Fresh Concrete

Mix #	Ambient		Concrete Temp	Unit Weight	Slump	Air Content
	Temp	Humidity				
	(F)	(%)	(F)	(lb/ft ³)	(in.)	(%)
1	70	40	60.8	144.8	1.25	4.8
2	70	40	59.2	145.2	0.25	4.8
3	70	40	60.5	142.0	0.25	5.6
4	70	40	66.7	138.8	4.50	6.0
5	70	40	62.9	147.2	0.25	4.6

SI Unit Conversion Factors

1 inch =	25.4 mm
1 lb =	0.4536 kg
lb/ft ³ =	16.02 kg/m ³

Table 6.3: Details of Specimen Designation

Mix #	Specimen #	Type	Number	Description of Procedure
1	1A	Cylinder	4	No Vibration
	1B	Cylinder	4	Rodding, 25 times each in two equal layers
	1C	Cylinder	4	10 seconds vibration of each layer, in two layers
	1D	Cylinder	4	20 seconds vibration of each layer, in two layers
	1E	Cylinder	4	30 seconds vibration of each layer, in two layers
	1F	Cylinder	4	For hardened concrete properties
	1G	Beams	4	For hardened concrete properties
2	2A	Cylinder	4	No Vibration
	2B	Cylinder	4	Rodding, 25 times each in two equal layers
	2C	Cylinder	4	10 seconds vibration of each layer, in two layers
	2D	Cylinder	4	20 seconds vibration of each layer, in two layers
	2E	Cylinder	4	30 seconds vibration of each layer, in two layers
	2F	Cylinder	4	For hardened concrete properties
	2G	Beams	4	For hardened concrete properties
3	3A	Cylinder	4	No Vibration
	3B	Cylinder	4	Rodding, 25 times each in two equal layers
	3C	Cylinder	4	10 seconds vibration of each layer, in two layers
	3D	Cylinder	4	20 seconds vibration of each layer, in two layers
	3E	Cylinder	4	30 seconds vibration of each layer, in two layers
	3F	Cylinder	4	For hardened concrete properties
	3G	Beams	4	For hardened concrete properties
4	4A	Cylinder	4	No Vibration
	4B	Cylinder	4	Rodding, 25 times each in two equal layers
	4C	Cylinder	4	10 seconds vibration of each layer, in two layers
	4D	Cylinder	4	20 seconds vibration of each layer, in two layers
	4E	Cylinder	4	30 seconds vibration of each layer, in two layers
	4F	Cylinder	4	For hardened concrete properties
	4G	Beams	4	For hardened concrete properties
5	5A	Cylinder	4	No Vibration
	5B	Cylinder	4	Rodding, 25 times each in two equal layers
	5C	Cylinder	4	10 seconds vibration of each layer, in two layers
	5D	Cylinder	4	20 seconds vibration of each layer, in two layers
	5E	Cylinder	4	30 seconds vibration of each layer, in two layers
	5F	Cylinder	4	For hardened concrete properties
	5G	Beams	4	For hardened concrete properties

Example: 1C4 is the fourth specimen from the first mix cast using 10 seconds vibration of each layer, in two layers

Note: The specimens numbering A to E (4 each) are used to determine density and permeability

Table 6.4: Cylinder Compressive strength and Static Modulus

Mix #	Specimen ID	Age (Days)	Diameter (in.)	Length (in.)	Unit weight (lb/ft ³)	Static modulus (x10 ⁶ psi)	Comp. strength (psi)
1	1F1	28	4.000	8.042	149	0.00	7760
	1F2	28	4.008	8.008	147	0.00	7810
	1F3	28	4.008	8.008	149	0.00	8130
	1F4	28	4.017	8.008	152	0.00	8050
	Average				149	0.00	7938
	Std.Dev				1.86	0.00	180
	% C.V				1.25	#DIV/0!	2.27
2	2F1	28	4.000	8.008	148	0.00	7600
	2F2	28	4.000	8.017	151	0.00	7600
	2F3	28	4.008	8.008	151	0.00	7490
	2F4	28	4.008	8.017	149	0.00	7690
	Average				150	0.00	7595
	Std.Dev				1.55	0.00	82
	% C.V				1.03	#DIV/0!	1.08
3	3F1	28	4.000	8.008	144	0.00	7110
	3F2	28	4.000	8.000	146	0.00	7090
	3F3	28	4.000	8.033	146	0.00	6530
	3F4	28	3.983	8.008	146	0.00	7145
	Average				145	0.00	6969
	Std.Dev				0.78	0.00	293
	% C.V				0.54	#DIV/0!	4.21
4	4F1	28	4.008	8.008	142	0.00	5390
	4F2	28	4.042	8.000	141	0.00	5300
	4F3	28	4.000	8.008	143	0.00	5370
	4F4	28	4.008	8.000	142	0.00	5350
	Average				142	0.00	5353
	Std.Dev				0.46	0.00	39
	% C.V				0.33	#DIV/0!	0.72
5	5F1	28	4.083	8.008	150	0.00	8480
	5F2	28	4.017	8.017	151	0.00	8685
	5F3	28	4.025	8.017	153	0.00	8730
	5F4	28	4.008	8.008	151	0.00	7930
	Average				151	0.00	8456
	Std.Dev				1.11	0.00	367
	% C.V				0.73	#DIV/0!	4.34

SI Unit Conversion Factors

1 inch = 25.4 mm

1 lb = 0.4536 kg

1 psi = 0.006895MPa

lb/ft³ = 16.02 kg/m³

Table 6.5: Plain Flexure Test

Mix #	Specimen ID	Avg Breadth	Avg Depth	Avg Length	Volume	Weight	Dry Unit Wt.	Ultimate load	Flexural strength
		(in.)	(in.)	(in.)	(in ³)	(lb)	(lb/cu.ft.)	(lbs)	(psi)
1	1G1	4.050	4.190	14.025	238.0	20.3	147.4	5946	1004
	1G2	4.150	4.130	14.000	240.0	20.3	146.2	5913	1002
	1G3	4.090	4.180	14.025	239.8	20.3	146.3	5750	966
	1G4	4.180	4.160	14.025	243.9	20.4	144.5	5875	975
Average									987
SD									19
%CV									0.02

Table 6.6: First Crack Strength and Maximum Flexural Strength

Mix #	Specimen #	Age (Days)	First Crack			Maximum Load (lbs)	Flexural Strength (psi)
			Load (lbs)	Deflection (inches)	Stress (psi)		
2	2G1	28	5500	0.0012	994	5584	1009
	2G2	28	5000	0.0007	831	5445	905
	2G3	28	4500	0.0012	803	4870	869
	2G4	28	5000	0.0036	823	5012	825
	Average				863		902
	SD				88		78
	%CV				0.10		0.09
3	3G1	28	3500	0.001	660	3885	733
	3G2	28	4500	0.001	745	4834	800
	3G3	28	4500	0.0014	882	4938	968
	3G4	28	4500	0.0013	743	4781	789
	Average				758		823
	SD				92		101
	%CV				0.12		0.12
4	4G1	28	4000	0.0003	732	4405	806
	4G2	28	3500	0.0003	604	3770	650
	4G3	28	3500	0.0001	665	3944	665
	4G4	28	4000	0.0003	639	4091	653
	Average				660		694
	SD				54		75
	%CV				0.08		0.11
5	5G1	28	4500	0.0008	754	4838	811
	5G2	28	5500	0.0009	926	5735	965
	5G3	28	4500	0.0005	853	4592	870
	5G4	28	3500	0.0012	670	3799	727
	Average				801		843
	SD				112		100
	%CV				0.14		0.12

SI Unit Conversion Factors

1 inch = 25.4 mm

1 lb = 0.4536 kg

1 psi = 0.006895MPa

Table 6.7: Japanese Standard - Toughness and Equivalent Strength

Mixture #	Specimen #	Toughness		Equivalent Flexural	
		(inch-lbs)	(Nm)	Strength (psi)	(MPa)
2					
	2G1	176.6	20.0	399	2.8
	2G2	186.2	21.0	389	2.7
	2G3	177.6	20.1	396	2.7
	2G4	176.0	19.9	364	2.5
	Average	179.1	20.2	387	2.7
	Std.Dev	4.8	0.5	15.9	0.1
	% C.V	2.7	2.7	4.1	4.1
3	3G1	194.6	22.0	459	3.2
	3G2	192.1	21.7	397	2.7
	3G3	190.0	21.5	442	3.0
	3G4	194.8	22.0	402	2.8
	Average	192.9	21.8	425	2.9
	Std.Dev	2.3	0.3	30.1	0.2
	% C.V	1.2	1.2	7.1	7.1
4	4G1	197.8	22.4	452	3.1
	4G2	196.0	22.1	422	2.9
	4G3	195.4	22.1	464	3.2
	4G4	194.7	22.0	389	2.7
	Average	196.0	22.1	432	3.0
	Std.Dev	1.3	0.2	33.7	0.2
	% C.V	0.7	0.7	7.8	7.8
5	5G1	176.2	19.9	369	2.5
	5G2	174.1	19.7	482	3.3
	5G3	176.2	19.9	417	2.9
	5G4	178.3	20.1	427	2.9
	Average	176.2	19.9	404	2.8
	Std.Dev	1.7	0.2	46.3	0.3
	% C.V	1.0	1.0	11.5	11.5

Conversion Factors:

1 MPa = 145 psi

1 in-lb = 0.113 Nm

Table 6.8: ASTM Toughness Indices - 28 Days

Mixture #	Specimen #	First Crack Toughness (in-lbs)	Toughness Indices				Toughness Ratios			Residual Strength Indices	
			I5	I10	I20	I30	I10/I5	I20/I10	I30/I20	R _{5,10}	R _{10,20}
2	2G1	4.0	4.62	8.88	16.12	18.94	1.92	1.82	1.17	85.2	72.4
	2G2	3.2	4.46	9.08	16.75	18.16	2.04	1.84	1.08	92.4	76.7
	2G3	3.4	4.57	8.59	17.03	20.21	1.88	1.98	1.19	80.4	84.4
	2G4	3.0	4.63	8.47	16.35	19.12	1.83	1.93	1.17	76.8	78.8
	Average	3.4	4.57	8.76	16.56	19.11	1.92	1.89	1.15	83.7	78.1
	Std.Dev	0.5	0.1	0.3	0.4	0.8	0.1	0.1	0.0	6.7	5.0
	% C.V	13.9	1.7	3.2	2.5	4.4	4.6	4.1	4.1	8.1	6.4
3	3G1	3.45	4.32	6.97	11.85	17.58	1.61	1.70	1.48	53.0	48.8
	3G2	3.50	4.07	7.11	11.39	14.04	1.75	1.60	1.23	60.8	42.8
	3G3	3.70	4.19	7.31	11.72	16.26	1.74	1.60	1.39	62.4	44.1
	3G4	3.78	4.12	7.25	11.91	14.89	1.76	1.64	1.25	62.6	46.6
	Average	3.61	4.18	7.16	11.72	15.69	1.72	1.64	1.34	59.7	45.6
	Std.Dev	0.2	0.1	0.2	0.2	1.6	0.1	0.0	0.1	4.5	2.7
	% C.V	4.4	2.6	2.1	2.0	9.9	4.0	2.8	8.9	7.6	5.9
4	4G1	2.60	4.59	8.58	15.95	25.66	1.87	1.86	1.61	79.8	73.7
	4G2	2.80	4.46	8.80	16.20	24.66	1.97	1.84	1.52	86.8	74.0
	4G3	2.87	4.89	8.94	16.11	25.55	1.83	1.80	1.59	81.0	71.7
	4G4	2.56	4.56	8.67	16.21	22.46	1.90	1.87	1.39	82.2	75.4
	Average	2.71	4.63	8.75	16.12	24.58	1.89	1.84	1.53	82.5	73.7
	Std.Dev	0.2	0.2	0.2	0.1	1.5	0.1	0.0	0.1	3.1	1.5
	% C.V	5.6	4.0	1.8	0.7	6.0	3.2	1.6	6.6	3.7	2.1
5	5G1	2.05	4.96	9.96	17.94	27.99	2.01	1.87	1.56	100.00	79.8
	5G2	1.96	5.10	9.78	17.84	23.68	1.92	1.82	1.33	93.60	80.6
	5G3	1.83	5.04	9.98	18.71	29.39	1.98	1.87	1.57	98.80	87.3
	5G4	1.75	4.98	9.77	17.43	29.67	1.96	1.78	1.70	95.80	76.6
	Average	1.90	5.02	9.87	17.98	27.68	1.97	1.84	1.54	97.05	81.1
	Std.Dev	0.1	0.1	0.1	0.5	2.8	0.0	0.0	0.2	2.9	4.5
	% C.V	7.0	1.3	1.1	3.0	10.0	1.9	2.3	10.1	3.0	5.5

Conversion Factor: 1in-lb = 0.113KN.m

**Table 6.9: Dry Density of Concrete with Different Compactive Efforts - (Mix 1) Plain LSD Concrete
(Same Mix Proportions as used in the North Bound Lane at Exit 212, I 90 (Vivian))**

Vibrtn. Type	Specimen No.	Diameter			Avg. Dia. (in.)	Height			Avg. Ht. (in.)	Vol. (in ³)	Wt. (lbs)	Density (lbs/ft ³)
		Dia. 1 (in.)	Dia. 2 (in.)	Dia. 3 (in.)		Ht. 1 (in.)	Ht. 2 (in.)	Ht. 3 (in.)				
No Vibration	1A1	4.000	4.000	4.000	4.000	2.075	2.100	2.050	2.075	26.062	2.14	142.0
	1A2	4.025	4.025	4.025	4.025	2.050	2.000	2.025	2.025	25.753	2.09	140.2
	1A3	4.000	4.025	4.025	4.017	2.075	2.025	2.050	2.050	25.963	2.14	142.7
	1A4	3.975	3.975	4.000	3.983	1.975	1.900	1.900	1.925	23.977	1.96	141.1
											Average SD	141.5 1.1
Rodding	1B1	4.000	4.025	4.025	4.017	1.975	1.925	1.975	1.958	24.802	2.08	144.9
	1B2	4.000	4.000	4.000	4.000	2.025	2.000	2.000	2.008	25.225	2.10	144.0
	1B3	4.000	4.000	4.000	4.000	1.950	1.975	2.000	1.975	24.806	2.04	141.9
	1B4	4.025	4.025	4.025	4.025	1.875	1.875	1.925	1.892	24.057	1.98	142.4
											Average SD	143.3 1.4
10 sec. Vibration	1C1	4.025	4.025	4.000	4.017	1.925	1.950	1.950	1.942	24.591	2.04	143.5
	1C2	4.025	4.025	4.025	4.025	1.875	1.850	1.825	1.850	23.527	1.94	142.2
	1C3	3.925	3.925	3.950	3.933	2.000	1.975	1.950	1.975	23.986	1.98	142.7
	1C4	4.025	4.075	4.025	4.042	2.025	2.025	1.850	1.967	25.219	2.09	143.1
											Average SD	142.9 0.5
20 sec. Vibration	1D1	4.000	4.000	4.000	4.000	1.975	2.000	1.975	1.983	24.911	2.09	145.2
	1D2	4.000	4.000	4.025	4.008	2.025	2.025	1.900	1.983	25.015	2.10	144.9
	1D3	4.000	4.000	4.000	4.000	1.975	1.950	2.000	1.975	24.806	2.07	144.4
	1D4	4.025	3.975	4.025	4.008	2.000	2.000	1.975	1.992	25.120	2.10	144.6
											Average SD	144.8 0.4
30 sec. Vibration	1E1	4.025	3.975	4.000	4.000	2.025	2.000	2.025	2.017	25.329	2.14	145.8
	1E2	3.975	4.000	3.975	3.983	2.025	2.025	1.975	2.008	25.015	2.12	146.2
	1E3	3.975	4.050	4.025	4.017	1.925	2.000	2.000	1.975	25.013	2.12	146.3
	1E4	4.050	4.075	4.050	4.058	1.975	1.900	1.900	1.925	24.888	2.11	146.4
											Average SD	146.2 0.2

**Table 6.10: Dry Density of Concrete with Different Compactive Efforts - (Mix 2) NMFRC; Fiber @ 20 lbs/cu.yd.
(Same Mix Proportions as used in the North Half of the South Bound Lane at Exit 212, I 90 (Vivian))**

Vibrtn. Type	Specimen No.	Diameter			Avg. Dia. (in.)	Height			Avg. Ht. (in.)	Vol. (in ³)	Wt. (lbs)	Density (lbs/ft ³)
		Dia. 1 (in.)	Dia. 2 (in.)	Dia. 3 (in.)		Ht. 1 (in.)	Ht. 2 (in.)	Ht. 3 (in.)				
No Vibration	2A1	4.050	4.050	4.050	4.050	2.000	2.000	2.025	2.008	25.859	2.13	142.7
	2A2	4.050	4.025	4.050	4.042	2.050	2.075	2.075	2.067	26.501	2.18	142.4
	2A3	4.125	4.025	4.010	4.053	2.025	2.025	2.050	2.033	26.224	2.18	143.4
	2A4	4.050	4.050	4.075	4.058	2.025	2.050	2.025	2.033	26.289	2.17	142.8
											Average	142.8
Rodding	2B1	4.025	4.025	4.050	4.033	1.975	1.950	1.975	1.967	25.115	2.11	145.1
	2B2	4.025	4.000	4.000	4.008	2.000	1.975	1.975	1.983	25.015	2.08	143.8
	2B3	3.950	3.950	3.975	3.958	2.025	2.075	2.025	2.042	25.112	2.11	144.9
	2B4	4.025	4.025	4.000	4.017	2.025	2.000	2.025	2.017	25.541	2.13	144.1
											Average	144.5
10 sec. Vibration	2C1	4.050	4.025	4.050	4.042	2.000	2.025	2.025	2.017	25.860	2.15	143.9
	2C2	4.075	4.075	4.075	4.075	1.975	1.975	1.925	1.958	25.528	2.13	143.9
	2C3	4.100	4.100	4.125	4.108	1.975	1.925	2.000	1.967	26.057	2.15	142.9
	2C4	3.975	4.025	4.000	4.000	2.000	2.050	2.050	2.033	25.539	2.12	143.3
											Average	143.5
20 sec. Vibration	2D1	3.925	3.975	4.050	3.983	2.025	2.025	2.025	2.025	25.222	2.11	144.4
	2D2	3.975	4.000	4.000	3.992	2.050	2.025	2.000	2.025	25.328	2.11	144.2
	2D3	3.975	3.975	3.975	3.975	2.000	1.975	1.950	1.975	24.497	2.06	145.5
	2D4	4.050	4.025	4.025	4.033	2.025	1.900	1.900	1.942	24.795	2.08	145.0
											Average	144.8
30 sec. Vibration	2E1	4.000	4.000	4.025	4.008	2.025	2.050	2.025	2.033	25.645	2.16	145.5
	2E2	4.000	4.025	4.075	4.033	2.000	2.025	1.975	2.000	25.540	2.15	145.3
	2E3	3.975	4.025	4.025	4.008	2.025	2.000	2.000	2.008	25.330	2.14	145.9
	2E4	4.000	4.000	4.025	4.008	2.025	2.000	2.025	2.017	25.435	2.13	144.8
											Average	145.4
											SD	0.5

**Table 6.11: Dry Density of Concrete with Different Compactive Efforts - (Mix 3) NMFC; Fiber @ 25 lbs/cu.yd.
(Same Mix Proportions as used in the South Half of the South Bound Lane at Exit 212, I 90 (Vivian))**

Vibrtn. Type	Specimen No.	Diameter			Avg. Dia. (in.)	Height			Avg. Ht. (in.)	Vol. (in ³)	Wt. (lbs)	Density (lbs/ft ³)
		Dia. 1 (in.)	Dia. 2 (in.)	Dia. 3 (in.)		Ht. 1 (in.)	Ht. 2 (in.)	Ht. 3 (in.)				
No Vibration	3A1	4.025	4.025	4.000	4.017	2.050	2.000	2.050	2.033	25.752	2.08	139.2
	3A2	3.975	3.975	3.975	3.975	1.975	1.950	1.950	1.958	24.290	1.98	140.9
	3A3	4.025	4.025	4.025	4.025	2.000	1.975	1.975	1.983	25.223	2.06	141.1
	3A4	4.000	4.000	4.025	4.008	1.925	2.025	2.000	1.983	25.015	2.04	140.9
											Average SD	140.5 0.9
Rodding	3B1	4.000	4.000	3.975	3.992	2.000	2.025	2.050	2.025	25.328	2.09	142.5
	3B2	4.025	4.000	4.000	4.008	1.975	2.100	2.125	2.067	26.066	2.16	143.3
	3B3	4.025	4.025	4.000	4.017	1.925	1.975	2.025	1.975	25.013	2.08	143.8
	3B4	4.025	4.000	4.025	4.017	2.025	2.025	2.025	2.025	25.646	2.13	143.7
											Average SD	143.3 0.6
10 sec. Vibration	3C1	4.025	4.025	4.025	4.025	2.025	2.000	2.025	2.017	25.647	2.09	140.7
	3C2	4.000	4.000	4.025	4.008	2.025	2.025	2.050	2.033	25.645	2.11	142.4
	3C3	4.000	4.025	4.025	4.017	1.925	1.975	1.925	1.942	24.591	2.00	140.7
	3C4	4.000	4.000	4.025	4.008	2.025	2.000	2.025	2.017	25.435	2.09	141.9
											Average SD	141.4 0.8
20 sec. Vibration	3D1	4.075	4.050	4.075	4.067	1.950	1.950	1.950	1.950	25.315	2.11	144.0
	3D2	4.000	4.025	4.025	4.017	2.000	2.000	2.000	2.000	25.330	2.11	143.9
	3D3	4.025	4.050	4.025	4.033	2.000	1.975	1.975	1.983	25.328	2.11	144.1
	3D4	4.000	4.025	4.050	4.025	2.000	1.975	2.050	2.008	25.541	2.12	143.4
											Average SD	143.9 0.3
30 sec. Vibration	3E1	4.000	4.000	4.025	4.008	1.950	1.975	1.975	1.967	24.804	2.10	146.0
	3E2	4.000	3.975	3.975	3.983	2.000	2.000	2.050	2.017	25.119	2.11	145.0
	3E3	4.025	4.000	4.000	4.008	1.950	1.975	1.975	1.967	24.804	2.10	146.4
	3E4	3.975	3.975	3.950	3.967	2.000	2.025	2.025	2.017	24.909	2.11	146.2
											Average SD	145.9 0.6

**Table 6.12: Dry Density of Concrete with Different Compactive Efforts - (Mix 4) Whitetopping; Fiber @ 25 lbs/cu.yd.
(Same Mix Proportions as used in the Approach to the Bridge at Exit 212, I 90 (Vivian))**

Vibrtn. Type	Specimen No.	Diameter			Avg. Dia. (in.)	Height			Avg. Ht. (in.)	Vol. (in ³)	Wt. (lbs)	Density (lbs/ft ³)
		Dia. 1 (in.)	Dia. 2 (in.)	Dia. 3 (in.)		Ht. 1 (in.)	Ht. 2 (in.)	Ht. 3 (in.)				
No Vibration	4A1	4.050	4.025	4.025	4.033	2.025	2.025	2.050	2.033	25.966	1.98	131.8
	4A2	4.000	3.975	3.975	3.983	2.075	2.075	2.125	2.092	26.053	1.97	130.8
	4A3	4.050	4.050	4.025	4.042	2.050	2.000	2.025	2.025	25.967	1.98	131.8
	4A4	4.000	4.000	3.975	3.992	2.000	2.125	2.000	2.042	25.537	1.99	134.7
											Average	132.2
											SD	1.7
Rodding	4B1	4.025	4.000	4.000	4.008	2.025	2.000	2.025	2.017	25.435	2.09	142.1
	4B2	4.050	4.000	4.000	4.017	2.025	1.950	1.975	1.983	25.119	2.10	144.7
	4B3	4.000	4.050	4.050	4.033	2.025	2.025	2.025	2.025	25.860	2.20	147.0
	4B4	4.100	4.050	3.975	4.042	1.975	1.975	2.000	1.983	25.432	2.10	143.0
											Average	144.2
											SD	2.2
10 sec. Vibration	4C1	4.000	4.075	4.025	4.033	2.025	2.075	2.075	2.058	26.285	2.10	137.9
	4C2	4.025	4.075	4.050	4.050	2.025	2.050	2.050	2.042	26.288	2.12	139.2
	4C3	4.025	4.025	4.025	4.025	2.025	2.050	2.050	2.042	25.965	2.11	140.3
	4C4	4.050	4.000	4.025	4.025	2.050	2.025	2.050	2.042	25.965	2.11	140.1
											Average	139.4
											SD	1.1
20 sec. Vibration	4D1	3.975	3.975	3.950	3.967	1.975	1.975	2.050	2.000	24.703	2.07	144.5
	4D2	3.975	4.000	4.000	3.992	1.950	1.950	2.000	1.967	24.599	2.02	142.2
	4D3	4.000	3.975	3.975	3.983	2.000	1.975	2.000	1.992	24.807	2.08	144.6
	4D4	4.025	3.975	4.000	4.000	1.975	2.000	1.975	1.983	24.911	2.06	143.0
											Average	143.6
											SD	1.2
30 sec. Vibration	4E1	3.975	4.000	3.975	3.983	1.975	1.975	2.000	1.983	24.704	2.09	146.5
	4E2	3.950	3.975	3.975	3.967	2.025	2.025	2.100	2.050	25.321	2.17	148.4
	4E3	4.000	4.000	4.000	4.000	1.975	2.000	2.025	2.000	25.120	2.15	147.9
	4E4	4.025	4.025	4.000	4.017	2.000	2.000	1.925	1.975	25.013	2.12	146.2
											Average	147.2
											SD	1.1

**Table 6.13: Dry Density of Concrete with Different Compactive Efforts - (Mix 5) NMFR; Fiber @ 25 lbs/cu.yd.
(Same Mix Proportions as used in the Bridge Deck Overlay at Exit 32, I 90 (Sturgis))**

Vibrtn. Type	Specimen No.	Diameter			Avg. Dia. (in.)	Height			Avg. Ht. (in.)	Vol. (in ³)	Wt. (lbs)	Density (lbs/ft ³)
		Dia. 1 (in.)	Dia. 2 (in.)	Dia. 3 (in.)		Ht. 1 (in.)	Ht. 2 (in.)	Ht. 3 (in.)				
No Vibration	5A1	3.925	3.975	4.000	3.967	2.025	2.000	1.950	1.992	24.600	1.97	138.2
	5A2	3.950	4.000	3.975	3.975	2.025	1.900	2.050	1.992	24.704	1.97	137.6
	5A3	3.925	4.000	4.000	3.975	2.000	1.950	1.975	1.975	24.497	1.97	139.2
	5A4	4.025	4.000	3.975	4.000	2.000	1.925	1.900	1.942	24.387	1.95	138.0
											Average	138.2
											SD	0.7
Rodding	5B1	4.000	4.025	4.000	4.008	2.025	2.000	2.025	2.017	25.435	2.07	140.6
	5B2	4.025	3.975	4.000	4.000	1.925	1.950	2.000	1.958	24.597	2.01	141.5
	5B3	3.925	3.925	3.975	3.942	2.025	2.025	2.000	2.017	24.596	2.01	141.3
	5B4	3.975	3.925	3.975	3.958	2.050	2.000	1.950	2.000	24.599	2.01	141.1
											Average	141.1
											SD	0.4
10 sec. Vibration	5C1	4.075	4.075	4.025	4.058	2.025	2.025	2.000	2.017	26.073	2.12	140.2
	5C2	4.025	4.050	4.025	4.033	2.025	2.025	2.050	2.033	25.966	2.12	141.2
	5C3	4.075	4.000	4.000	4.025	2.025	2.025	2.025	2.025	25.753	2.09	140.1
	5C4	4.000	4.025	4.025	4.017	2.050	1.975	2.050	2.025	25.646	2.10	141.5
											Average	140.8
											SD	0.7
20 sec. Vibration	5D1	4.025	3.975	4.000	4.000	2.025	1.950	1.900	1.958	24.597	2.06	144.6
	5D2	4.025	4.000	4.025	4.017	2.025	1.900	1.925	1.950	24.697	2.06	144.2
	5D3	4.025	4.025	4.000	4.017	1.950	1.950	1.950	1.950	24.697	2.07	144.9
	5D4	4.000	4.025	4.000	4.008	1.975	2.000	1.975	1.983	25.015	2.08	143.8
											Average	144.4
											SD	0.5
30 sec. Vibration	5E1	4.025	4.025	4.000	4.017	1.975	2.025	1.925	1.975	25.013	2.12	146.4
	5E2	3.975	3.975	4.075	4.008	2.000	2.025	2.000	2.008	25.330	2.13	145.2
	5E3	4.000	4.000	4.000	4.000	2.025	2.050	2.100	2.058	25.853	2.17	145.3
	5E4	4.025	4.100	4.075	4.067	1.975	1.950	1.975	1.967	25.532	2.14	145.1
											Average	145.5
											SD	0.6

Table 6.14: Rapid Chloride Permeability Test Results for the Specimens Cast in Laboratory

Mix # 1 (North Bound Lane at Exit 212, I 90 - Plain Concrete)											
Rodding			10 sec. Vibration			20 sec. Vibration			30 sec. Vibration		
Spec. No.	Charge (Coulomb)	Remark	Spec. No.	Charge (Coulomb)	Remark	Spec. No.	Charge (Coulomb)	Remark	Spec. No.	Charge (Coulomb)	Remark
1B1	4064	HIGH	1C1	4949	HIGH	1D1	3717	MOD	1E1	2828	MOD
1B2	4165	HIGH	1C2	5119	HIGH	1D2	3246	MOD	1E2	2200	MOD
1B3	3876	MOD	1C3	4764	HIGH	1D3	4568	HIGH	1E3	2146	MOD
1B4	4083	HIGH	1C4	5323	HIGH	1D4	3437	MOD	1E4	2159	MOD
AVG	4047	HIGH		5039	HIGH		3742	MOD		2333	MOD
SD	122			239			584			331	
CV	0.03			0.05			0.16			0.14	
Mix # 2 (South Bound Lane at Exit 212, I 90 - NMFRC: 20 lbs/cu.yd.)											
Rodding			10 sec. Vibration			20 sec. Vibration			30 sec. Vibration		
Spec. No.	Charge (Coulomb)	Remark	Spec. No.	Charge (Coulomb)	Remark	Spec. No.	Charge (Coulomb)	Remark	Spec. No.	Charge (Coulomb)	Remark
2B1	4658	HIGH	2C1	3885	MOD	2D1	3105	MOD	2E1	2928	MOD
2B2	4352	HIGH	2C2	4778	HIGH	2D2	4156	HIGH	2E2	2279	MOD
2B3	4486	HIGH	2C3	4349	HIGH	2D3	2544	MOD	2E3	2747	MOD
2B4	4126	HIGH	2C4	4956	HIGH	2D4	3568	MOD	2E4	2489	MOD
AVG	4406	HIGH		4492	HIGH		3343	MOD		2611	MOD
SD	225			478			685			285	
CV	0.05			0.11			0.20			0.11	
Mix # 3 (South Bound Lane at Exit 212, I 90 - NMFRC: 25 lbs/cu.yd.)											
Rodding			10 sec. Vibration			20 sec. Vibration			30 sec. Vibration		
Spec. No.	Charge (Coulomb)	Remark	Spec. No.	Charge (Coulomb)	Remark	Spec. No.	Charge (Coulomb)	Remark	Spec. No.	Charge (Coulomb)	Remark
3B1	4079	HIGH	3C1	4546	HIGH	3D1	4251	HIGH	3E1	2817	MOD
3B2	4307	HIGH	3C2	4629	HIGH	3D2	4512	HIGH	3E2	2203	MOD
3B3	4268	HIGH	3C3	4823	HIGH	3D3	4215	HIGH	3E3	2156	MOD
3B4	4632	HIGH	3C4	4253	HIGH	3D4	4189	HIGH	3E4	2289	MOD
AVG	4322	HIGH		4563	HIGH		4292	HIGH		2366	MOD
SD	230			237			149			306	
CV	0.05			0.05			0.03			0.13	

Table 6.14: (Contd..) Rapid Chloride Permeability Test Results for the Specimens Cast in Laboratory

Mix # 4 (Approach to Bridge at Exit 212, I 90 - Whitetopping)

Rodding			10 sec. Vibration			20 sec. Vibration			30 sec. Vibration		
Spec. No.	Charge (Coulomb)	Remark	Spec. No.	Charge (Coulomb)	Remark	Spec. No.	Charge (Coulomb)	Remark	Spec. No.	Charge (Coulomb)	Remark
4B1	4020	HIGH	4C1	4109	MOD	4D1	3986	MOD	4E1	3698	MOD
4B2	4198	HIGH	4C2	4000	MOD	4D2	3569	MOD	4E2	3458	MOD
4B3	4169	HIGH	4C3	4069	MOD	4D3	3968	MOD	4E3	3558	MOD
4B4	4683	HIGH	4C4	3989	MOD	4D4	3987	MOD	4E4	3458	MOD
AVG	4268	HIGH		4042	MOD		3878	MOD		3543	MOD
SD	288			57			206			114	
CV	0.07			0.01			0.05			0.03	

Mix # 5 (Bridge at Exit 32, I 90 - FRC: 25 lbs/cu.yd.)

Rodding			10 sec. Vibration			20 sec. Vibration			30 sec. Vibration		
Spec. No.	Charge (Coulomb)	Remark	Spec. No.	Charge (Coulomb)	Remark	Spec. No.	Charge (Coulomb)	Remark	Spec. No.	Charge (Coulomb)	Remark
5B1	3880	MOD	5C1	4587	HIGH	5D1	3698	MOD	5E1	2135	MOD
5B2	2956	MOD	5C2	4365	HIGH	5D2	2959	MOD	5E2	2038	MOD
5B3	2774	MOD	5C3	3689	MOD	5D3	3246	MOD	5E3	2132	MOD
5B4	3056	MOD	5C4	4179	HIGH	5D4	2827	MOD	5E4	2260	MOD
AVG	3167	MOD		4205	HIGH		3183	MOD		2141	MOD
SD	490			382			386			91	
CV	0.15			0.09			0.12			0.04	

Research Task 7: Compare the permeabilities and densities of the samples taken for Task 3 with those of Task 6.

The permeability and density values of the cores from the field (Task 3) and the cylinders cast in the laboratory (Task 6) were compared in this Research task. Table 7.1 gives the values of chloride permeability of cores from field and those cast in the laboratory. Figures 7.1 to 7.5 give the comparison of permeabilities of cores from various locations and the corresponding cylinder specimens cast in the laboratory.

Chloride permeability**Chloride permeability of cores from field**

Three samples (cores) were taken from the plain LSD concrete overlay and the chloride permeability values for these cores varied from 1491 to 2984 coulombs, with an average of 2033 coulombs. If more samples were taken from the plain concrete section of the bridge, a more reasonable value for the chloride permeability would have been obtained. Due to the inherent variability of the test results in this method, a minimum of 5 specimens would be needed to estimate the chloride permeability correctly. Since the difference in the chloride permeability of plain concrete and NMFRC was only 485 coulombs, which was within the experimental variation possible for chloride permeability test, it was difficult to positively conclude that the addition of fibers would increase the permeability of the concrete.

The difference in the chloride permeability of fiber reinforced concrete with 11.9 Kg/m^3 (20 lbs/yd³) and 14.8 Kg/m^3 (25 lbs/yd³) was less than 10% which was within the experimental variation possible for this test. Therefore it could be stated that the chloride permeability of both fiber concretes was the same.

There was not much difference in the chloride permeability of the NMFRC overlay used at the Exit 212, I90 (Vivian) and that used at the Exit 32, I90 (Sturgis). The same mixture proportions were used for both the NMFRC overlays in Vivian and Sturgis with 14.8 Kg/m^3 (25 lbs/yd³) polyolefin fiber. The average chloride permeability values were 2796 and 2492 coulombs respectively. The minor difference between the two was within the tolerance allowed for this test.

The FRC used in the approach (whitetopping) to the bridge at Exit 212, 190, had higher chloride permeability (4686 coulombs.) than that of the overlay concretes (2033, 2518 & 2796 coulombs). This was due to the lower cement content used in the whitetopping (342.1 Kg/m^3 - 575 lbs/yd^3) than that used for the NMFRC in the overlay (489.7 Kg/m^3 - 823 lbs/yd^3). A plain concrete with the same mix proportions as used in the whitetopping would likely give the same chloride permeability (4500 to 5000 coulombs). Therefore it can be concluded that the addition of fibers did not significantly influence the chloride permeability of the field concrete.

Chloride permeability of specimens cast in the laboratory

Specimens cast in the laboratory using the same mix proportions used in the construction of the bridge deck at Exit 32 and Exit 212, 190 showed that the chloride permeability largely depends on the compaction effort used to make the specimens. The specimens made without any vibration or rodding showed numerous voids and continuous capillary holes in the 50.8 mm (2 in.) depth. When one specimen was tested the chloride permeability was so high for the specimen that it was beyond the limit of the equipment to measure it. Therefore we did not do the chloride permeability test for other specimens.

When only rodding, as specified in the ASTM, was used as the compaction effort, the chloride permeability was between 3100 to 4400 coulombs. When 10 sec. vibration was used where the cylinders were made using the vibrating table in the laboratory (high-speed vibrating table with a capacity of 136 Kg (300 lbs) and which provided 3600 vibrations per minute with a constant amplitude of vibration of 0.317 mm (0.012 in.)), the permeability (4200 to 5000 coulombs) was even higher than that of specimens made using rodding, where as when 20 sec. vibration was used the chloride permeability reduced considerably to a range of 3200 to 3700 coulombs. The 30 sec. vibration further reduced the chloride permeability to a range of 2100 to 2400 coulombs.

In the laboratory, four specimens were used for the determination of chloride permeability and identical consolidation effort (30 sec. vibration) was used for all the specimens. Therefore the comparison would be more reliable. The average chloride permeability values were 2333, 2611, 2366 and 2141 coulombs, respectively for plain

LSDC, NMFRC with 11.9 Kg/m^3 (20 lbs/yd^3), NMFRC with 14.8 Kg/m^3 (25 lbs/yd^3) and the NMFRC with 14.8 Kg/m^3 (25 lbs/yd^3) used in Sturgis overlay. Comparing these results it can be stated that the chloride permeability values were almost the same, the differences are within the tolerance allowed for the chloride permeability test.

Comparison of permeability of cores from field and specimens from Laboratory

As shown in Table 7.1, the chloride permeability of field samples and laboratory samples for a compaction effort of 30 sec. were 2033 and 2333 coulombs., 2518 and 2611 coulombs., 2786 and 2366 coulombs., and 2492 and 2141 respectively for plain LSDC, NMFRC with 11.9 Kg/m^3 (20 lbs/yd^3), NMFRC with 14.8 Kg/m^3 (25 lbs/yd^3), and NMFRC with 14.8 Kg/m^3 (25 lbs/yd^3) used in Sturgis bridge overlay.

The chloride permeability of the cores from the field was almost equal to the permeability of the specimens cast in the laboratory with 30 sec. vibration. This indicated that the consolidation used in the field concrete was the same as the consolidation provided in the laboratory for NMFRC. However the field concrete as well as the laboratory concrete needed more consolidation in order to eliminate the small amounts of voids. If NMFRC had been consolidated more, then its permeability would be lower than that of LSDC. It was observed in a few cases that the cores, which had voids, had higher permeability than the average. Therefore we could conclude that chloride permeability mainly depends on two major factors: the cement content and the compaction effort used. The addition of fibers did not seem to have much influence on the chloride permeability of the concrete.

Based on the field and laboratory study, it can be concluded that the addition of fibers either at 11.9 or 14.8 Kg/m^3 (20 or 25 lbs/yd^3) did not change the potential for chloride permeability in the plain LSDC.

Comparison of dry densities of cores from field and specimens cast in the laboratory

The dry density of the field concrete seemed to be the same for NMFRC and for plain LSDC except for the NMFRC concrete from the North half of the South bound lane of the bridge at Exit 212, I 90 (Vivian), which had a higher value. The densities of concrete cast in the laboratory depended on the compaction effort used. As the

compaction effort increased, there was a consistent increase in the density as seen from the Table 7.2.

It was observed that the densities of the concrete cores taken from the field were less than the densities of the concrete specimens cast in laboratory. The field concrete was drier with considerably less moisture content during the test when compared to the specimens cast in laboratory which had more moisture since the test was conducted on surface dried specimens after 28 days of curing. Figures 7.6 to 7.10 give the comparison of the dry densities for the specimens cast in the laboratory with different compacting efforts.

Comparison of fresh and hardened concrete properties for the field and laboratory concretes

Even though it was not required according to the contract, this comparison was done in order to make the study more complete. Table 7.3 gives the comparison of fresh concrete properties of the lab mixes with the data from the field. Figures 7.11 to 7.14 give the comparison of concrete temperature, unit weight, slump and air content of the concrete cast in the laboratory with the field data. Table 7.4 gives the comparison of the hardened concrete properties of the laboratory mixes with the data from the field concrete. Figures 7.15 to 7.20 give the comparison of the compressive strength, static modulus, first crack strength, maximum flexural strength, Japanese standard toughness and the Japanese standard equivalent flexural strength for the laboratory mixes and the field data. Table 7.5 gives the comparison of the ASTM toughness indices for the laboratory mixes and the field data. Figures 7.21 to 7.26 give the comparison of the first crack toughness, toughness indices I5, I10 and I20 and toughness ratios I10/I5 and I20/I10 for the laboratory mixes and the field data from records.

Both fresh concrete and hardened concrete properties of the concrete made in the laboratory were almost the same as the values recorded for the corresponding mixes made in the field. All the differences in values between laboratory and field concretes were found to be within the tolerance allowed in concrete testing.

**Table 7.1: Comparison of Permeabilities of Cores from Field
and Cylinders Cast in Lab**

Cores from field		Cylinders Cast in Lab		
Location	Charge * (Coloumbs)	Specimen #	Compactive Effort	Charge ** (Coloumbs)
North Bound Lane of Bridge at Exit 212, I 90 (Vivian) Plain LSD Concrete	2033	1A-1 to 4	No Vibration	***
		1B-1 to 4	Rodding	4047
		1C-1 to 4	10 sec. Vibration	5039
		1D-1 to 4	20 sec. Vibration	3742
		1E-1 to 4	30 sec. Vibration	2333
North Half of the South Bound Lane of the Bridge at Exit 212, I 90 (Vivian) NMFRC - Fiber @ 20 lbs/cu.yd.	2518	2A-1 to 4	No Vibration	***
		2B-1 to 4	Rodding	4406
		2C-1 to 4	10 sec. Vibration	4492
		2D-1 to 4	20 sec. Vibration	3343
		2E-1 to 4	30 sec. Vibration	2611
South Half of the South Bound Lane of the Bridge at Exit 212, I 90 (Vivian) NMFRC - Fiber @ 25 lbs/cu.yd.	2796	3A-1 to 4	No Vibration	***
		3B-1 to 4	Rodding	4322
		3C-1 to 4	10 sec. Vibration	4563
		3D-1 to 4	20 sec. Vibration	4292
		3E-1 to 4	30 sec. Vibration	2366
Approach to the bridge at Exit 212, I 90 (Vivian) Whitetopping: Fiber @ 25 lbs/cu.yd.	4686	4A-1 to 4	No Vibration	***
		4B-1 to 4	Rodding	
		4C-1 to 4	10 sec. Vibration	
		4D-1 to 4	20 sec. Vibration	
		4E-1 to 4	30 sec. Vibration	
Overlay on Bridge at Exit 32, I 90 (Sturgis) NMFRC - Fiber @ 25 lbs/cu.yd.	2492	5A-1 to 4	No Vibration	***
		5B-1 to 4	Rodding	3167
		5C-1 to 4	10 sec. Vibration	4205
		5D-1 to 4	20 sec. Vibration	3183
		5E-1 to 4	30 sec. Vibration	2141

* The permeability values of the cores from field are the average of three readings for all the locations on the interchange bridge at exit 212, I 90 (Vivian) and are the average of seven readings from the bridge at Exit 32, I 90 (Sturgis)

** The permeability values of the cylinders cast in lab are the average of four readings

*** The permeability of the specimens in the series A were not determined, because there were too many voids and hence they were expected to give very high permeability values and damage the instrument.

Note: The individual laboratory and field RCPT values are given in Appendix B

Table 7.2: Comparison of Dry Densities of Cores from Field and Cylinders Cast in Lab

Cores from field		Cylinders Cast in Lab		
Location	Density (lbs/ft ³)	Specimen #	Compactive Effort	Density (lbs/ft ³)
North Bound Lane of Bridge at Exit 212, I 90 (Vivian) Plain LSD Concrete	136.9	1A-1 to 4	No Vibration	141.5
		1B-1 to 4	Rodding	143.3
		1C-1 to 4	10 sec. Vibration	142.9
		1D-1 to 4	20 sec. Vibration	144.8
		1E-1 to 4	30 sec. Vibration	146.2
North Half of the South Bound Lane of the Bridge at Exit 212, I 90 (Vivian) NMFRC - Fiber @ 20 lbs/cu.yd.	141.5	2A-1 to 4	No Vibration	142.8
		2B-1 to 4	Rodding	144.5
		2C-1 to 4	10 sec. Vibration	143.5
		2D-1 to 4	20 sec. Vibration	144.8
		2E-1 to 4	30 sec. Vibration	145.6
South Half of the South Bound Lane of the Bridge at Exit 212, I 90 (Vivian) NMFRC - Fiber @ 25 lbs/cu.yd.	139.2	3A-1 to 4	No Vibration	140.5
		3B-1 to 4	Rodding	143.3
		3C-1 to 4	10 sec. Vibration	141.4
		3D-1 to 4	20 sec. Vibration	143.9
		3E-1 to 4	30 sec. Vibration	145.9
Approach to the bridge at Exit 212, I 90 (Vivian) Whitetopping: Fiber @ 25 lbs/cu.yd.	136.0	4A-1 to 4	No Vibration	132.2
		4B-1 to 4	Rodding	144.2
		4C-1 to 4	10 sec. Vibration	139.4
		4D-1 to 4	20 sec. Vibration	143.6
		4E-1 to 4	30 sec. Vibration	147.2
Overlay on Bridge at Exit 32, I 90 (Sturgis) NMFRC - Fiber @ 25 lbs/cu.yd.	137.0	5A-1 to 4	No Vibration	138.2
		5B-1 to 4	Rodding	141.1
		5C-1 to 4	10 sec. Vibration	140.8
		5D-1 to 4	20 sec. Vibration	144.4
		5E-1 to 4	30 sec. Vibration	145.5

- Notes:
1. The density values of the cores from field are the average of three readings for all the locations on the interchange bridge at exit 212, I 90 (Vivian) and are the average of eight readings from the bridge at Exit 32, I 90 (Sturgis)
 2. The density values of the cylinders cast in lab are the average of four readings

Table 7.3: Comparison of the Properties of Fresh Concrete from Record and Lab Mixes

Property	Location	From Record		From the lab Mix	
		Value	Record #	Value	Mix #
Concrete Temperature (F)	NB Lane @ Exit 212 (Plain Concrete)	75.0	SD94-04-I	60.8	1
	SB Lane @ Exit 212 (NMFRFC-20 lbs/cu.yd.)	68.5	SD94-04-I	59.2	2
	SB Lane @ Exit 212 (NMFRFC-25 lbs/cu.yd.)	82.0	SD94-04-I	60.5	3
	Approach @ Exit 212 (Whitetopping)	77.0	SD94-04-I	66.7	4
	Bridge @ Exit 32	67.0	SD97-11-F	62.9	5
Unit Weight (lb/cu.ft.)	NB Lane @ Exit 212 (Plain Concrete)	145.0	SD94-04-I	144.8	1
	SB Lane @ Exit 212 (NMFRFC-20 lbs/cu.yd.)	145.6	SD94-04-I	145.2	2
	SB Lane @ Exit 212 (NMFRFC-25 lbs/cu.yd.)	148.3	SD94-04-I	142.0	3
	Approach @ Exit 212 (Whitetopping)	143.7	SD94-04-I	138.8	4
	Bridge @ Exit 32	146.0	SD97-11-F	147.2	5
Slump (in.)	NB Lane @ Exit 212 (Plain Concrete)	1.0	SD94-04-I	1.3	1
	SB Lane @ Exit 212 (NMFRFC-20 lbs/cu.yd.)	0.8	SD94-04-I	0.3	2
	SB Lane @ Exit 212 (NMFRFC-25 lbs/cu.yd.)	0.5	SD94-04-I	0.3	3
	Approach @ Exit 212 (Whitetopping)	4.0	SD94-04-I	4.5	4
	Bridge @ Exit 32	0.5	SD97-11-F	0.3	5
Air Content (%)	NB Lane @ Exit 212 (Plain Concrete)	6.2	SD94-04-I	4.8	1
	SB Lane @ Exit 212 (NMFRFC-20 lbs/cu.yd.)	5.4	SD94-04-I	4.8	2
	SB Lane @ Exit 212 (NMFRFC-25 lbs/cu.yd.)	6.0	SD94-04-I	5.6	3
	Approach @ Exit 212 (Whitetopping)	6.1	SD94-04-I	6.0	4
	Bridge @ Exit 32	3.9	SD97-11-F	4.6	5

Table 7.4: Comparison of the Properties of Hardened Concrete from Record and Lab Mixes

Property	Location	From Record		From the lab Mix	
		Value	Record #	Value	Mix #
Compressive Strength (psi)	NB Lane @ Exit 212 (Plain Concrete)	6420	SD94-04-I	7938	1
	SB Lane @ Exit 212 (FRC-20 lbs/cu.yd.)	6160	SD94-04-I	7595	2
	SB Lane @ Exit 212 (FRC-25 lbs/cu.yd.)	5445	SD94-04-I	6969	3
	Approach @ Exit 212 (Whitetopping)	5155	SD94-04-I	5353	4
	Bridge @ Exit 32	6539	SD97-11-F	8456	5
Static Modulus (x10⁶ psi)	NB Lane @ Exit 212 (Plain Concrete)	5.34	SD94-04-I	5.84	1
	SB Lane @ Exit 212 (FRC-20 lbs/cu.yd.)	5.33	SD94-04-I	5.46	2
	SB Lane @ Exit 212 (FRC-25 lbs/cu.yd.)	4.26	SD94-04-I	5.03	3
	Approach @ Exit 212 (Whitetopping)	4.86	SD94-04-I	4.98	4
	Bridge @ Exit 32	5.32	SD97-11-F	6.15	5
First Crack Strength (psi)	NB Lane @ Exit 212 (Plain Concrete)	800	SD94-04-I	987	1
	SB Lane @ Exit 212 (FRC-20 lbs/cu.yd.)	803	SD94-04-I	863	2
	SB Lane @ Exit 212 (FRC-25 lbs/cu.yd.)	778	SD94-04-I	758	3
	Approach @ Exit 212 (Whitetopping)	654	SD94-04-I	660	4
	Bridge @ Exit 32	647	SD97-11-F	801	5
Maximum Flexural Strength (psi)	NB Lane @ Exit 212 (Plain Concrete)	800	SD94-04-I	987	1
	SB Lane @ Exit 212 (FRC-20 lbs/cu.yd.)	845	SD94-04-I	902	2
	SB Lane @ Exit 212 (FRC-25 lbs/cu.yd.)	810	SD94-04-I	823	3
	Approach @ Exit 212 (Whitetopping)	708	SD94-04-I	694	4
	Bridge @ Exit 32	858	SD97-11-F	843	5
Japanese Standard Toughness (in.lbs)	NB Lane @ Exit 212 (Plain Concrete)		SD94-04-I		1
	SB Lane @ Exit 212 (FRC-20 lbs/cu.yd.)	176	SD94-04-I	179	2
	SB Lane @ Exit 212 (FRC-25 lbs/cu.yd.)	190	SD94-04-I	193	3
	Approach @ Exit 212 (Whitetopping)	194	SD94-04-I	196	4
	Bridge @ Exit 32	171	SD97-11-F	176	5
Japanese Standard Equivalent Flexural Strength (psi)	NB Lane @ Exit 212 (Plain Concrete)		SD94-04-I		1
	SB Lane @ Exit 212 (FRC-20 lbs/cu.yd.)	392	SD94-04-I	387	2
	SB Lane @ Exit 212 (FRC-25 lbs/cu.yd.)	415	SD94-04-I	425	3
	Approach @ Exit 212 (Whitetopping)	420	SD94-04-I	432	4
	Bridge @ Exit 32	378	SD97-11-F	404	5

**Table 7.5: Comparison of the Properties of Hardened Concrete from
Record and Lab Mixes
(ASTM Toughness Indices)**

Property		Location	From Record		From the lab Mix	
			Value	Record #	Value	Mix #
First Crack Toughness (in.lbs)		SB Lane @ Exit 212 (NMFC-20 lbs/cu.yd.)	3.1	SD94-04-I	3.4	2
		SB Lane @ Exit 212 (NMFC-25 lbs/cu.yd.)	3.4	SD94-04-I	3.6	3
		Approach @ Exit 212 (Whitetopping)	2.5	SD94-04-I	2.7	4
		Bridge @ Exit 32	1.9	SD97-11-F	1.9	5
Toughness Indices	I 5	SB Lane @ Exit 212 (NMFC-20 lbs/cu.yd.)	4.56	SD94-04-I	4.57	2
		SB Lane @ Exit 212 (NMFC-25 lbs/cu.yd.)	4.09	SD94-04-I	4.18	3
		Approach @ Exit 212 (Whitetopping)	4.58	SD94-04-I	4.63	4
		Bridge @ Exit 32	4.88	SD97-11-F	5.02	5
	I 10	SB Lane @ Exit 212 (NMFC-20 lbs/cu.yd.)	8.72	SD94-04-I	8.76	2
		SB Lane @ Exit 212 (NMFC-25 lbs/cu.yd.)	7.27	SD94-04-I	7.16	3
		Approach @ Exit 212 (Whitetopping)	8.69	SD94-04-I	8.75	4
		Bridge @ Exit 32	9.67	SD97-11-F	9.87	5
	I 20	SB Lane @ Exit 212 (NMFC-20 lbs/cu.yd.)	16.03	SD94-04-I	16.56	2
		SB Lane @ Exit 212 (NMFC-25 lbs/cu.yd.)	11.83	SD94-04-I	11.72	3
		Approach @ Exit 212 (Whitetopping)	15.78	SD94-04-I	16.12	4
		Bridge @ Exit 32	17.70	SD97-11-F	17.98	5
Toughness Ratios	I 10/15	SB Lane @ Exit 212 (NMFC-20 lbs/cu.yd.)	1.91	SD94-04-I	1.92	2
		SB Lane @ Exit 212 (NMFC-25 lbs/cu.yd.)	1.78	SD94-04-I	1.72	3
		Approach @ Exit 212 (Whitetopping)	1.89	SD94-04-I	1.89	4
		Bridge @ Exit 32	1.98	SD97-11-F	1.97	5
	I 20/10	SB Lane @ Exit 212 (NMFC-20 lbs/cu.yd.)	1.84	SD94-04-I	1.89	2
		SB Lane @ Exit 212 (NMFC-25 lbs/cu.yd.)	1.62	SD94-04-I	1.64	3
		Approach @ Exit 212 (Whitetopping)	1.81	SD94-04-I	1.84	4
		Bridge @ Exit 32	1.83	SD97-11-F	1.84	5

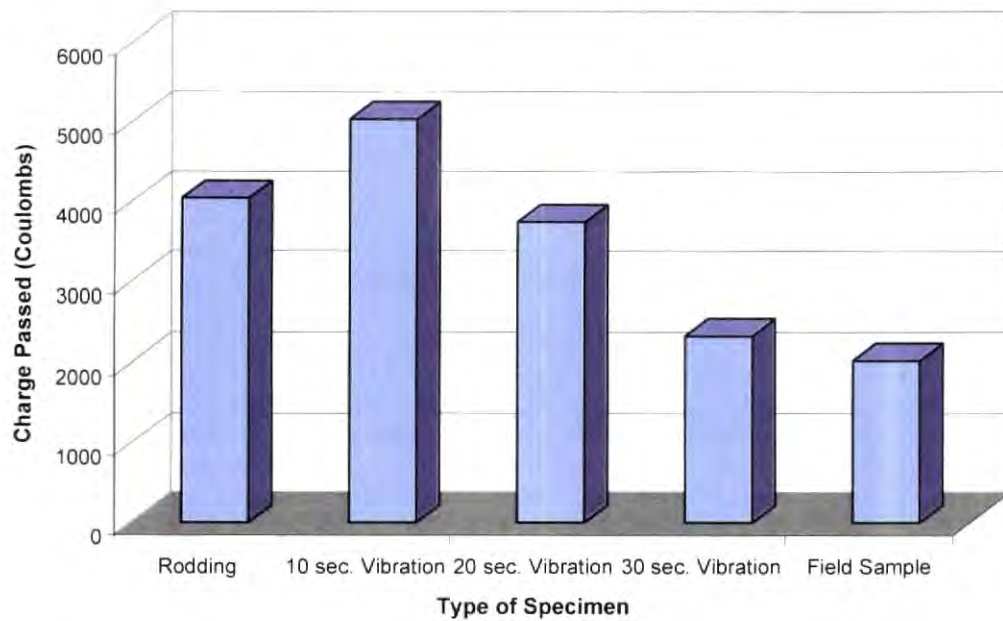


Figure 7.1: Comparison of Permeabilities of Cores from Field on the North Bound Lane of the Bridge at Exit 212, I 90 (Vivian) and Cylinders cast in Lab

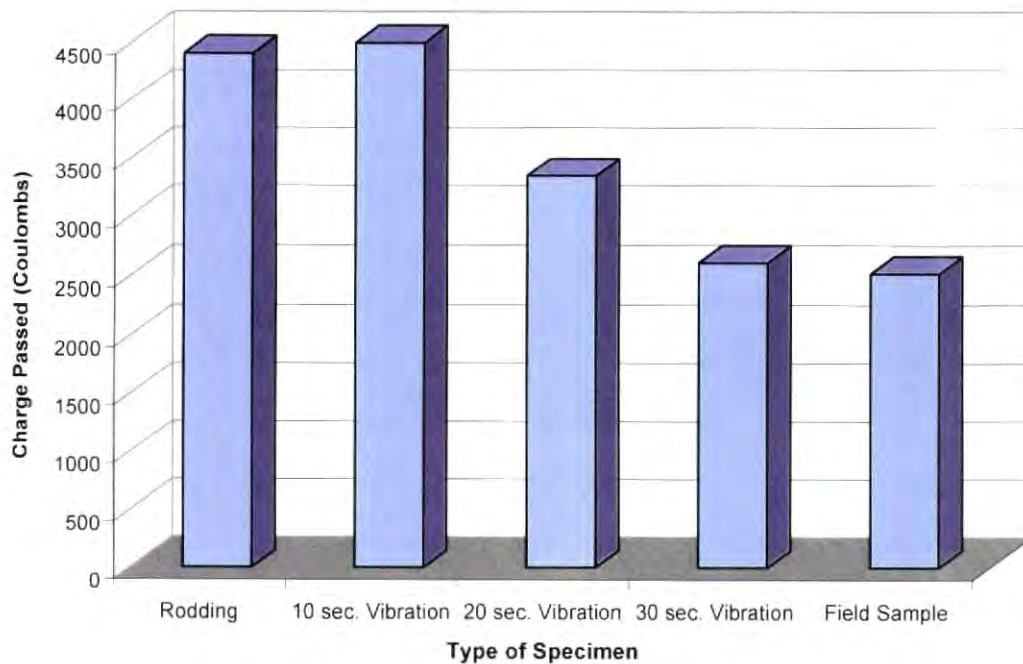


Figure 7.2: Comparison of Permeabilities of Cores from Field on the North Half of the South Bound Lane of the Bridge at Exit 212, I 90 (Vivian) and Cylinders cast in Lab

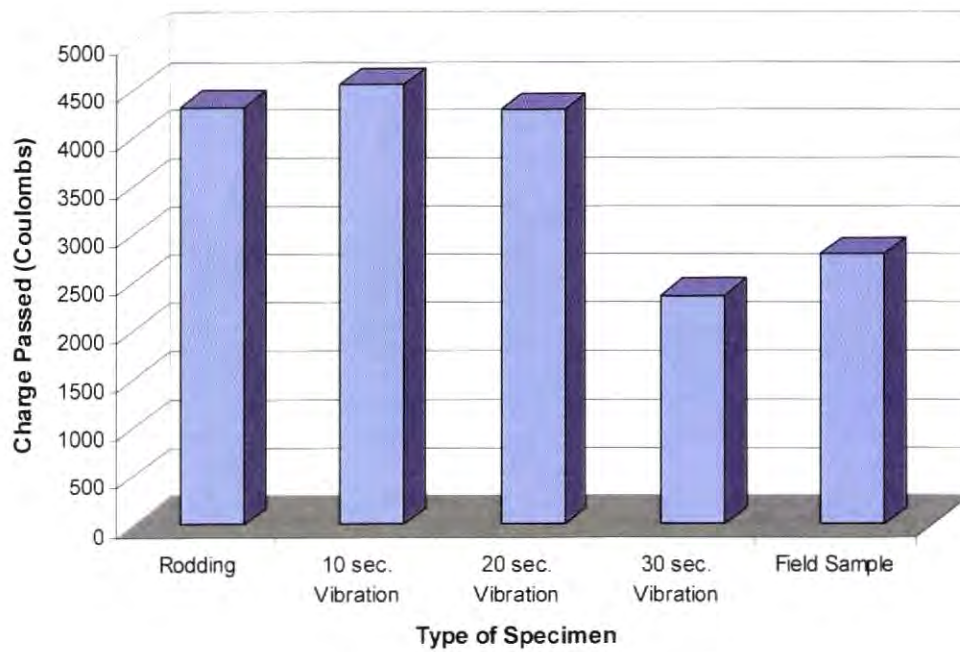


Figure 7.3: Comparison of Permeabilities of Cores from Field on the South Half of the South Bound Lane of the Bridge at Exit 212, I 90 (Vivian) and Cylinders cast in Lab

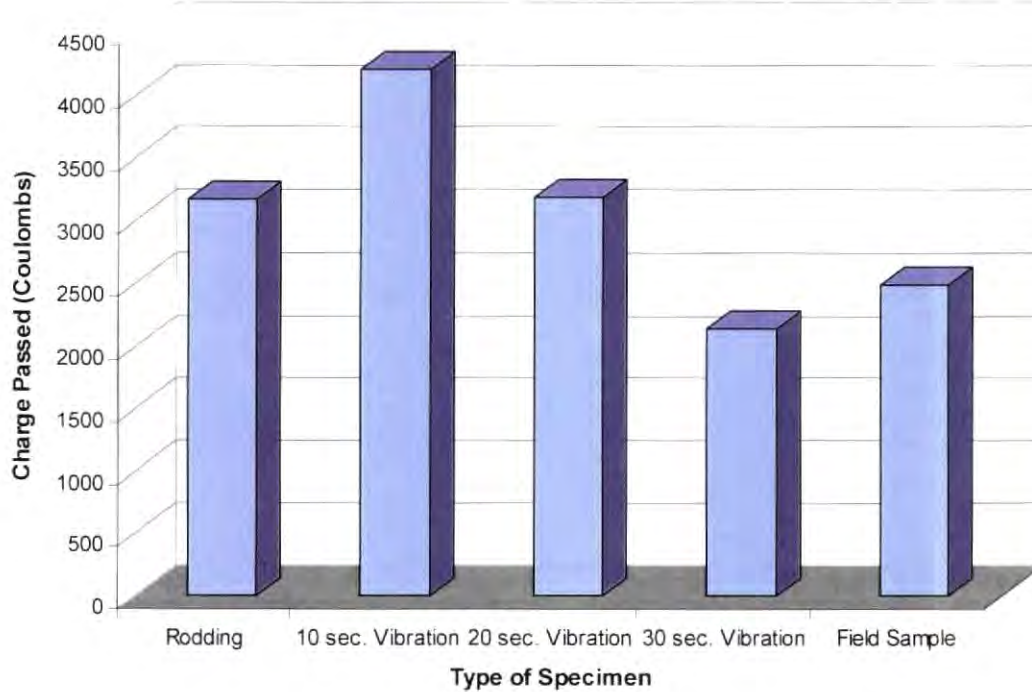


Figure 7.5: Comparison of Permeabilities of Cores from Field on the Bridge at Exit 32, I 90 (Sturgis) and Cylinders cast in Lab

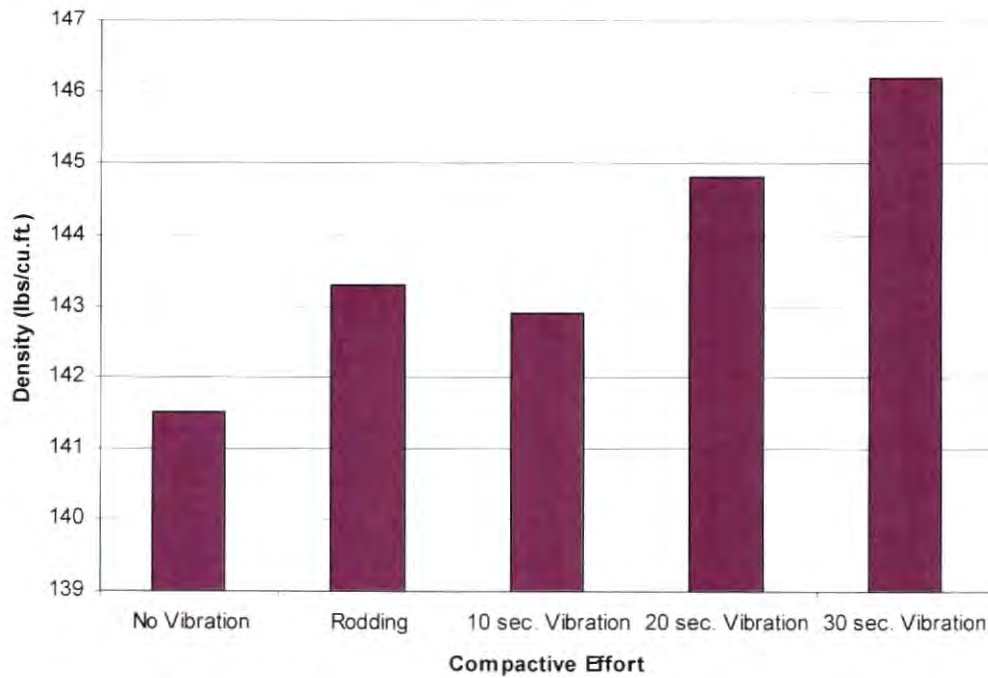


Figure 7.6: Comparison of Densities of Cylinders cast in Lab (North Bound lane of the Bridge at Exit 212, I 90 (Vivian))

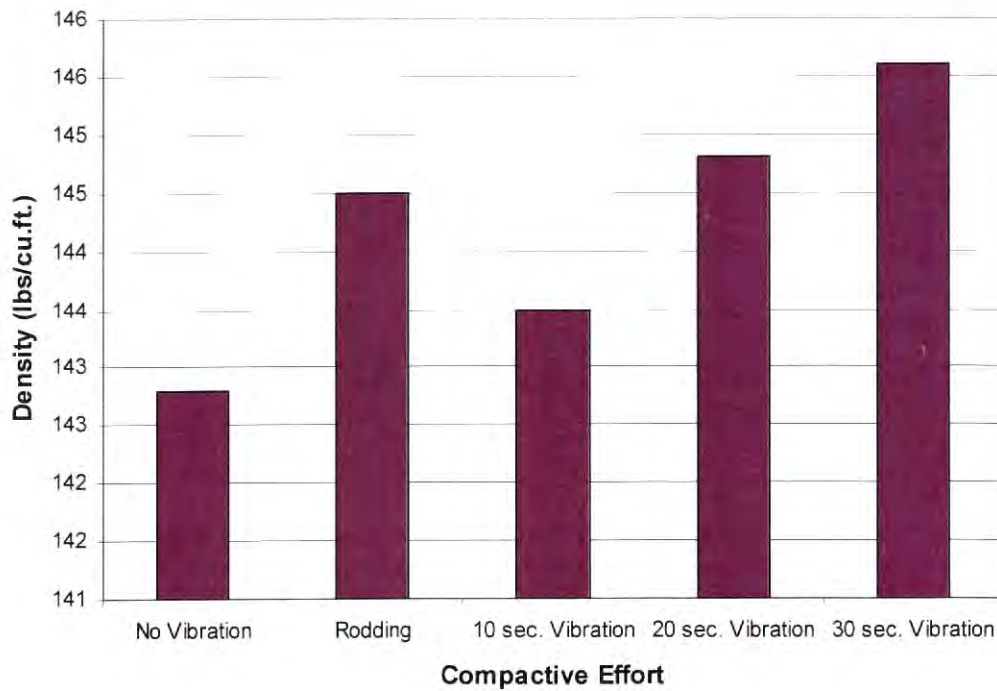


Figure 7.7: Comparison of Densities of Cylinders cast in Lab (North Half of South Bound lane of the Bridge at Exit 212, I 90 (Vivian))

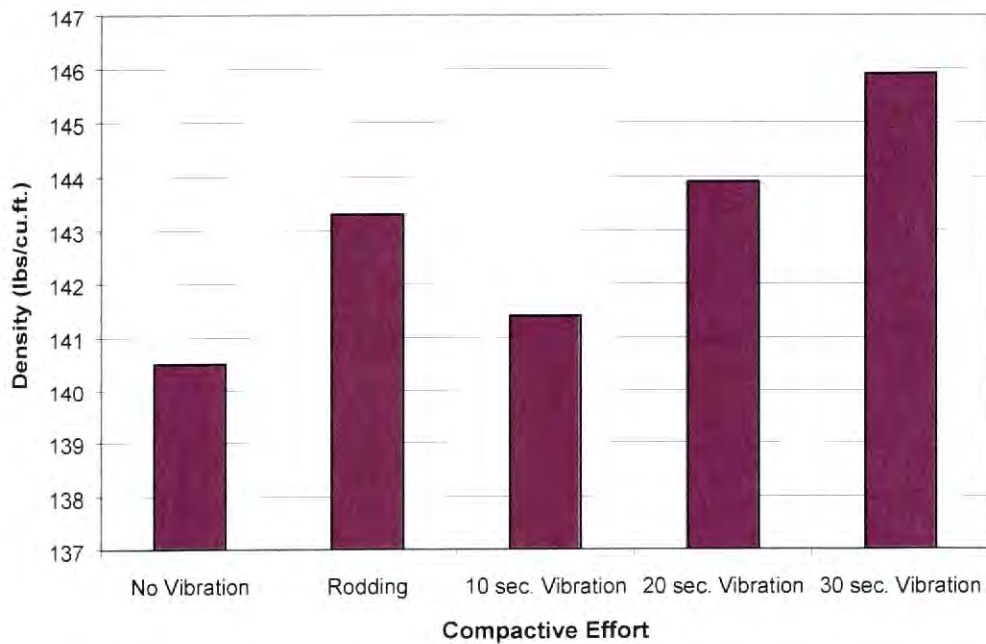


Figure 7.8: Comparison of Densities of Cylinders cast in Lab (South Half of South Bound lane of the Bridge at Exit 212, I 90 (Vivian))

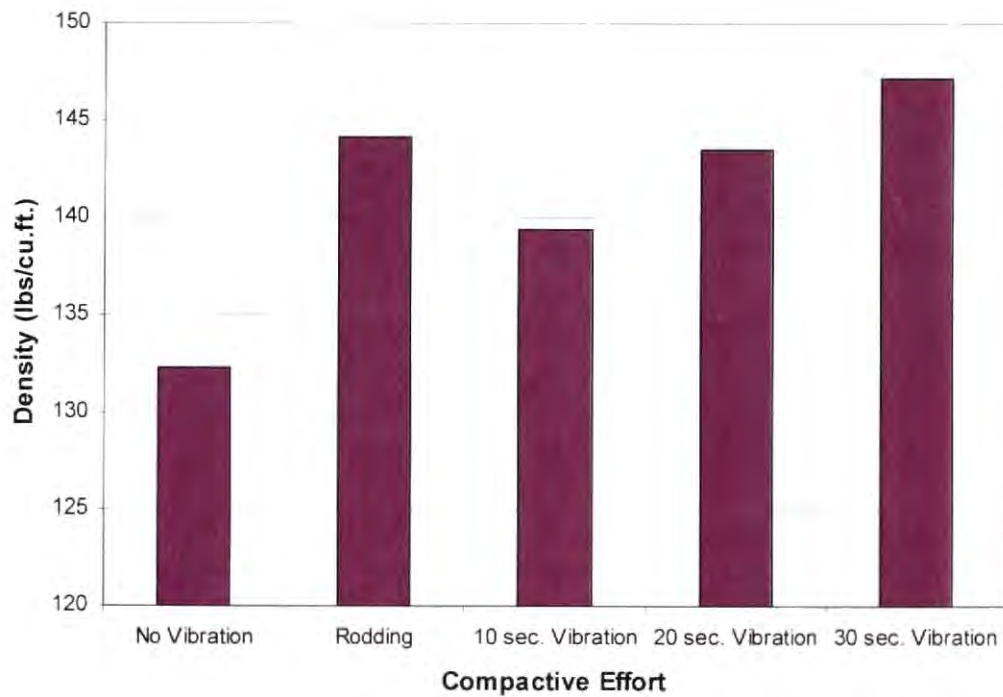


Figure 7.9: Comparison of Densities of Cylinders cast in Lab (Approach to the Bridge at Exit 212, I 90 (Vivian))

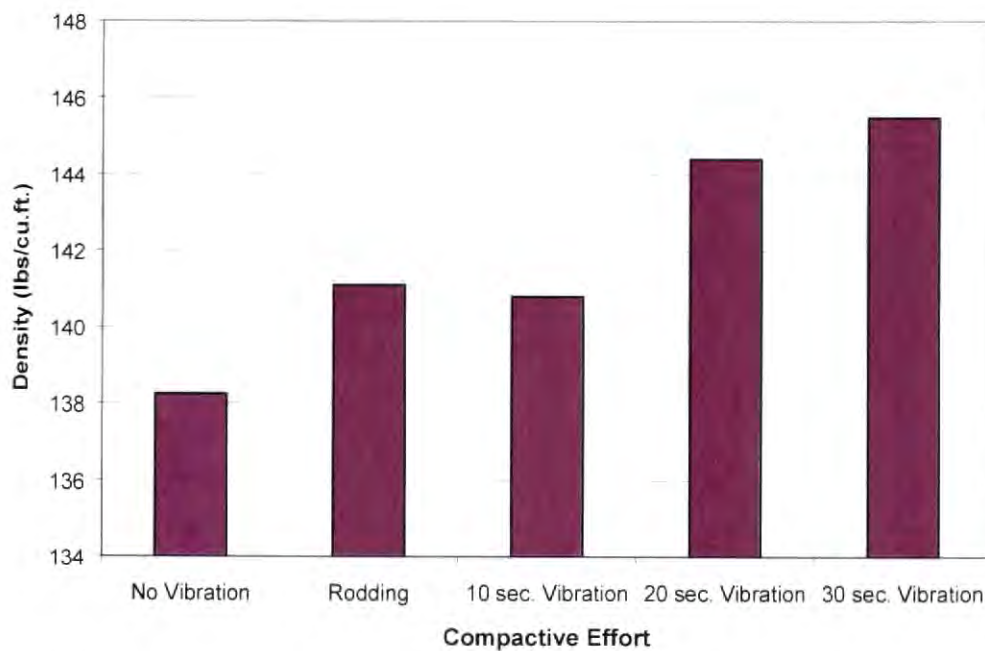


Figure 7.10: Comparison of Densities of Cylinders cast in Lab (Bridge at Exit 32, I 90 (Sturgis))

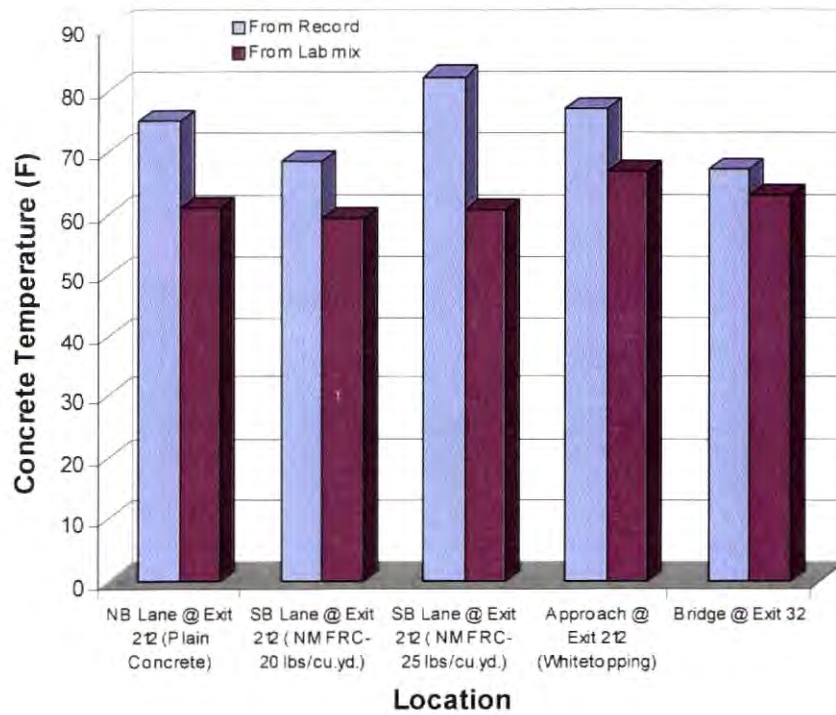


Figure 7.11: Comparison of the Concrete Temperature from Record and Lab Mixes

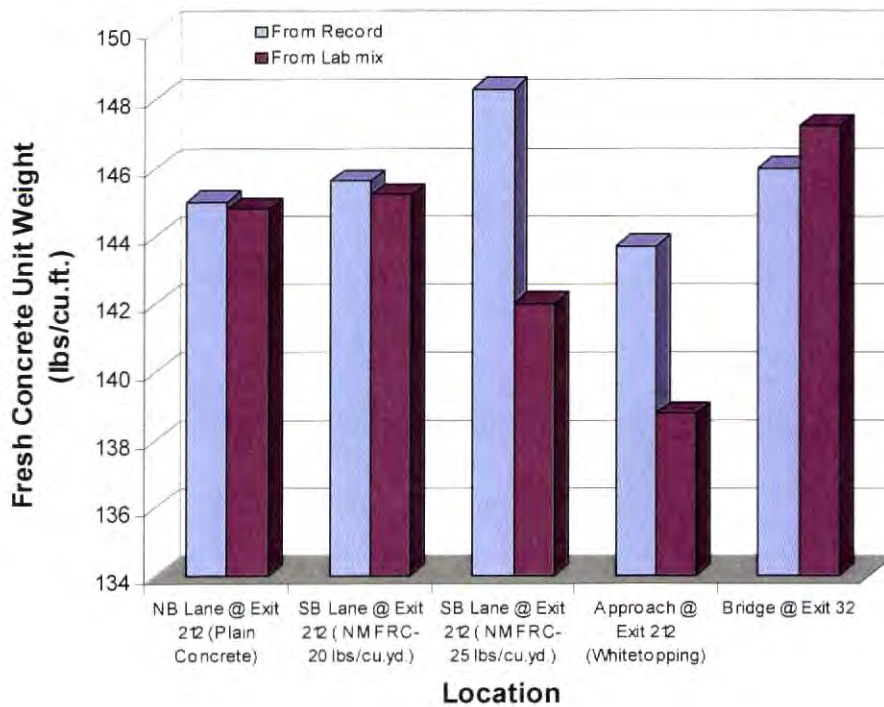


Figure 7.12: Comparison of the Fresh Concrete Unit Weight from Record and Lab Mixes

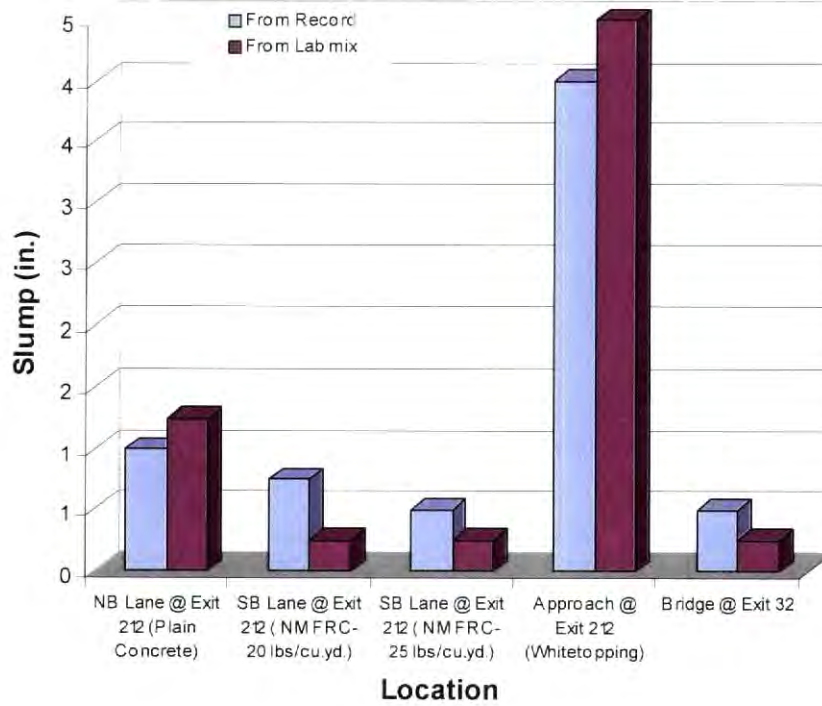


Figure 7.13: Comparison of the Slump from Record and Lab Mixes

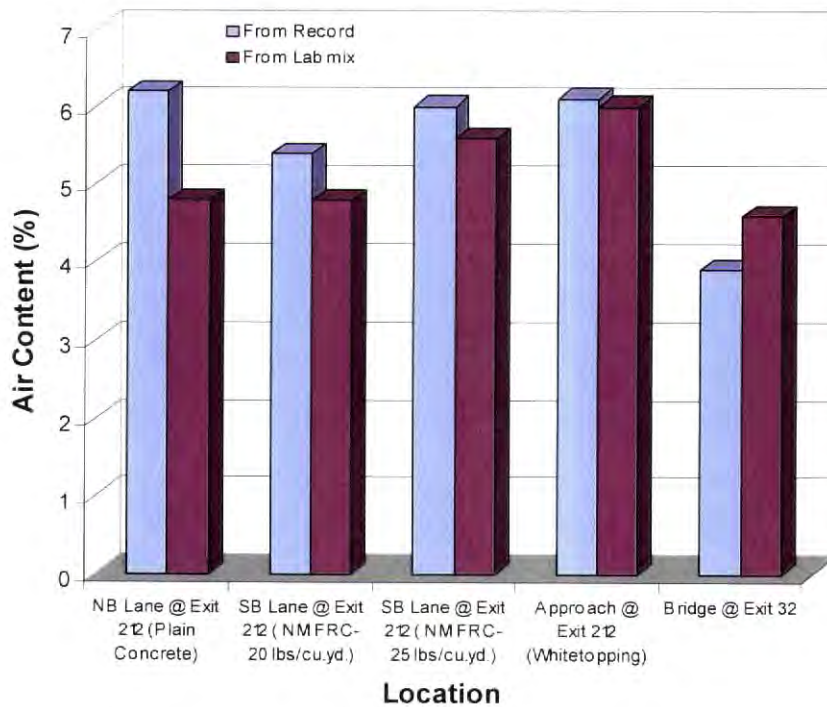


Figure 7.14: Comparison of the Air Content from Record and Lab Mixes

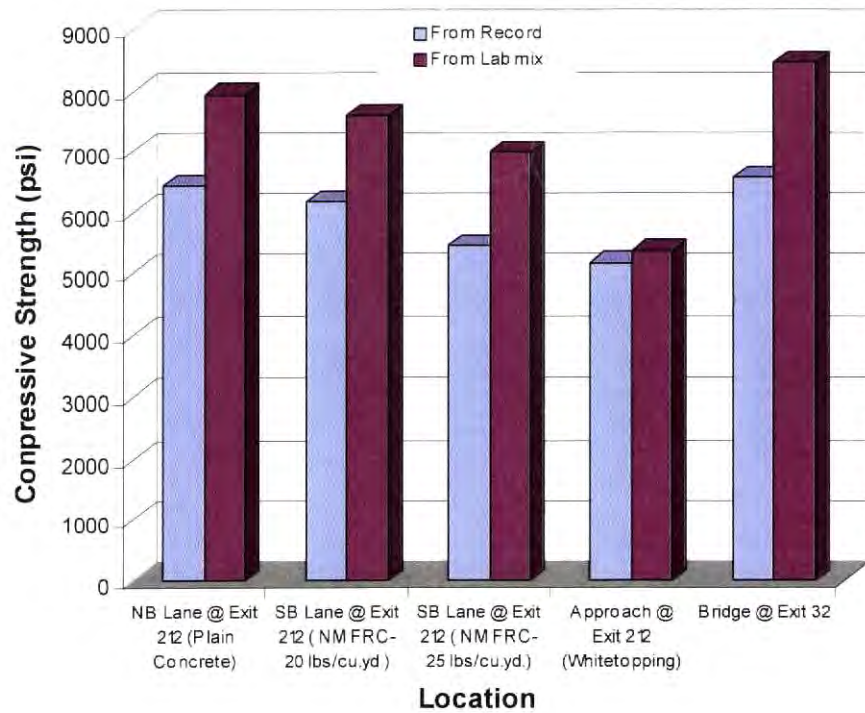


Figure 7.15: Comparison of Compressive Strength from Record and Lab Mixes

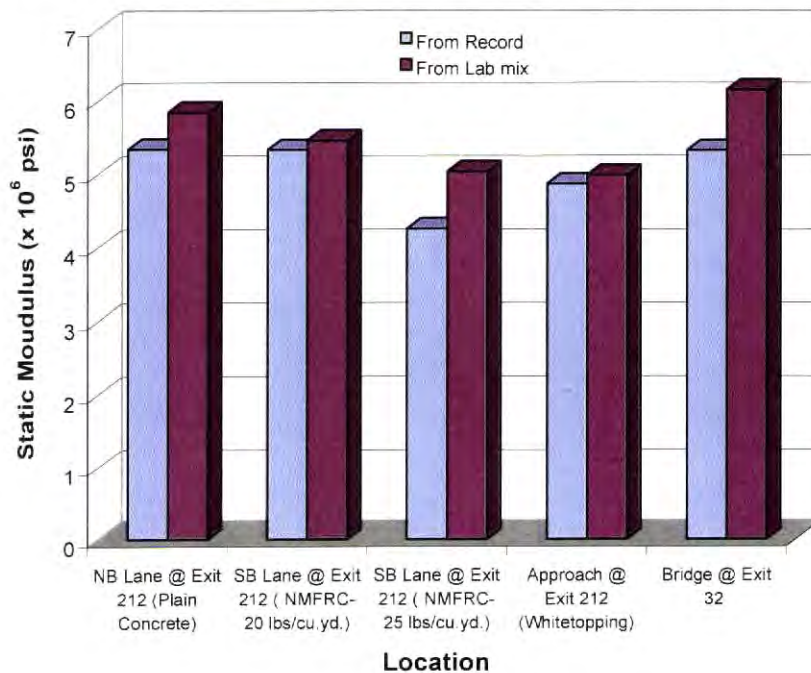


Figure 7.16: Comparison of Static Modulus from Record and Lab Mixes

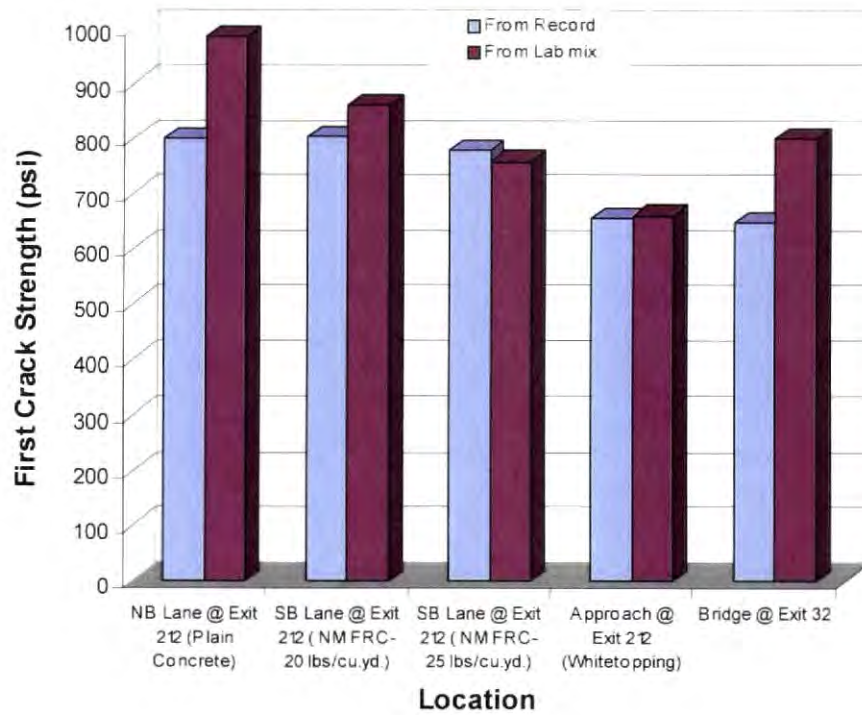


Figure 7.17: Comparison of First Crack Strength from Record and Lab Mixes

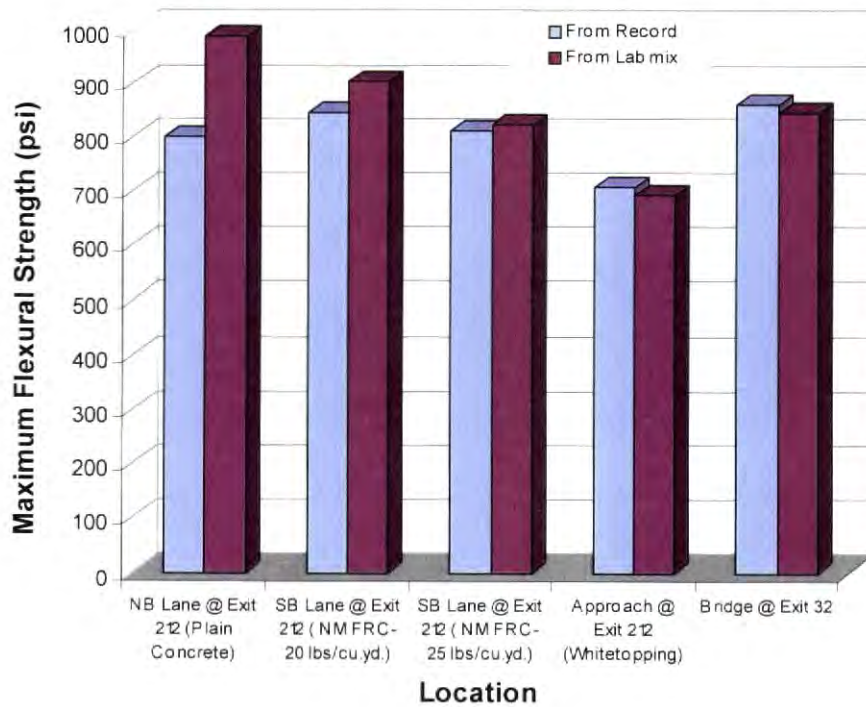


Figure 7.18: Comparison of Maximum Flexural Strength from Record and Lab Mixes

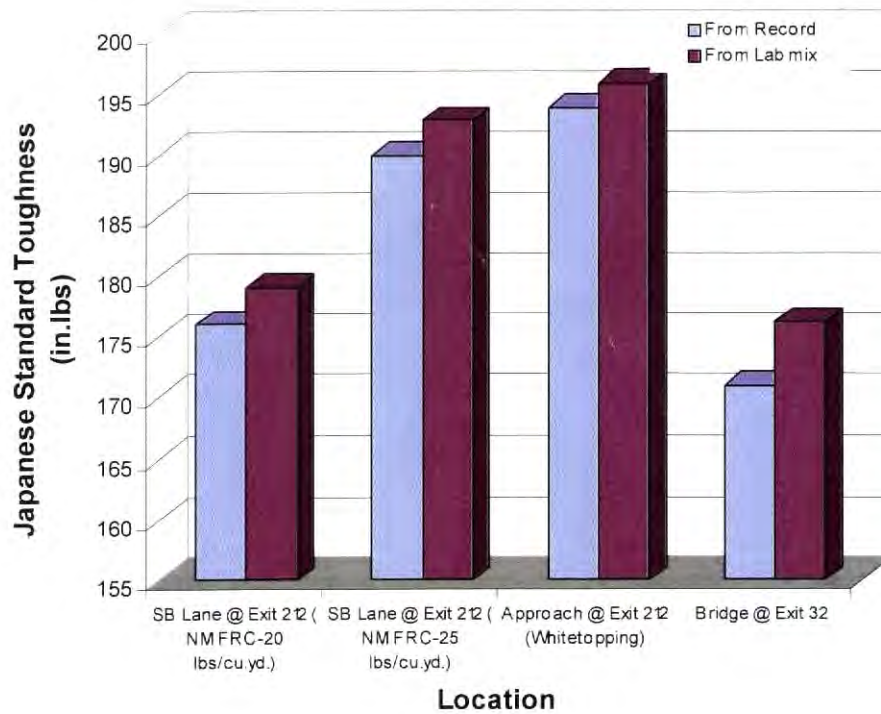


Figure 7.19: Comparison of Japanese Standard Toughness from Record and Lab Mixes

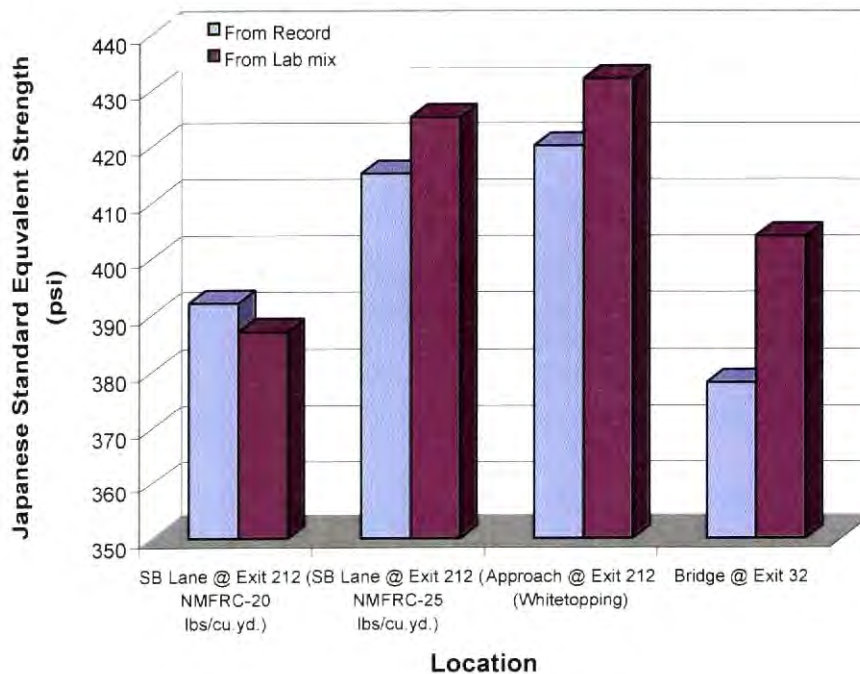


Figure 7.20: Comparison of Japanese Standard Equivalent Strength from Record and Lab Mixes

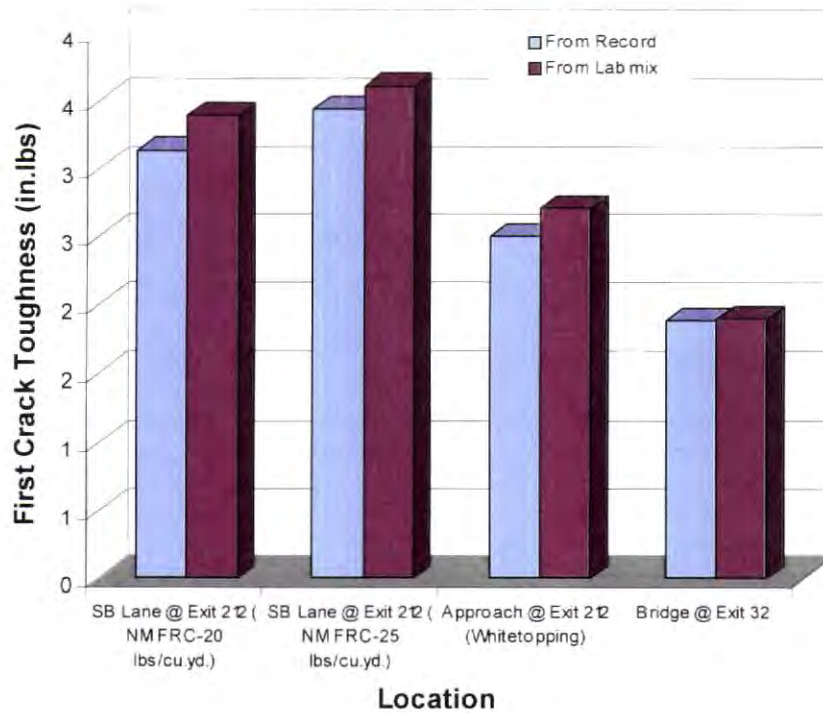


Figure 7.21: Comparison of First Crack Toughness from Record and Lab Mixes

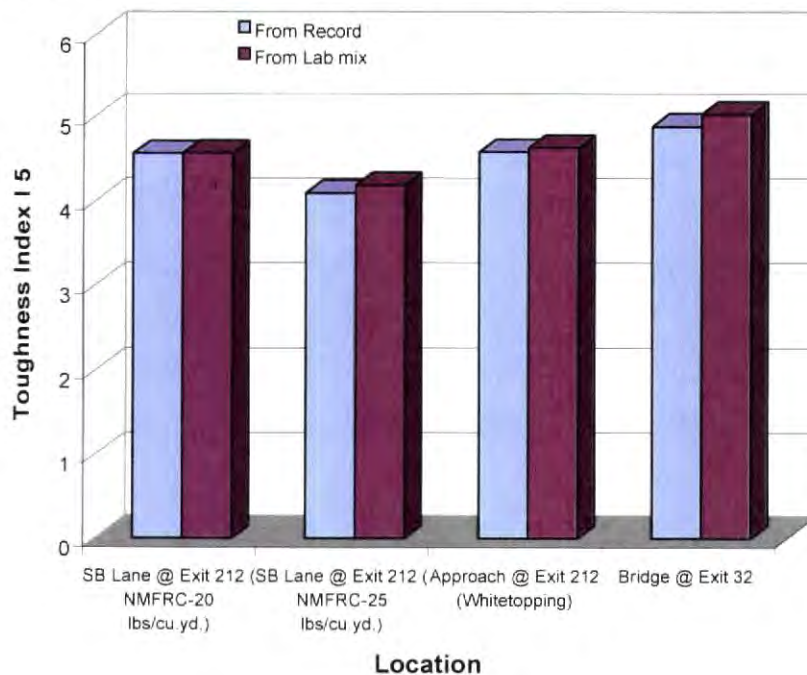


Figure 7.22: Comparison of Toughness Index I 5 from Record and Lab Mixes

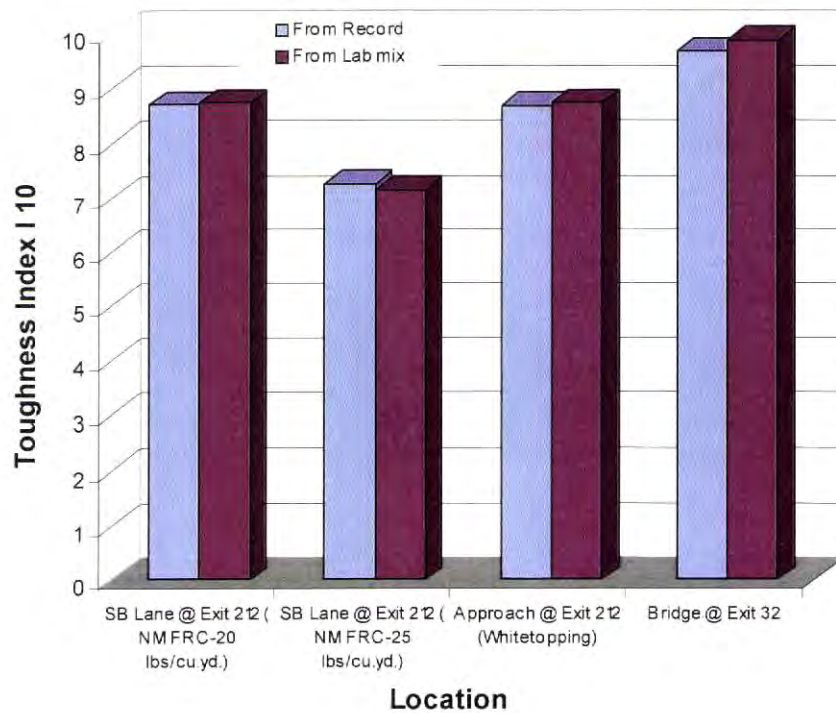


Figure 7.23: Comparison of Toughness Index I 10 from Record and Lab Mixes

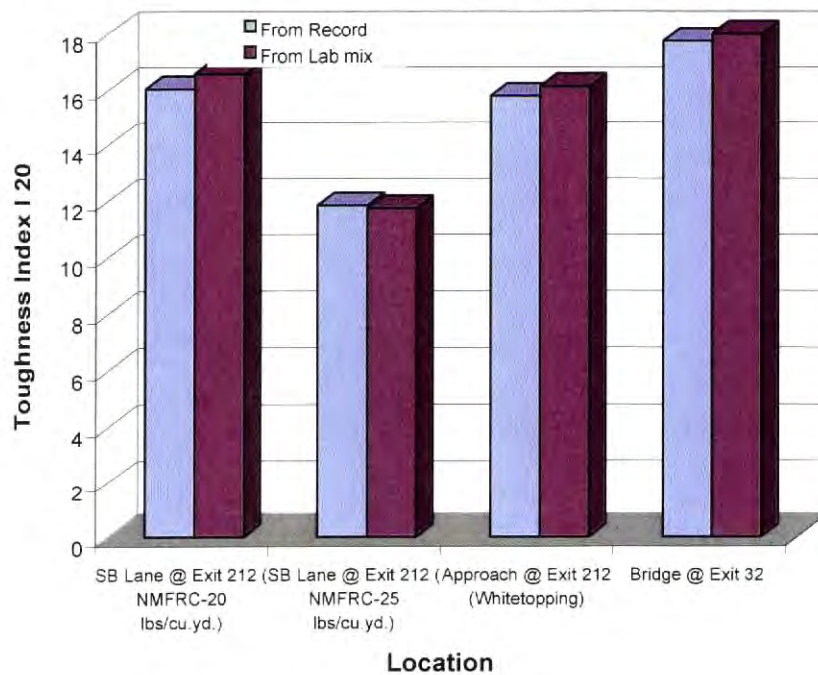


Figure 7.24: Comparison of Toughness Index I 20 from Record and Lab Mixes

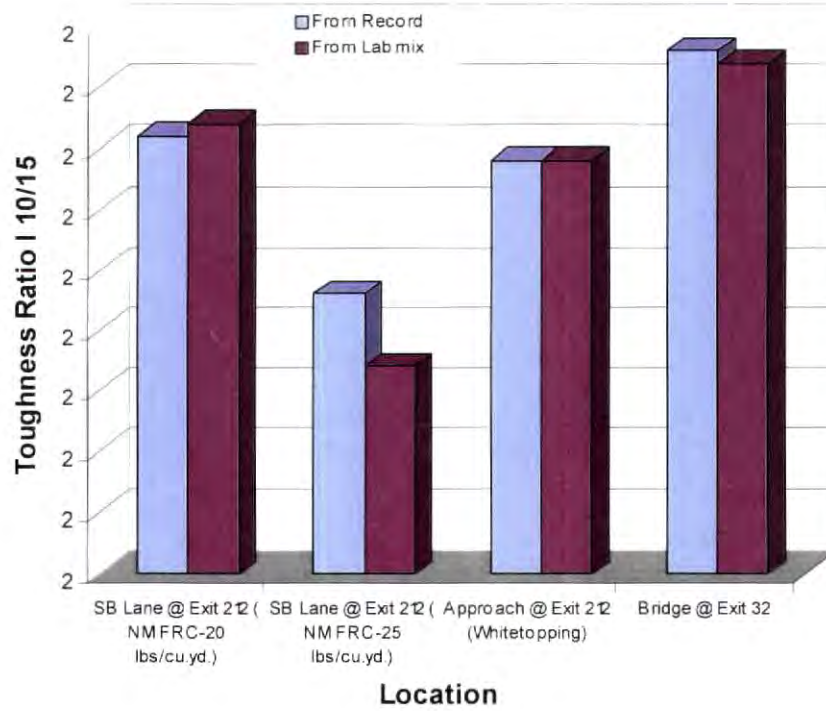


Figure 7.25: Comparison of Toughness Ratio I 10/15 from Record and Lab Mixes

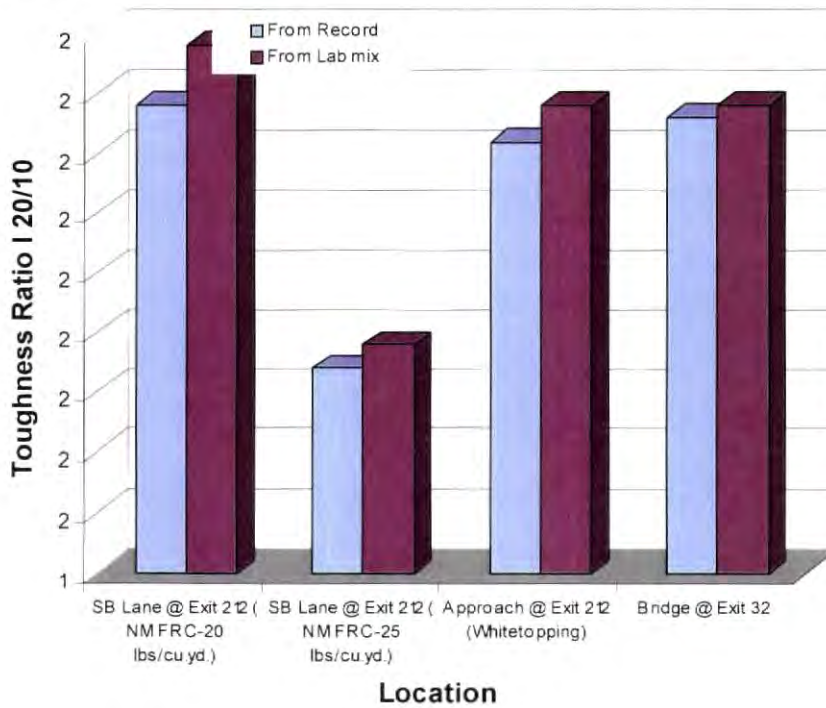


Figure 7.26: Comparison of Toughness Ratio I 20/10 from Record and Lab Mixes

Research Task 8: Identify and recommend equipment and testing requirements necessary for the development of bridge deck overlay NMFRC mix designs.

For the development of bridge deck overlay NMFRC mix designs, standard equipment available in a good concrete testing laboratory will be adequate. The equipment needed would be a concrete mixer preferably 9 cu.ft. capacity, equipment for conducting the inverted cone test ASTM C995 or a slump test if the slump is more than 50 mm (2.0 in.), air content, concrete temperature, accurate weighing scale (0.1g least count), molds (beams and cylinders), curing chamber, etc. for determination of fresh concrete properties. The equipment needed for hardened concrete property determination would be a universal testing machine for compression, flexure, and tension testing. For conducting ASTM C1018 and ASTM C 1399, the machine must be capable of deflection control and load control tests. A good data logging system would be needed to record the load and deflections automatically and continuously. The laboratory must have the facilities to conduct all the quality control tests mentioned in Task 9.

With trial and error, it is possible to optimize the mix design for the specified fresh and hardened concrete properties with varying the fiber dosages. Extensive research done at SDSM&T had shown that the addition of 14.8 Kg/m³ (25 lbs/yd³) would be an ideal fiber dosage for bridge deck overlay concrete.

Research Task 9: Identify and recommend necessary equipment, tests, and procedures required for quality control testing in the field.

Based on comparison of the permeability and density values of the cores from the field and the well-compacted laboratory specimens, it could be stated that the construction technique used and the construction equipment used in the field produced satisfactory compaction. When NMFRC is used a mobile mixture could not be used, only truck delivered concrete could be used. NMFRC needs possibly more consolidation to achieve higher impermeability than LSDC. In the case of NMFRC, the slump of the initial concrete before the addition of fibers should be higher (above 75mm (3 in.)) and reduced angle of tining fork. Other than the above mentioned modifications, all other construction techniques and

construction equipment normally used in the construction of bridge deck overlays could be used in the construction of NMFRC bridge deck overlays.

It is recommended that the same quality control tests conducted in this project for NMFRC fresh concrete namely, slump, unit weight, air content and test for actual fiber content could be specified. When the slump is less than 25 mm (1 in.), then inverted cone test ASTM C995 can be specified. The standard test procedures are described in Research Task 6. It is also recommended that the concrete temperature, the ambient temperature, humidity and the wind velocity should be recorded.

Field samples should be collected and cured using ASTM standard procedures and the following hardened concrete performance tests should be conducted for NMFRC at 28-days: compressive strength, elastic modulus, flexural strength (modulus of rupture), and toughness values (ASTM and Japanese standards). An optional test that could be specified is the fatigue test for FRC. The test procedure is included in a previous report (1). The standard test procedures to be followed are described in Research Task 6. Another test which is not included in this project and which need to be performed on the NMFRC is the ASTM C1399, to determine the average residual strength of the FRC. The ASTM C1399 was introduced in the late 1999.

The tests indicated that the field bond test and the laboratory bond test gave very similar results. These tests are not yet included in the ASTM standard test procedures. Both tests indicated the real tensile strength of the concrete. Therefore it is recommended that either one or both tests could be specified, depending on the time available for closing of the highway to traffic. If longer closing time (2 hours additional) was permissible then the field bond test could be specified. The advantage of the field bond test is that it would have smaller cores drilled on the bridge deck, (which is also easy to repair) and the results would be known immediately. If longer closing of highways was not permissible, then the lab bond test is recommended. The same procedure as developed and used in this research project (Research Task 5) could be specified. This was a simple test and it gave reliable results.

For the determination of rapid chloride permeability, the ASTM C1202 test is recommended. Currently this is the best test available, even though some deficiencies had been reported in recent publications.

It is recognized that currently SDDOT does not specify any of the above recommended tests except the compressive strength test.

Research Task 10: Submit a final report summarizing relevant literature, research methodology, test results, NMFRC mix design specifications, required testing equipment, laboratory and field testing procedures, conclusions and recommendations.

The final report has been submitted which summarized all aspects of the study.

Research Task 11: Make an executive presentation to the SDDOT Research Review Board summarizing the findings and conclusions.

An executive presentation summarizing the findings and conclusions was made to the SDDOT Research Review Board on June 8, 2000.

CONCLUSIONS

1. The chloride permeability and density values of NMFRC were found to be similar to the values of the plain LSDC. This was true in both field and laboratory tests. The addition of fibers did not seem to have much influence on the chloride permeability and the density of the concrete.
2. The chloride permeability of the field cores was similar to the permeability values obtained for the specimens made in the laboratory with 30 sec. vibration. The higher initial slump, prior to the addition of fiber, did not affect the compactive effort of the deck overlay machine. The NMFRC cores taken from the field had small voids indicating that NMFRC possibly needed more consolidation. With more consolidation NMFRC would have higher impermeability than LSDC.
3. Truck delivered concrete was needed for NMFRC. Initially higher slump and reduced angle on tining fork were needed for NMFRC. The same operations for consolidation, and finishing, used for plain concrete were adequate for NMFRC.
4. Visual inspection of the cores from the bridge deck showed that many major cracks in the underlying old concrete did not propagate to the overlay concrete. Therefore it could be concluded that the NMFRC would improve the performance of the overlay by

minimizing large cracks, spalling and loss of material from the top of the deck and thus reduce the potential for hazards to the public.

5. The field and the laboratory bond strength test showed that the NMFRC was adequately bonded with the underlying concrete on the bridge deck which strengthens the acceptability of NMFRC for its usage in bridge decks overlays.
6. Both types of bond tests (field and laboratory) indicated that the failure was always due to the tensile failure of the old concrete. The bond between the old and new concrete was stronger than the tensile strength of the old concrete.

RECOMMENDATIONS

1. It is recommended that NMFRC be used for deck overlays when an overlay would be placed over badly deteriorated bridge decks. Bonded overlay is desirable to provide a composite action for the slab, which would reduce the potential tensile stresses and cracking in concrete overlays. A thin layer of cement-slurry bonding agent should be used.
2. It is recommended that the NMFRC should have the same specifications and mixture proportions as that for SDDOT's plain LSDC with the exception of the inclusions of 3M's polyolefin fibers (type 50/63) at a rate of 14.8 Kg/m^3 (25 lbs/yd^3). The LSDC specification is in SDDOT's *Standard Specifications for Roads and Bridges*. A higher slump can be permitted for NMFRC overlays. The initial slump before the addition of fibers should be high enough to accommodate these fibers such that when they are added, the slump comes down to the specified amount.
3. The same construction procedures for transporting, placing, consolidating, finishing, and curing used for construction with plain concrete be used for construction of NMFRC. For tining a reduced angle on tining fork should be used for NMFRC. The mixing should be done in a ready-mix truck or in a batch plant.
4. When NMFRC is used the following quality control tests according to ASTM procedures be conducted for the fresh concrete: slump (ASTM C143), unit weight (ASTM C138), and air content (ASTM C231). The fiber content should be determined as per the procedure given in this report. The concrete temperature, the ambient temperature,

humidity and the wind velocity be recorded during placing of the concrete. The following hardened concrete tests be conducted on field samples collected and cured according to ASTM standard procedures for NMFRC at 28 days: compressive strength (ASTM C39), elastic modulus (ASTM C469), flexural strength (ASTM C78), fatigue strength (ACI Committee 544) and toughness values (ASTM and Japanese standards). Additionally it is recommended that the test for the average residual strength (ASTM C 1399) be conducted on the hardened NMFRC. SDDOT should establish minimum specifications for each of these above tests for acceptable testing.

5. It is recommended that either the field or the laboratory bond test or both tests should be specified, depending on the time available for closing of the highway for traffic. If the longer closing time (2 hours additional) is permissible then the field bond test could be specified. If longer closing of highways was not permissible, then the lab bond test is recommended. These tests are not yet adopted as ASTM standards. Therefore the same procedure as developed and used in this research project (Research Task 5) could be specified for conducting the bond tests. Both tests are simple tests and they gave reliable results. A minimum bond strength of 0.69Mpa (100 psi) should be specified.
6. The ASTM C1202 test should be used for the determination of rapid chloride permeability. SDDOT should establish a minimum value for acceptance testing.

REFERENCES

1. Ramakrishnan, V., "Evaluation of Non-Metallic Fiber Reinforced Concrete in PCC Pavements and Structures", Report submitted to the SDDOT, No. SD94-04 I, September 1995.
2. Ramakrishnan, V., "Demonstration of Polyolefin Fiber Reinforced Concrete in a Bridge Deck Replacement", Report submitted to the SDDOT, No. SD95-22, February 1998.
3. Ramakrishnan, V., "Evaluation of Non-Metallic Fiber Reinforced Concrete in new Full Depth PCC Pavements", Report submitted to the SDDOT, No. SD96-15 F, December 1998.
4. Ramakrishnan, V., "Evaluation of Two Low-Slump Dense Non-Metallic Fiber Reinforced Concrete Deck Overlays at Exit 32 on I 90 in South Dakota", Report submitted to the SDDOT, No. SD97-11 F, June 1998.
5. Ramakrishnan, V., "Evaluation of Non-Metallic Fiber Reinforced Concrete Whitetopping", Report submitted to the SDDOT, No. SD96-13, August 1999.
6. Clear, K.C., "Time-to-Corrosion of Reinforcing Steel in Concrete Slabs", Report No. FHWA-RD-76-70, April, 1976.
7. Ramakrishnan, V., "Properties and Applications of Latex Modified Concrete", *Proceedings CANMET International Conference on Advances in Concrete Technology*, ed. V. M. Malhotra, Ottawa, Ontario, 1980, pp. 839-890.
8. Whiting, D., "Permeability of Selected Concretes", *Permeability of Concrete*, SP 108, American Concrete Institute, Detroit, 1988, pp. 195-222.
9. AASHTO Designation: T259-80 "Standard Method of Test for Resistance of Concrete to Chloride ion Penetration".
10. Perenchio, W.F., and Marusin, S.L., "Short -Term Chloride Penetration into Relatively Impermeable Concretes", *Concrete International*, Vol. 5, No. 4, pp. 37-41, April, 1983.
11. Whiting, D., "In Situ Measurement of the Permeability of Concrete to Chloride Ions" SP 82-25, *Proceedings CANMET/ACI International Conference on In Situ/Nondestructive Testing of Concrete*, ed. V. M. Malhotra, Ottawa, Canada, October, 1984, pp. 501-524.
12. Slater, J., Lankard, D., and Moreland, P.J., "Electro-Chemical Removal of Chlorides from Concrete Bridge Decks", *Materials Performance*, Vol. 15, No. 11, pp. 21-26, 1976.

13. Morrison, G.L., Virmani, Y.P., Stratten, F.W., and Gilliland, W.J., "Chloride Removal and Monomer Impregnation of Bridge deck Concrete by Electro-Osmosis", Report No. FHWA KS-RD-71-1, 1976.
14. Daniels, F., and Alberty, R., *Physical Chemistry*, 3rd Edition, Chapter 11, pp. 394-397, Wiley, new york, 1967.
15. Whiting, D., "Rapid Determination of the Chloride permeability of Concrete", Report No. FHWA-RD-81/119, *Federal highway Administration*, Washington, D. C, 1981.
16. Goro, S., and Roy, D.M., "Diffusion of ions Through Hardened Cement Paste", *Cem. Concr. Res.*, Vol. 11, No. 5/6, pp. 751-757, 1981.
17. Dhir, R.K., Jones, M.R., Ahmed, H.E.H., and Seneviratne, A.M.G., "Rapid estimation of Chloride Diffusion Coefficient in Concrete", *Magazine of Concrete Research*, Vol. 42, No. 152, pp. 177-185, September, 1990.
18. ASTM Designation C 1202-97, "Test method for Electrical Indication of Concrete's Ability to Resist Chloride Ion Penetration", *Annual Book of ASTM Standards, Section 4, Construction*, Vol. 04.02, "Concrete and Concrete Aggregates", ASTM, Philadelphia, PA, 1998.
19. Perraton, D., Aitcin, P.C., and Vezina, D., "Permeabilities of Silica Fume Concrete", *Permeability of Concrete*, SP-108, American Concrete Institute, Detroit, pp. 63-84, 1988.
20. "Guide to Nondestructive Testing of Concrete", Publication no. FHWA-SA-97-105, pp. 31-36, September 1997.
21. ASTM Designation C 882-91, "Standard Test method for Bond Strength of Epoxy-Resin Systems Used with Concrete by Slant shear", *Annual Book of ASTM Standards, Section 4, Construction*, Vol. 04.02, "Concrete and Concrete Aggregates", ASTM, Philadelphia, PA, 1998.
22. Bagate, M., McCullough, B.F., and Fowler, D., "Construction and Performance of an Experimental Thin-Bonded Concrete Overlay pavement in Houston", *Transportation Research Record* 1040, 1983.
23. Bergren, V.J., "Bonded Portland Cement Concrete Resurfacing", *Division of Highways*, Iowa Department of Transportation, Ames, Iowa.
24. Furr, H and Ingram, L., "Concrete Overlays for Bridge Deck Repair", *Highway Research Record* 400, HRB, National Research Council, Washington, D. C., p.93, 1972.

25. Struble, L. and Waters, N., "Tensile Test to Measure Adhesion between old and New cement paste", NBSIR 87-3685, National Bureau of Standards, Gaithersburg, MD, January 1988.
26. Knab, L.I and Spring, C.B., "Evaluation of Test Methods for Measuring the Bond Strength of Portland-Cement Based Repair Materials to Concrete", NBSIR 88-3746, National Bureau of Standards, Gaithersburg, MD, April, 1988.
27. ASTM Designation C 1245-93, "Test Method for Determining Bond Strength Between Hardened Roller-Compacted Concrete and Other Hardened Cementitious Mixtures (Point Load Test)". Annual Book of ASTM Standards, Section 4, *Construction*, Vol. 04.02, "Concrete and Concrete Aggregates", ASTM, Philadelphia, PA, 1998.
28. British Standard Institution, *Guide to the Use of Non-Destructive Methods of Test for Hardened concrete*, BS 1881, 1986, Part 201.

Appendix A

Core Locations for Field and Lab Bond Tests

- **Exit 32, I 90 (Sturgis)**
- **Exit 212, I 90 (Vivian)**

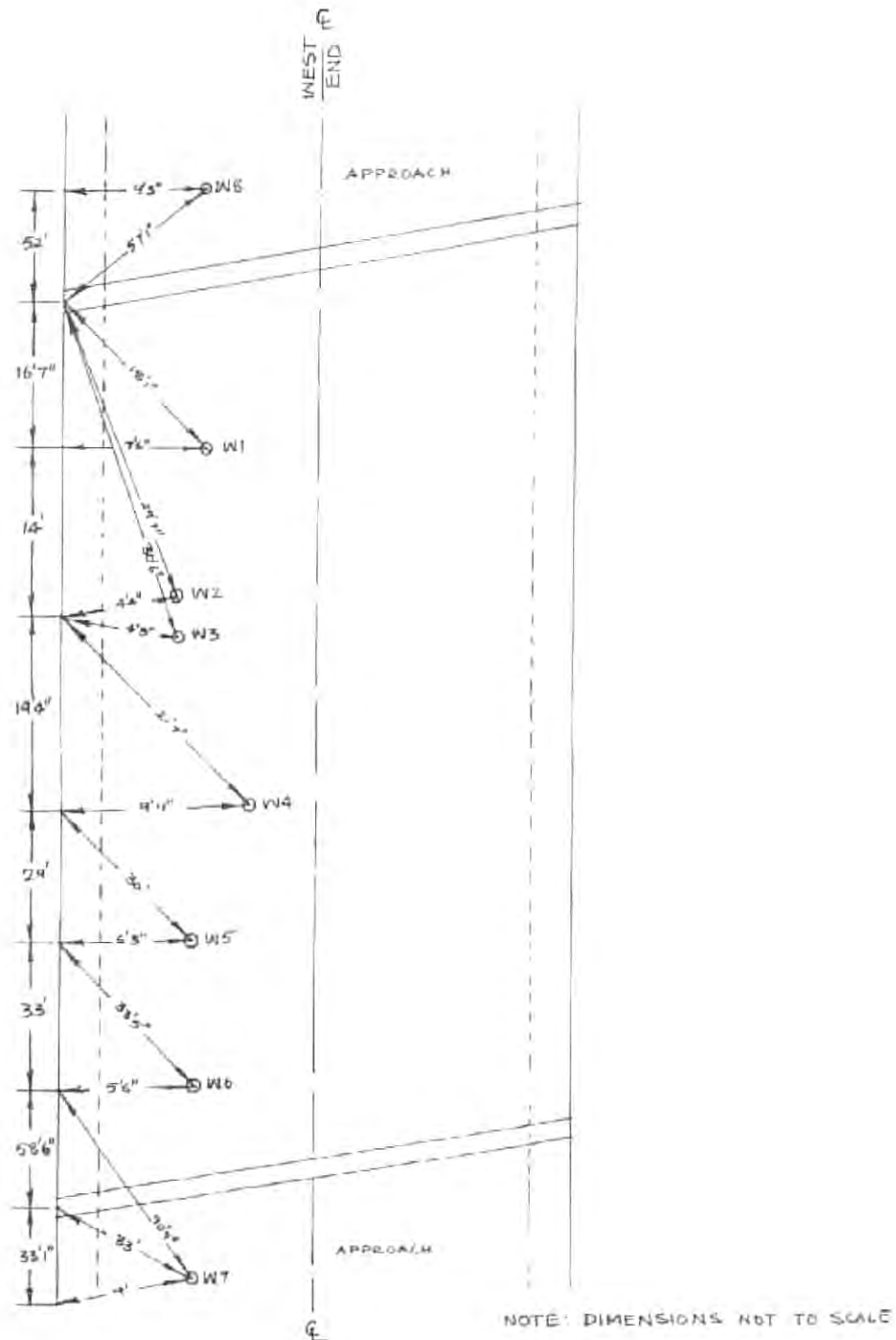


Figure A1: Location of Field Bond Test on West Round lane of the Interchange Bridge at Exit 32, 190 (Sturgis)

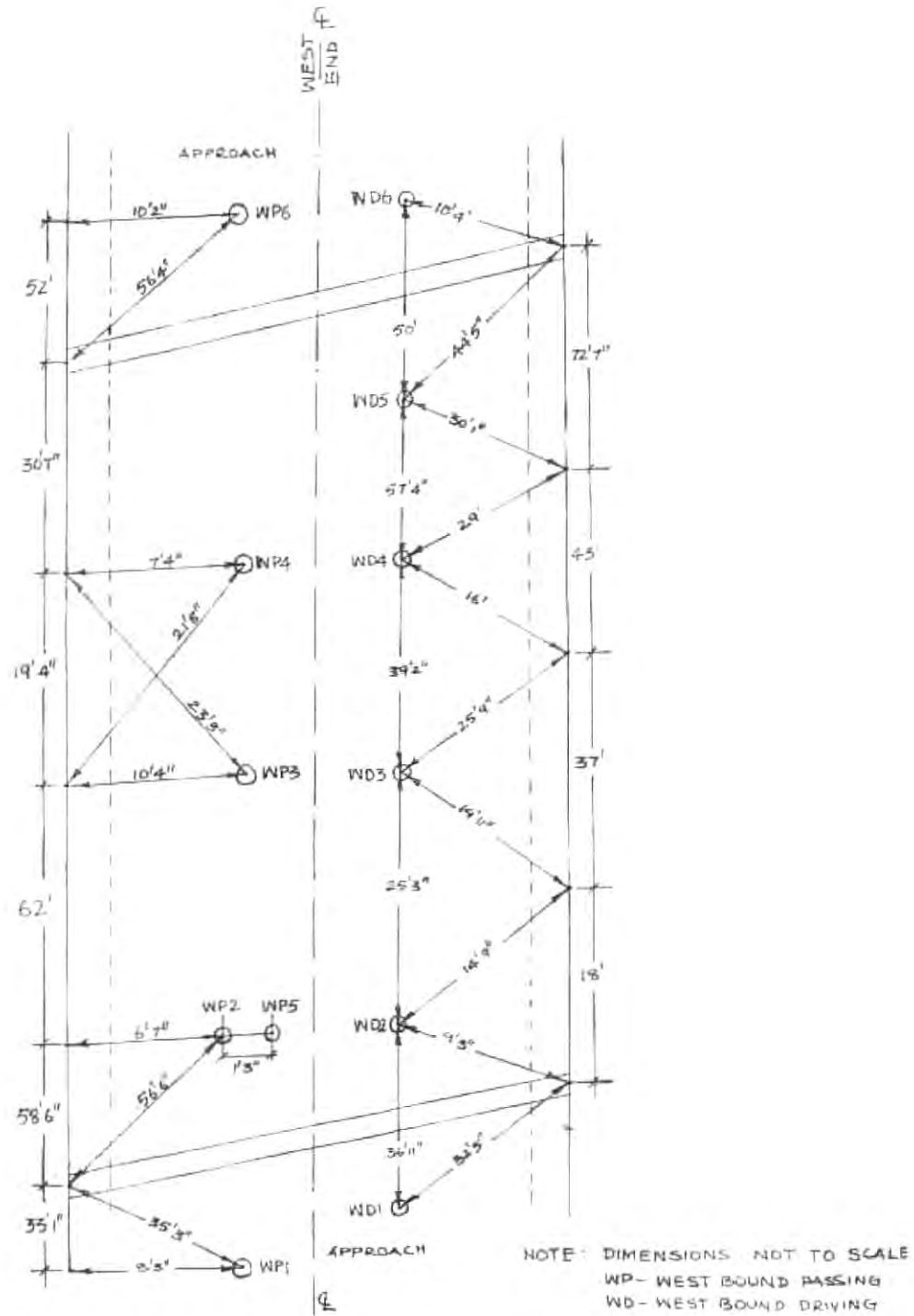


Figure A2: Location of 4" Cores for the Laboratory Tests on the West Bound lane of the Interchange Bridge at Exit 32, I 90 (Sturgis)

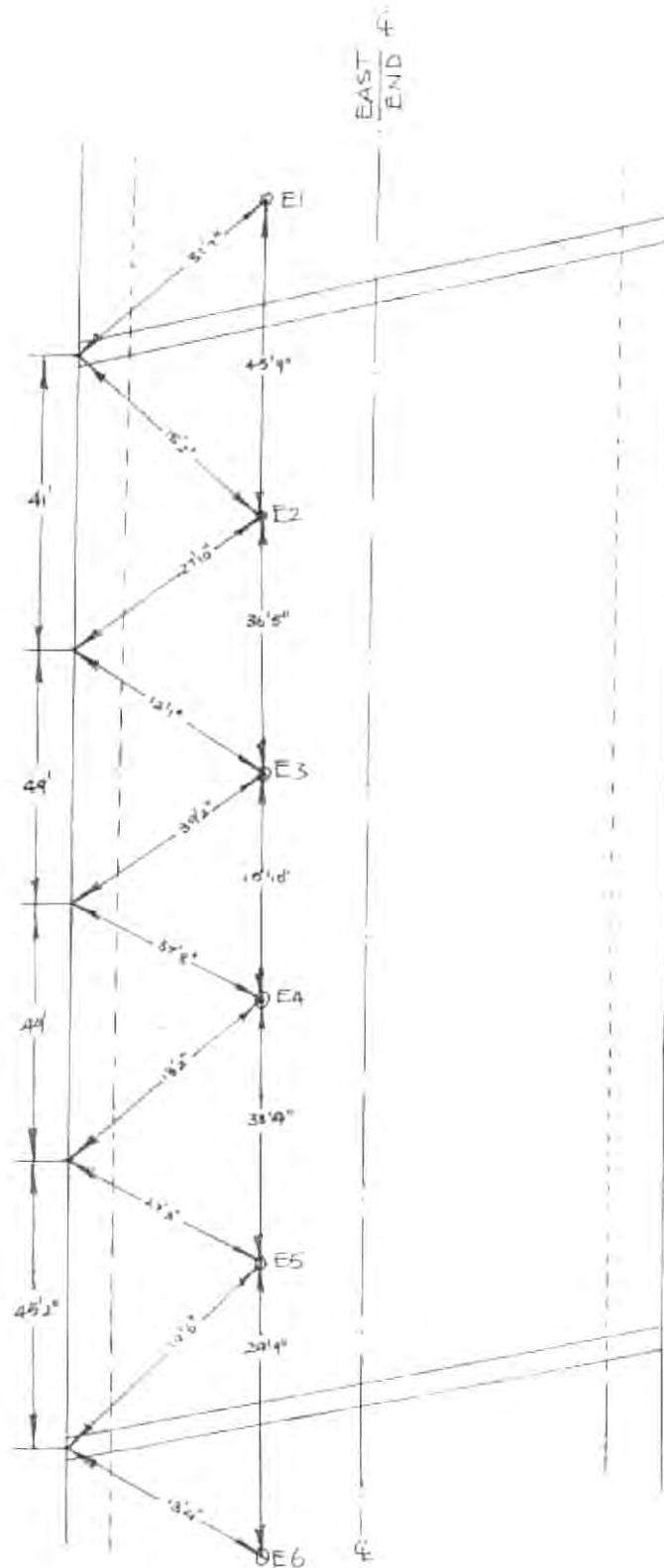


Figure A3: Location of Field Bond Test on East Bound lane on the Interchange Bridge at Exit 32, I 90 (Sturgis)

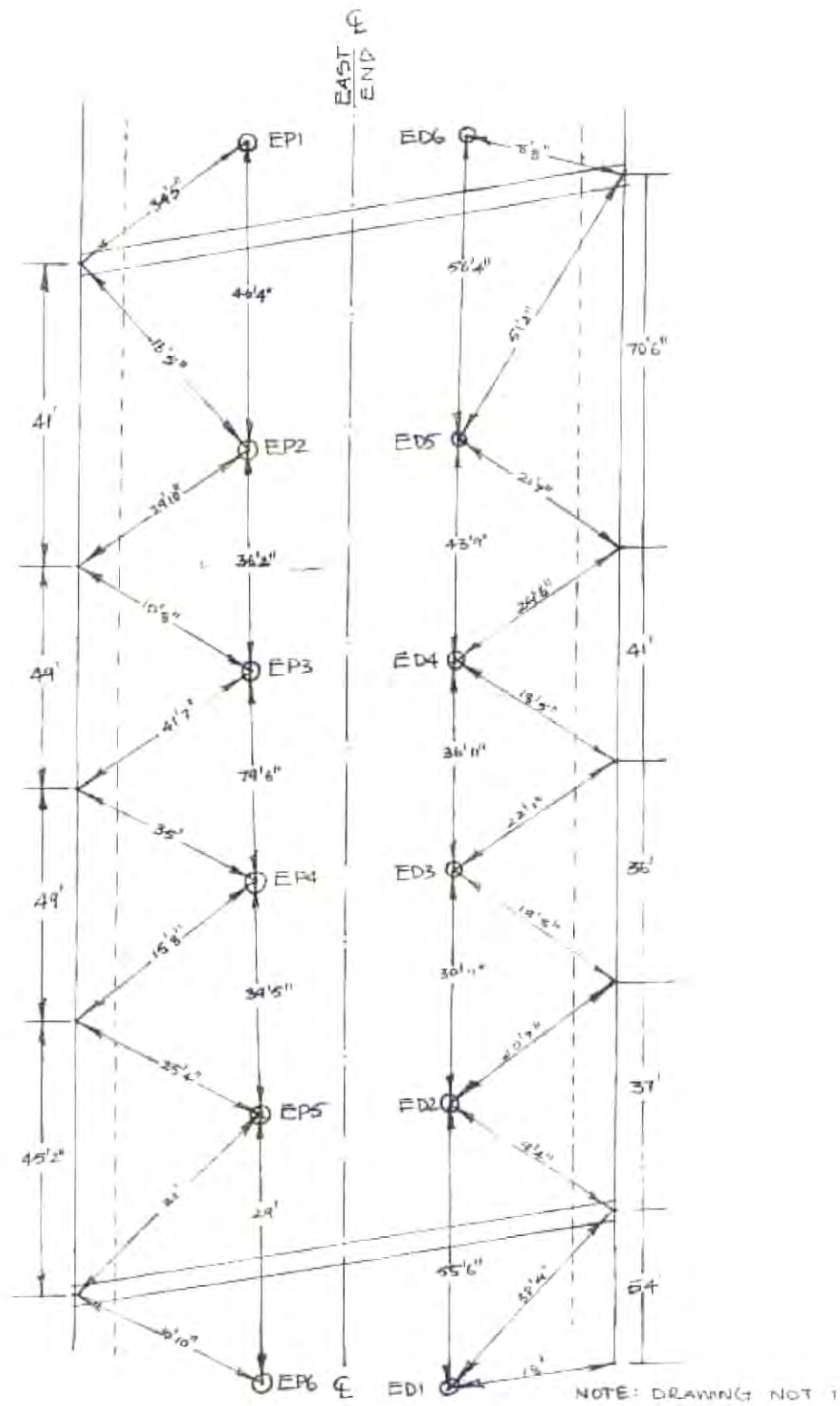


Figure A4: Location of 4" Cores for the Laboratory Tests on the East Bound lane of the Interchange Bridge at Exit 32, I 90 (Sturgis)

East (towards Rapid City)																													
<table> <tr><th>Dia. of Core (in)</th><th>No. of Cores</th><th>Naming</th></tr> <tr><td>4</td><td>1</td><td>ED6</td></tr> <tr><td>2</td><td>0</td><td></td></tr> </table>	Dia. of Core (in)	No. of Cores	Naming	4	1	ED6	2	0		<table> <tr><th>Dia. of Core (in)</th><th>No. of Cores</th><th>Naming</th></tr> <tr><td>4</td><td>4</td><td>ED-2 to 5</td></tr> <tr><td>2</td><td>0</td><td></td></tr> </table>	Dia. of Core (in)	No. of Cores	Naming	4	4	ED-2 to 5	2	0		<table> <tr><th>Dia. of Core (in)</th><th>No. of Cores</th><th>Naming</th></tr> <tr><td>4</td><td>1</td><td>ED1</td></tr> <tr><td>2</td><td>0</td><td></td></tr> </table>	Dia. of Core (in)	No. of Cores	Naming	4	1	ED1	2	0	
Dia. of Core (in)	No. of Cores	Naming																											
4	1	ED6																											
2	0																												
Dia. of Core (in)	No. of Cores	Naming																											
4	4	ED-2 to 5																											
2	0																												
Dia. of Core (in)	No. of Cores	Naming																											
4	1	ED1																											
2	0																												
East Bound Driving Lane																													
<table> <tr><th>Dia. of Core (in)</th><th>No. of Cores</th><th>Naming</th></tr> <tr><td>4</td><td>1</td><td>EP1</td></tr> <tr><td>2</td><td>1</td><td>E1</td></tr> </table>	Dia. of Core (in)	No. of Cores	Naming	4	1	EP1	2	1	E1	<table> <tr><th>Dia. of Core (in)</th><th>No. of Cores</th><th>Naming</th></tr> <tr><td>4</td><td>4</td><td>EP-2 to 5</td></tr> <tr><td>2</td><td>4</td><td>E-2 to 5</td></tr> </table>	Dia. of Core (in)	No. of Cores	Naming	4	4	EP-2 to 5	2	4	E-2 to 5	<table> <tr><th>Dia. of Core (in)</th><th>No. of Cores</th><th>Naming</th></tr> <tr><td>4</td><td>1</td><td>EP6</td></tr> <tr><td>2</td><td>1</td><td>E6</td></tr> </table>	Dia. of Core (in)	No. of Cores	Naming	4	1	EP6	2	1	E6
Dia. of Core (in)	No. of Cores	Naming																											
4	1	EP1																											
2	1	E1																											
Dia. of Core (in)	No. of Cores	Naming																											
4	4	EP-2 to 5																											
2	4	E-2 to 5																											
Dia. of Core (in)	No. of Cores	Naming																											
4	1	EP6																											
2	1	E6																											
East Bound Passing Lane																													
West (towards Sturgis)																													
<table> <tr><th>Dia. of Core (in)</th><th>No. of Cores</th><th>Naming</th></tr> <tr><td>4</td><td>1</td><td>WP1</td></tr> <tr><td>2</td><td>1</td><td>W7</td></tr> </table>	Dia. of Core (in)	No. of Cores	Naming	4	1	WP1	2	1	W7	<table> <tr><th>Dia. of Core (in)</th><th>No. of Cores</th><th>Naming</th></tr> <tr><td>4</td><td>4</td><td>WP-2 to 5</td></tr> <tr><td>2</td><td>6</td><td>W-1 to 5</td></tr> </table>	Dia. of Core (in)	No. of Cores	Naming	4	4	WP-2 to 5	2	6	W-1 to 5	<table> <tr><th>Dia. of Core (in)</th><th>No. of Cores</th><th>Naming</th></tr> <tr><td>4</td><td>1</td><td>WP6</td></tr> <tr><td>2</td><td>1</td><td>W8</td></tr> </table>	Dia. of Core (in)	No. of Cores	Naming	4	1	WP6	2	1	W8
Dia. of Core (in)	No. of Cores	Naming																											
4	1	WP1																											
2	1	W7																											
Dia. of Core (in)	No. of Cores	Naming																											
4	4	WP-2 to 5																											
2	6	W-1 to 5																											
Dia. of Core (in)	No. of Cores	Naming																											
4	1	WP6																											
2	1	W8																											
West Bound Passing Lane																													
<table> <tr><th>Dia. of Core (in)</th><th>No. of Cores</th><th>Naming</th></tr> <tr><td>4</td><td>1</td><td>WVD1</td></tr> <tr><td>2</td><td>0</td><td></td></tr> </table>	Dia. of Core (in)	No. of Cores	Naming	4	1	WVD1	2	0		<table> <tr><th>Dia. of Core (in)</th><th>No. of Cores</th><th>Naming</th></tr> <tr><td>4</td><td>4</td><td>WD-2 to 5</td></tr> <tr><td>2</td><td>0</td><td></td></tr> </table>	Dia. of Core (in)	No. of Cores	Naming	4	4	WD-2 to 5	2	0		<table> <tr><th>Dia. of Core (in)</th><th>No. of Cores</th><th>Naming</th></tr> <tr><td>4</td><td>1</td><td>WVD6</td></tr> <tr><td>2</td><td>0</td><td></td></tr> </table>	Dia. of Core (in)	No. of Cores	Naming	4	1	WVD6	2	0	
Dia. of Core (in)	No. of Cores	Naming																											
4	1	WVD1																											
2	0																												
Dia. of Core (in)	No. of Cores	Naming																											
4	4	WD-2 to 5																											
2	0																												
Dia. of Core (in)	No. of Cores	Naming																											
4	1	WVD6																											
2	0																												
West Bound Driving Lane																													

Figure A5: Details of the number of cores of different diameters in different parts of the bridge and its naming at Exit 32, I 90 (Sturgis)

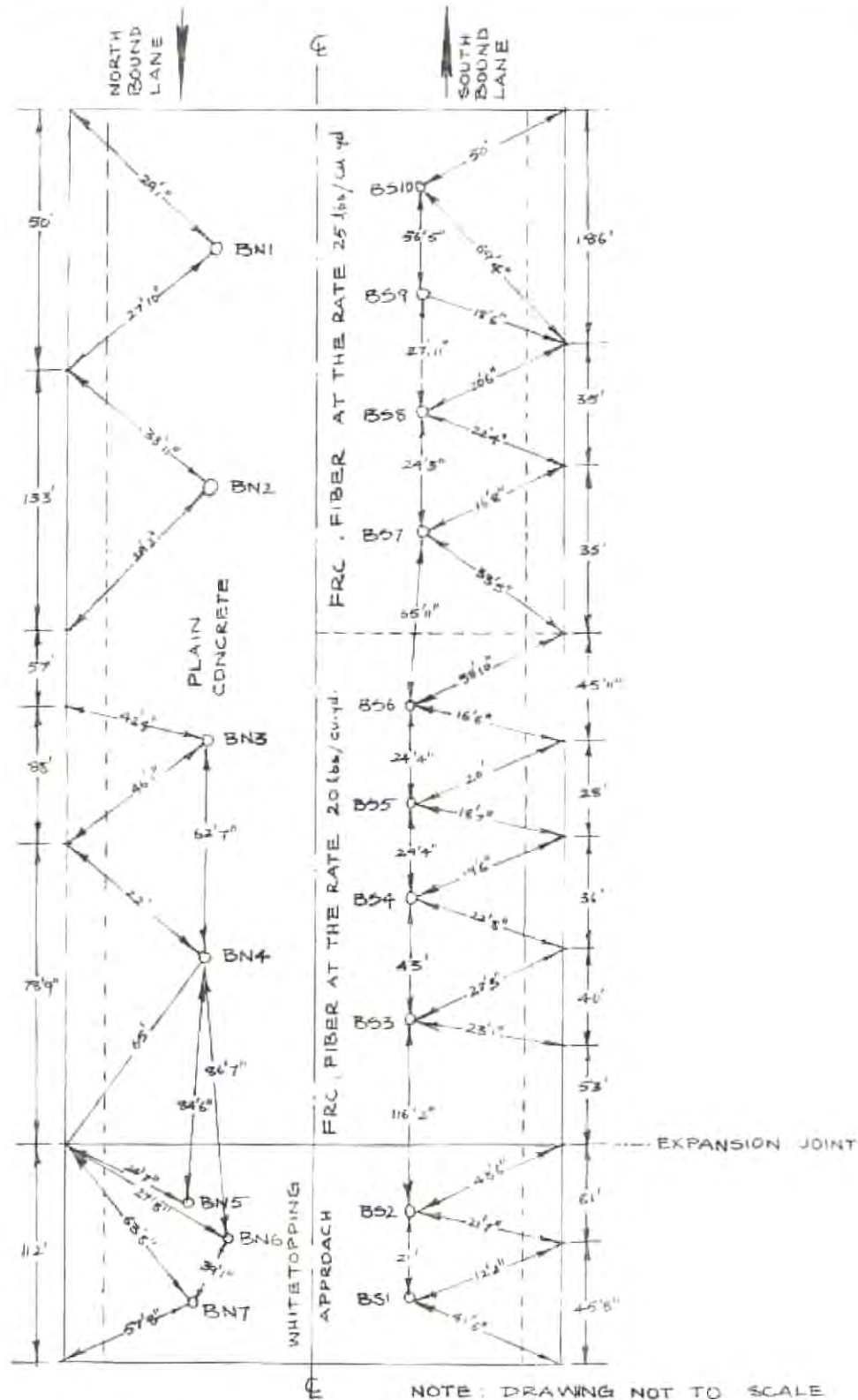


Figure A6: Location of Field Bond Test on North and South Bound Lanes of the Interchange Bridge at Exit 212, I 90 (Vivian)

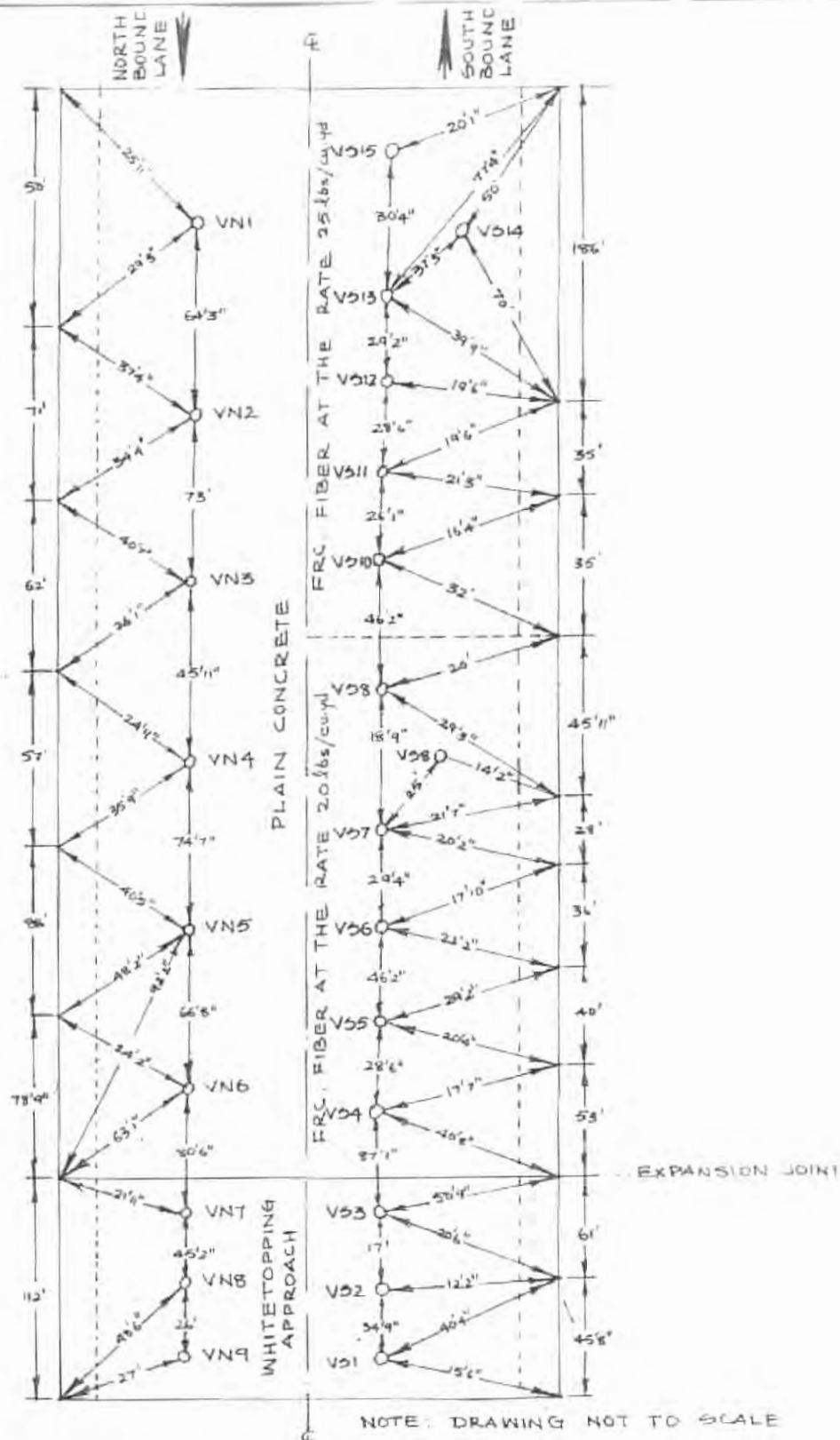


Figure A7: Location of 4" Cores for the Laboratory Tests on the North and South Bound lanes of the Interchange Bridge at Exit 212, I 90 (Vivian)

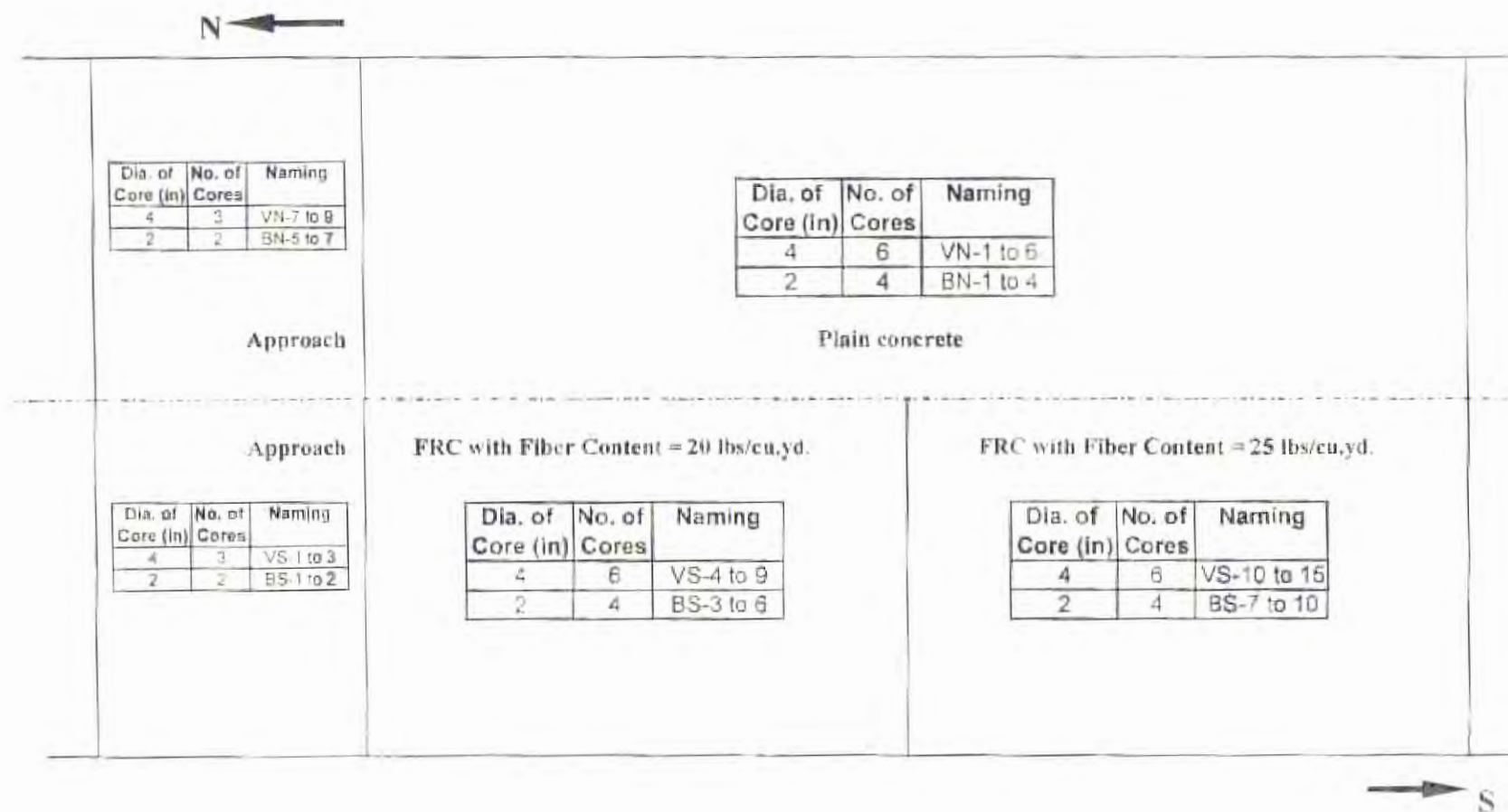


Figure A8: Details of the number of cores of different diameters in different parts of the bridge and its naming at Exit 212, I 90 (Vivian)

Appendix B
Tables and Figures

**Rapid Chloride Permeability Test
Of Core Samples From**

- **Exit 32, I 90 (Sturgis)**
- **Exit 212, I 90 (Vivian)**

Table B1: RCPT Test Results of Specimens from the West Bound lane at Exit 32, I 90 (Sturgis)

Specimen ID: WD1(Approach)			Specimen ID: WD2 (Drv-lane)			Specimen ID: WD5 (Drv-lane)		
Elapsed Time	Current	Area Under Curve	Elapsed Time	Current	Area Under Curve	Elapsed Time	Current	Area Under Curve
(hrs)	(mA)	(coulombs)	(hrs)	(mA)	(coulombs)	(hrs)	(mA)	(coulombs)
0.5	180.8	0.0	0.5	107.8	0.0	0.5	83.0	0.0
1.0	207.4	349.4	1.0	118.5	203.7	1.0	89.8	155.5
1.5	229.1	392.9	1.5	127.8	221.7	1.5	96.0	167.2
2.0	249.6	430.8	2.0	136.7	238.1	2.0	102.0	178.2
2.5	268.0	465.8	2.5	145.1	253.6	2.5	107.2	188.3
3.0	285.4	498.1	3.0	153.0	268.3	3.0	113.3	198.5
3.5	301.8	528.5	3.5	160.4	282.1	3.5	118.4	208.5
4.0	318.1	557.9	4.0	166.0	293.8	4.0	123.7	217.9
4.5	334.3	587.2	4.5	173.3	305.4	4.5	128.5	227.0
5.0	348.9	614.9	5.0	179.5	317.5	5.0	134.1	236.3
5.5	363.1	640.8	5.5	184.9	328.0	5.5	138.8	245.6
6.0	375.3	664.6	6.0	190.3	337.7	6.0	144.0	254.5
Total		5730.8	Total		3049.7	Total		2277.5
Specimen ID: WP2 (Pass-lane)			Specimen ID: WP4 (Pass-lane)					
Elapsed Time	Current	Area Under Curve	Elapsed Time	Current	Area Under Curve			
(hrs)	(mA)	(coulombs)	(hrs)	(mA)	(coulombs)			
0.5	72.4	0.0	0.5	60.9	0.0			
1.0	77.0	134.5	1.0	64.4	112.8			
1.5	81.1	142.3	1.5	66.8	118.1			
2.0	84.9	149.4	2.0	69.7	122.9			
2.5	88.5	156.1	2.5	71.9	127.4			
3.0	91.9	162.4	3.0	74.0	131.3			
3.5	95.0	168.2	3.5	76.7	135.6			
4.0	98.1	173.8	4.0	78.3	139.5			
4.5	101.0	179.2	4.5	80.5	142.9			
5.0	103.6	184.1	5.0	81.8	146.1			
5.5	106.2	188.8	5.5	83.5	148.8			
6.0	108.7	193.4	6.0	84.5	151.2			
Total		1832.1	Total		1476.5			

**Table B2: RCPT Test Results of Specimens from the East Bound lane at Exit 32, I
90 (Sturgis)**

Specimen ID: ED1 (Approach)			Specimen ID: ED2 (Drv-lane)			Specimen ID: ED4 (Drv-lane)		
Elapsed Time	Current	Area Under Curve	Elapsed Time	Current	Area Under Curve	Elapsed Time	Current	Area Under Curve
(hrs)	(mA)	(coulombs)	(hrs)	(mA)	(coulombs)	(hrs)	(mA)	(coulombs)
0.5	81.9	0.0	0.5	66.9	0.0	0.5	41.8	0.0
1.0	87.2	152.2	1.0	70.9	124.0	1.0	43.5	76.8
1.5	92.9	162.1	1.5	74.4	130.8	1.5	44.8	79.5
2.0	97.3	171.2	2.0	77.5	136.7	2.0	46.7	82.4
2.5	101.5	178.9	2.5	80.5	142.2	2.5	48.2	85.4
3.0	104.4	185.3	3.0	83.4	147.5	3.0	50.9	89.2
3.5	108.2	191.3	3.5	86.3	152.7	3.5	52.3	92.9
4.0	111.8	198.0	4.0	88.4	157.2	4.0	53.2	95.0
4.5	115.4	204.5	4.5	90.7	161.2	4.5	54.6	97.0
5.0	118.3	210.3	5.0	93.0	165.3	5.0	57.8	101.2
5.5	120.5	214.9	5.5	95.0	169.2	5.5	59.3	105.4
6.0	123.1	219.2	6.0	97.2	173.0	6.0	60.7	108.0
Total		2088.0	Total		1659.9	Total		1012.6
Specimen ID: ED6 (Approach)			Specimen ID: EP2 (Pass-lane)			Specimen ID: EP5 (Pass-lane)		
Elapsed Time	Current	Area Under Curve	Elapsed Time	Current	Area Under Curve	Elapsed Time	Current	Area Under Curve
(hrs)	(mA)	(coulombs)	(hrs)	(mA)	(coulombs)	(hrs)	(mA)	(coulombs)
0.5	189.7	0.0	0.5	142.0	0.0	0.5	54.2	0.0
1.0	217.1	366.1	1.0	158.4	270.4	1.0	56.2	99.4
1.5	240.8	412.1	1.5	171.2	296.6	1.5	58.8	103.5
2.0	262.6	453.1	2.0	184.2	319.9	2.0	61.5	108.3
2.5	282.5	490.6	2.5	194.3	340.7	2.5	64.0	113.0
3.0	301.8	525.9	3.0	203.7	358.2	3.0	66.6	117.5
3.5	321.9	561.3	3.5	213.5	375.5	3.5	69.1	122.1
4.0	341.9	597.4	4.0	221.9	391.9	4.0	71.0	126.1
4.5	361.8	633.3	4.5	230.6	407.3	4.5	73.0	129.6
5.0	377.6	665.5	5.0	238.4	422.1	5.0	74.7	132.9
5.5	397.2	697.3	5.5	245.0	435.1	5.5	76.4	136.0
6.0	412.3	728.6	6.0	249.0	444.6	6.0	78.3	139.2
Total		6131.2	Total		4062.1	Total		1327.6

Table B3: RCPT Test Results of Specimens from the Approach and the Plain Concrete Section at Exit 212, I90 (Vivian)

Approach	Specimen ID: VS1			Specimen ID: VS3			Specimen ID: VN9		
	Elapsed Time	Current	Area Under Curve	Elapsed Time	Current	Area Under Curve	Elapsed Time	Current	Area Under Curve
	(hrs)	(mA)	(coulombs)	(hrs)	(mA)	(coulombs)	(hrs)	(mA)	(coulombs)
	0.5	171.4	0.0	0.5	133.4	0.0	0.5	122.5	0.0
	1.0	200.1	334.4	1.0	147.8	253.1	1.0	134.2	231.0
	1.5	230.5	387.5	1.5	159.1	276.2	1.5	144.4	250.7
	2.0	264.8	445.8	2.0	170.8	296.9	2.0	153.5	268.1
	2.5	303.3	511.3	2.5	178.6	314.5	2.5	161.5	283.5
	3.0	347.8	586.0	3.0	185.6	327.8	3.0	169.1	297.5
	3.5	397.5	670.8	3.5	191.1	339.0	3.5	174.0	308.8
	4.0	447.5	760.5	4.0	197.4	349.7	4.0	179.4	318.1
	4.5	476.6	831.7	4.5	201.4	358.9	4.5	184.3	327.3
	5.0	478.4	859.5	5.0	205.2	365.9	5.0	188.3	335.3
	5.5	479.0	861.7	5.5	208.8	372.6	5.5	191.7	342.0
	6.0	479.8	862.9	6.0	212.8	379.4	6.0	195.1	348.1
	Total		7112.0	Total		3634.0	Total		3310.6
Plain Concrete	Specimen ID: VN1			Specimen ID: VN2			Specimen ID: VN6		
	Elapsed Time	Current	Area Under Curve	Elapsed Time	Current	Area Under Curve	Elapsed Time	Current	Area Under Curve
	(hrs)	(mA)	(coulombs)	(hrs)	(mA)	(coulombs)	(hrs)	(mA)	(coulombs)
	0.5	63.5	0.0	0.5	98.4	0.0	0.5	68.0	0.0
	1.0	66.6	117.1	1.0	107.1	185.0	1.0	72.0	126.0
	1.5	69.1	122.1	1.5	116.3	201.1	1.5	75.3	132.6
	2.0	71.7	126.7	2.0	125.2	217.4	2.0	77.9	137.9
	2.5	73.3	130.5	2.5	134.8	234.0	2.5	80.5	142.6
	3.0	75.5	133.9	3.0	144.5	251.4	3.0	81.6	145.9
	3.5	77.2	137.4	3.5	154.3	268.9	3.5	83.4	148.5
	4.0	78.7	140.3	4.0	164.7	287.1	4.0	85.5	152.0
	4.5	79.8	142.7	4.5	175.4	306.1	4.5	86.7	155.0
	5.0	81.4	145.1	5.0	185.7	325.0	5.0	88.6	157.8
	5.5	82.0	147.1	5.5	196.7	344.2	5.5	90.6	161.3
	6.0	82.9	148.4	6.0	208.3	364.5	6.0	92.4	164.7
	Total		1491.3	Total		2984.5	Total		1624.1

Table B4: RCPT Test Results of Specimens from the South Bound lane at Exit 212, I 90 (Vivian)

Fiber Reinforced Concrete (20 lbs/yd3)	Specimen ID: VS4			Specimen ID: VS5			Specimen ID: VS7		
	Elapsed	Current	Area Under	Elapsed	Current	Area Under	Elapsed	Current	Area Under
	Time		Curve	Time		Curve	Time		Curve
	(hrs)	(mA)	(coulombs)	(hrs)	(mA)	(coulombs)	(hrs)	(mA)	(coulombs)
	0.5	123.0	0.0	0.5	105.5	0.0	0.5	66.8	0.0
	1.0	133.3	230.7	1.0	113.0	196.7	1.0	70.2	123.3
	1.5	142.5	248.2	1.5	119.5	209.3	1.5	73.1	129.0
	2.0	151.2	264.3	2.0	125.7	220.7	2.0	76.0	134.2
	2.5	159.1	279.3	2.5	131.6	231.6	2.5	78.6	139.1
	3.0	164.7	291.4	3.0	137.2	241.9	3.0	81.1	143.7
Fiber Reinforced Concrete (25 lbs/yd3)	3.5	170.3	301.5	3.5	142.5	251.7	3.5	83.3	148.0
	4.0	175.8	311.5	4.0	146.8	260.4	4.0	84.9	151.4
	4.5	179.5	319.8	4.5	150.6	267.7	4.5	86.2	154.0
	5.0	182.6	325.9	5.0	154.1	274.2	5.0	87.2	156.1
	5.5	185.6	331.4	5.5	157.0	280.0	5.5	88.1	157.8
	6.0	187.3	335.6	6.0	160.2	285.5	6.0	88.7	159.1
	Total		3239.6	Total		2719.5	Total		1595.6
	Specimen ID: VS11			Specimen ID: VS12			Specimen ID: VS13		
	Elapsed	Current	Area Under	Elapsed	Current	Area Under	Elapsed	Current	Area Under
	Time		Curve	Time		Curve	Time		Curve
	(hrs)	(mA)	(coulombs)	(hrs)	(mA)	(coulombs)	(hrs)	(mA)	(coulombs)
	0.5	124.2	0.0	0.5	92.3	0.0	0.5	108.3	0.0
	1.0	134.8	233.1	1.0	98.7	171.9	1.0	116.1	202.0
	1.5	144.5	251.4	1.5	104.2	182.6	1.5	123.2	215.4
	2.0	153.1	267.8	2.0	108.8	191.7	2.0	129.3	227.3
	2.5	161.0	282.7	2.5	113.4	200.0	2.5	134.8	237.7
	3.0	167.9	296.0	3.0	116.8	207.2	3.0	140.2	247.5
	3.5	173.9	307.6	3.5	120.8	213.8	3.5	144.8	256.5
	4.0	179.2	317.8	4.0	123.3	219.7	4.0	148.8	264.2
	4.5	184.2	327.1	4.5	125.9	224.3	4.5	152.7	271.4
	5.0	188.1	335.1	5.0	128.3	228.8	5.0	156.1	277.9
	5.5	191.4	341.6	5.5	130.4	232.8	5.5	158.8	283.4
	6.0	194.3	347.1	6.0	132.2	236.3	6.0	162.3	289.0
	Total		3307.2	Total		2309.1	Total		2772.2

Plain concrete								
Specimen ID: VN1			Specimen ID: VN2			Specimen ID: VN6		
Elapsed	Current	Area Under	Elapsed	Current	Area Under	Elapsed	Current	Area Under
Time		Curve	Time		Curve	Time		Curve
(hrs)	(mA)	(coulombs)	(hrs)	(mA)	(coulombs)	(hrs)	(mA)	(coulombs)
0.5	63.5	0.0	0.5	98.4	0.0	0.5	68.0	0.0
1.0	66.6	117.1	1.0	107.1	185.0	1.0	72.0	126.0
1.5	69.1	122.1	1.5	116.3	201.1	1.5	75.3	132.6
2.0	71.7	126.7	2.0	125.2	217.4	2.0	77.9	137.9
2.5	73.3	130.5	2.5	134.8	234.0	2.5	80.5	142.6
3.0	75.5	133.9	3.0	144.5	251.4	3.0	81.6	145.9
3.5	77.2	137.4	3.5	154.3	268.9	3.5	83.4	148.5
4.0	78.7	140.3	4.0	164.7	287.1	4.0	85.5	152.0
4.5	79.8	142.7	4.5	175.4	306.1	4.5	86.7	155.0
5.0	81.4	145.1	5.0	185.7	325.0	5.0	88.6	157.8
5.5	82.0	147.1	5.5	196.7	344.2	5.5	90.6	161.3
6.0	82.9	148.4	6.0	208.3	364.5	6.0	92.4	164.7
Total		1491.3	Total		2984.5	Total		1624.1

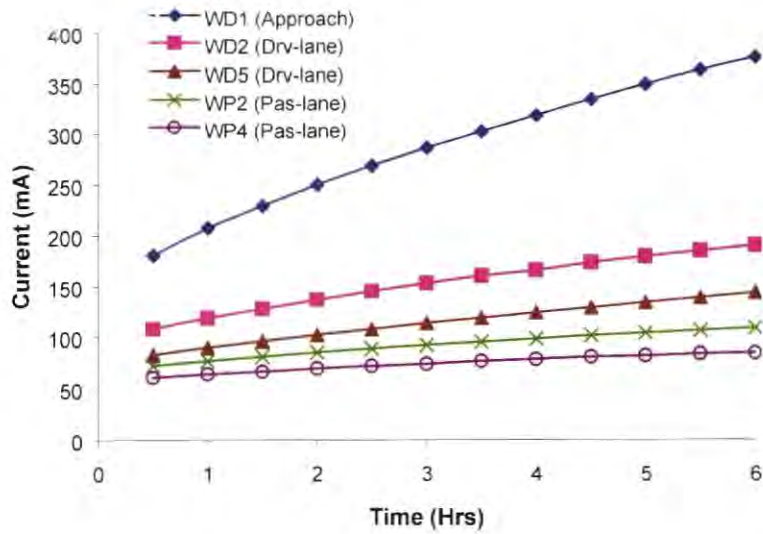


Figure B1: RCPT Results of Specimens from West Bound Lane at Exit 32, I 90 (Sturgis)

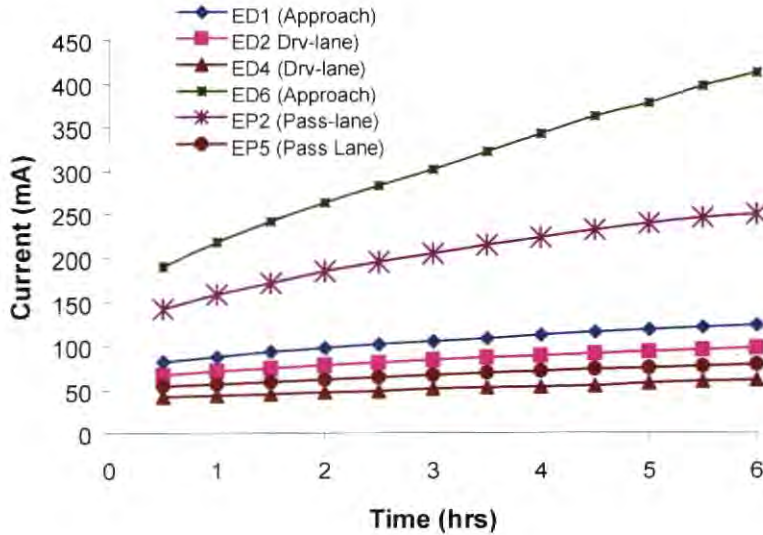


Figure B2: RCPT Results of Specimens from East Bound Lane at Exit 32, I 90 (Sturgis)

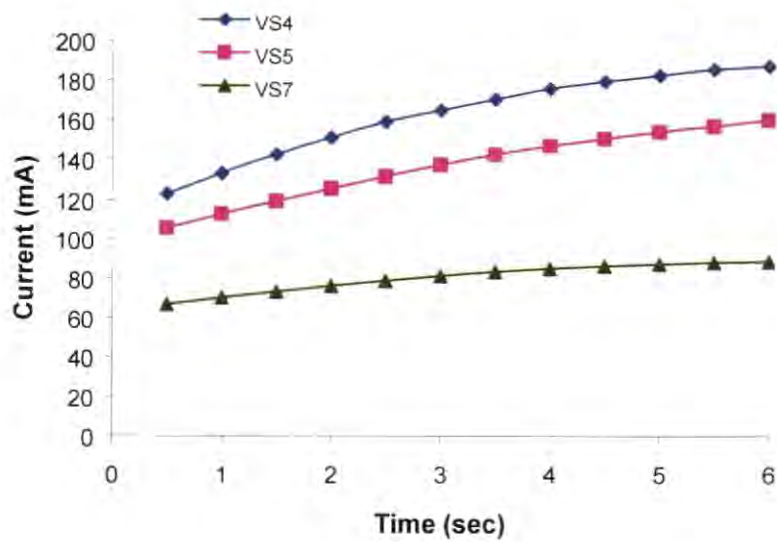


Figure B3: RCPT Results of Specimens from North Half of South Bound lane at Exit 212, I 90 (Vivian)

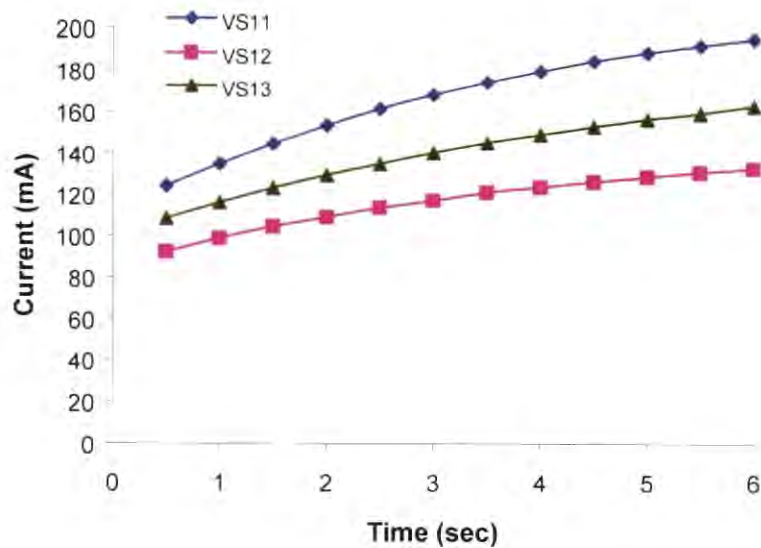


Figure B4: RCPT Results of Specimens from South Half of South Bound lane at Exit 212, I 90 (Vivian)

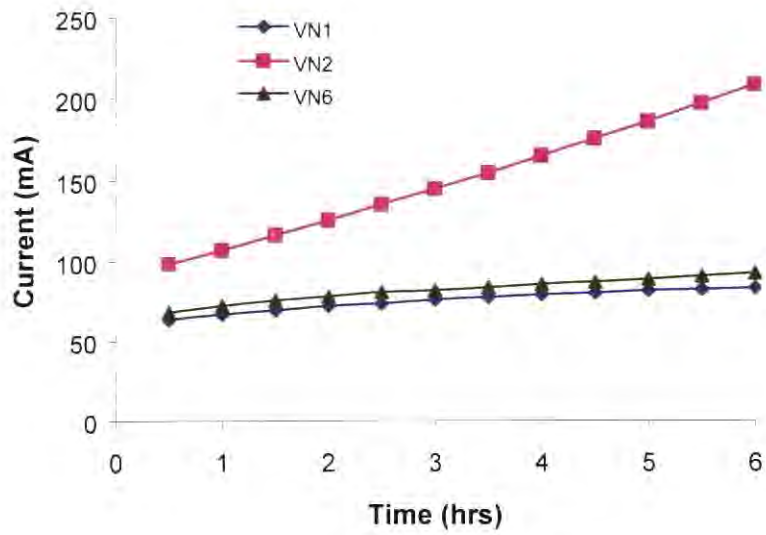


Figure B5: RCPT Results of Specimens from the North Bound Lane at Exit 212, I 90 (Vivian)

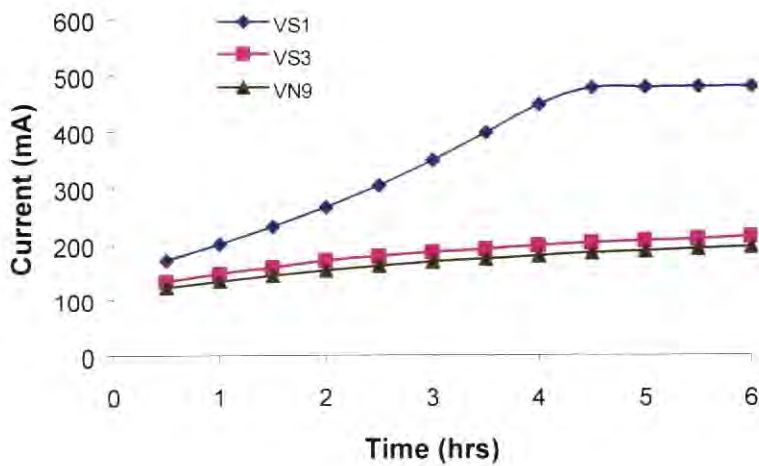


Figure B6: RCPT Results of Specimens from the Approach Section at Exit 212, I 90 (Vivian)

Laboratory Mixes

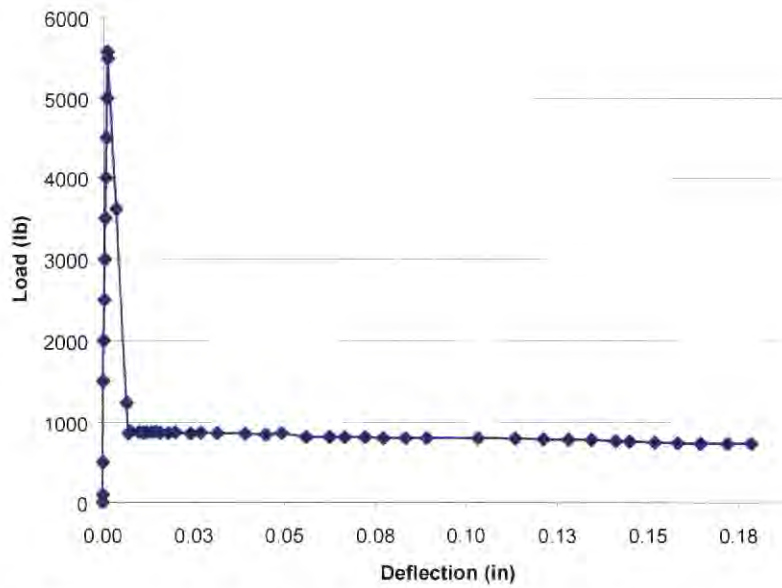


Figure B7: Load Deflection Curve (ASTM C 1018) Specimen 2G1

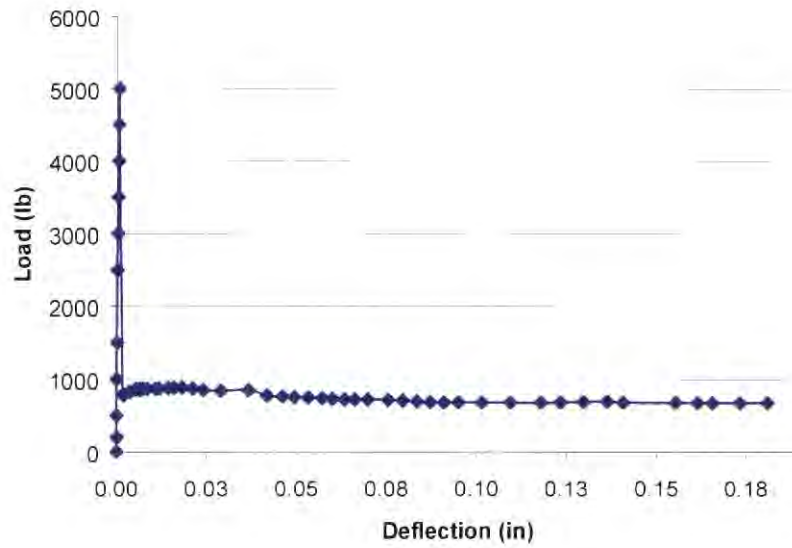


Figure B8: Load Deflection Curve (ASTM C 1018) Specimen 2G2

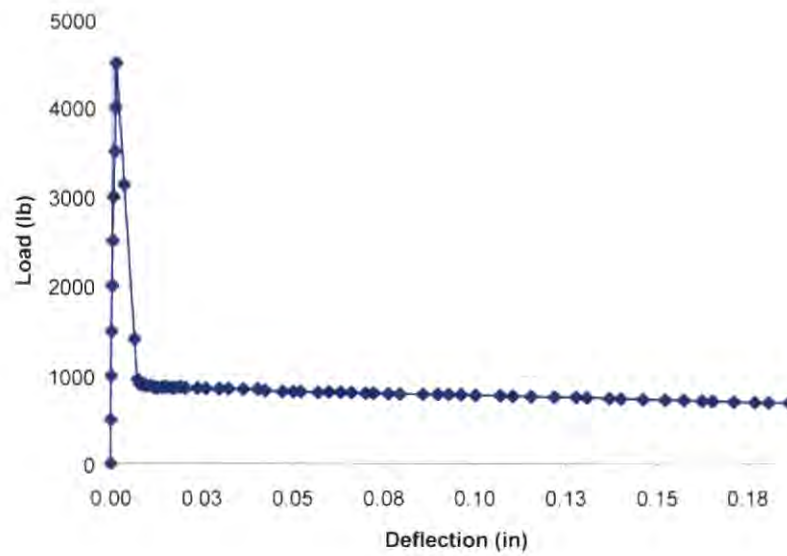


Figure B9: Load Deflection Curve (ASTM C 1018) Specimen 2G3

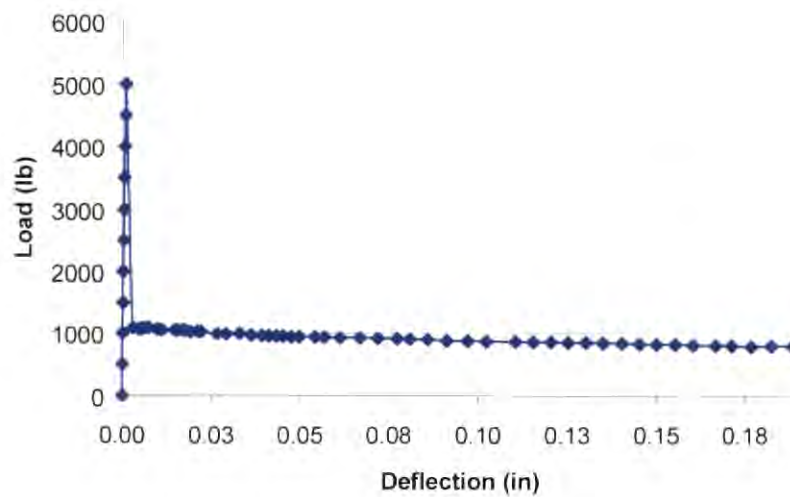


Figure B10: Load Deflection Curve (ASTM C 1018) Specimen 2G4

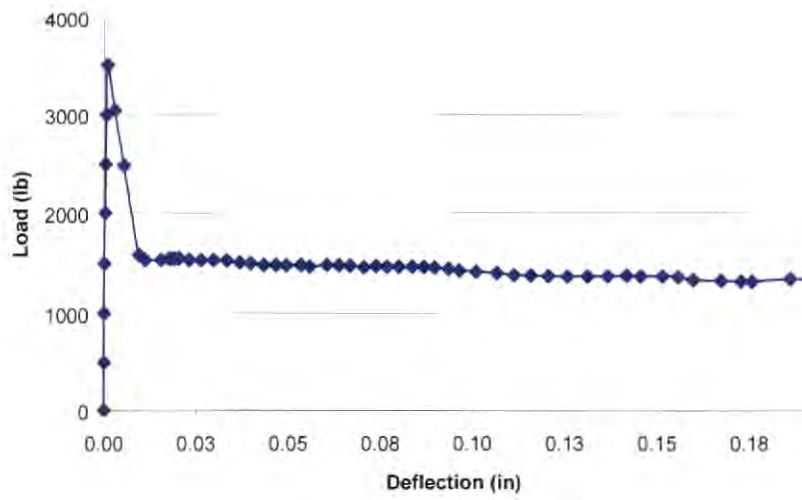


Figure B11: Load Deflection Curve (ASTM C 1018) Specimen 3G1

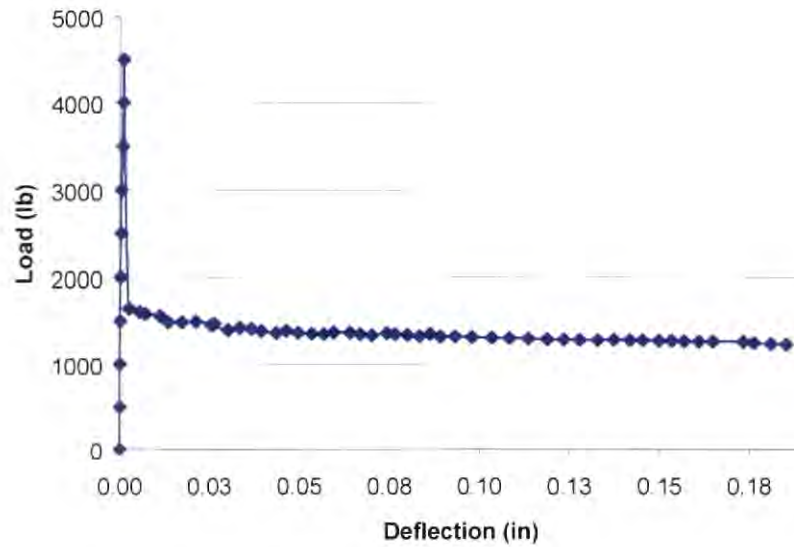


Figure B12: Load Deflection Curve (ASTM C 1018) Specimen 3G2

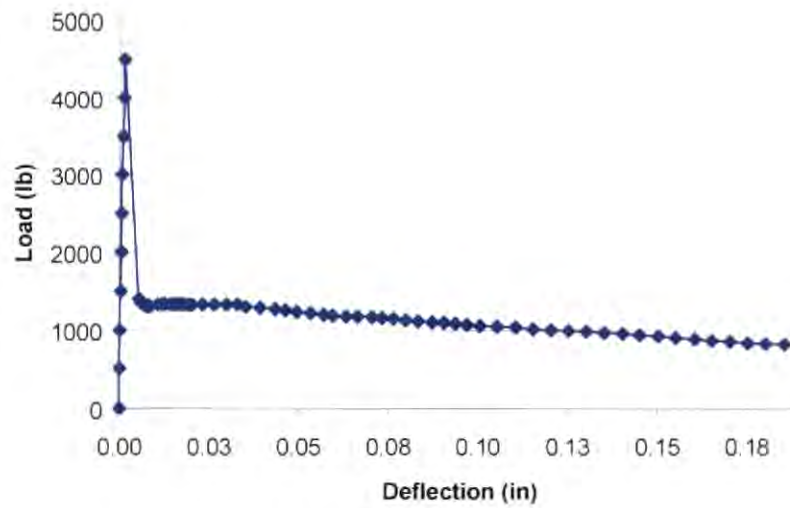


Figure B13: Load Deflection Curve (ASTM C 1018) Specimen 3G3

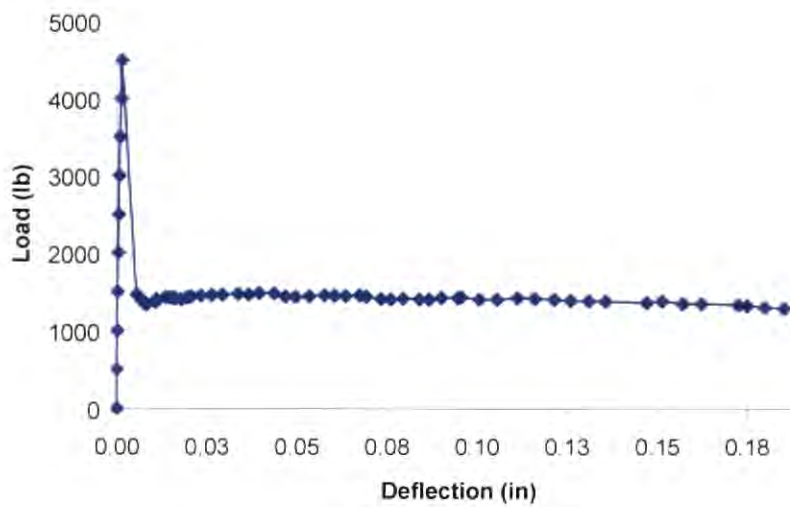


Figure B14: Load Deflection Curve (ASTM C 1018) Specimen 3G4

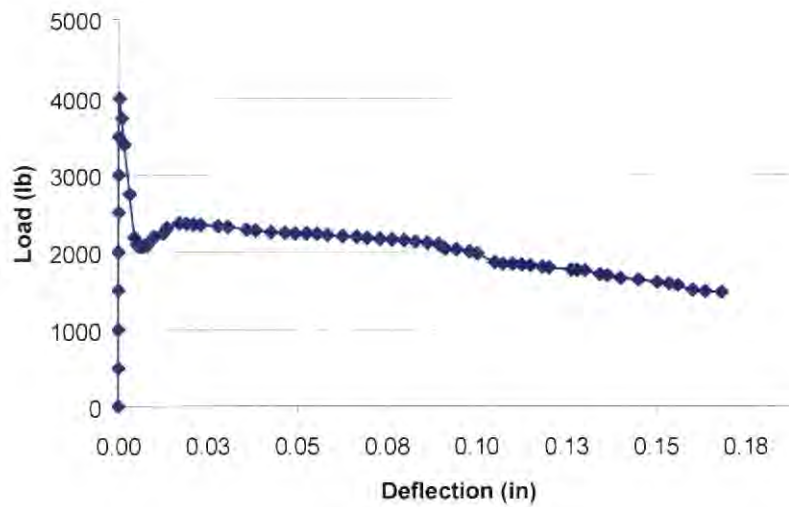


Figure B15: Load Deflection Curve (ASTM C 1018) Specimen 4G1

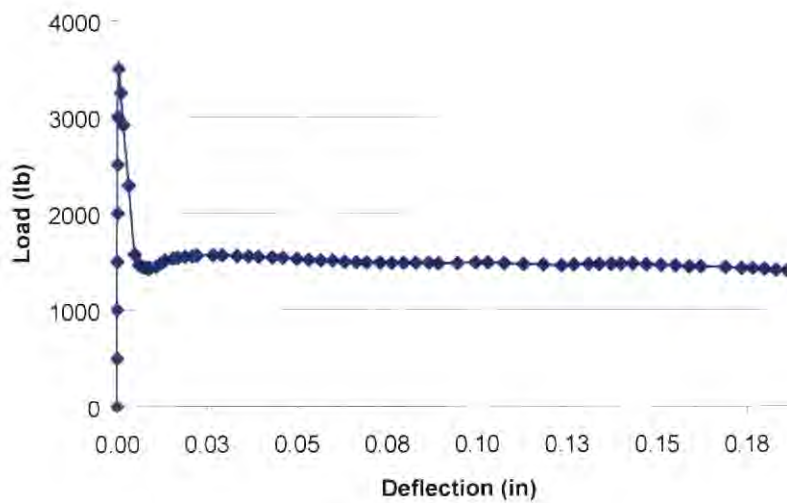


Figure B16: Load Deflection Curve (ASTM C 1018) Specimen 4G2

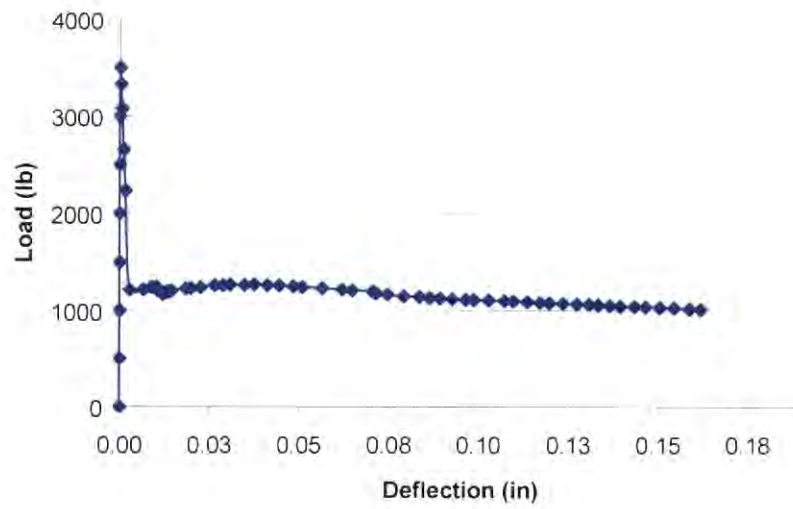


Figure B17: Load Deflection Curve (ASTM C 1018) Specimen 4G3

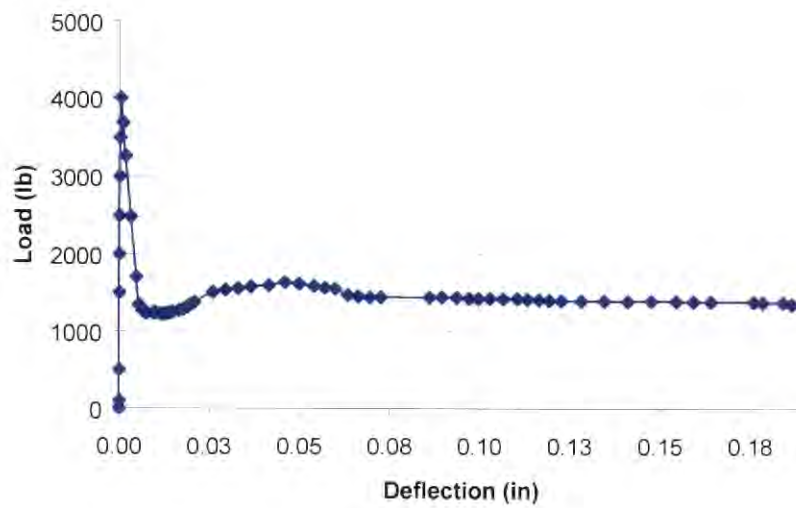


Figure B18: Load Deflection Curve (ASTM C 1018) Specimen 4G4

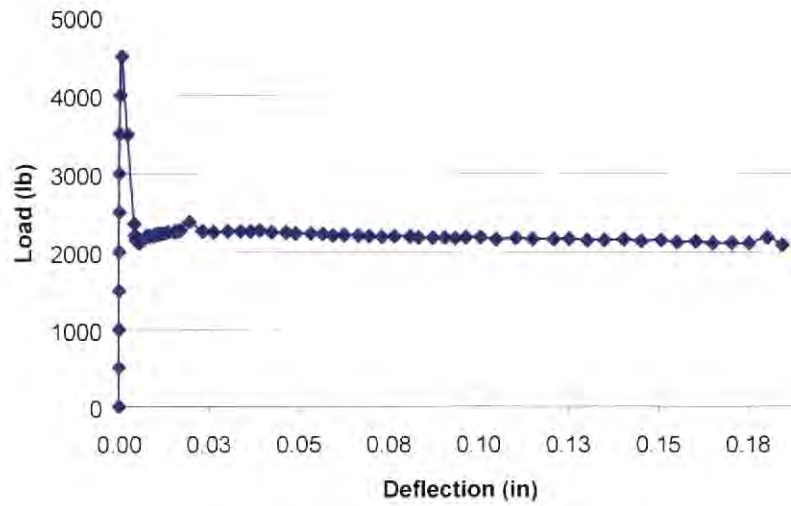


Figure B19: Load Deflection Curve (ASTM C 1018) Specimen 5G1

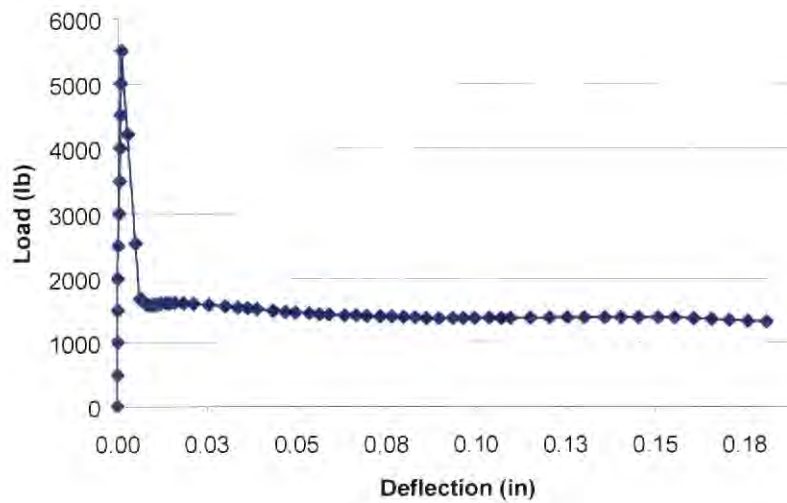


Figure B20: Load Deflection Curve (ASTM C 1018) Specimen 5G2

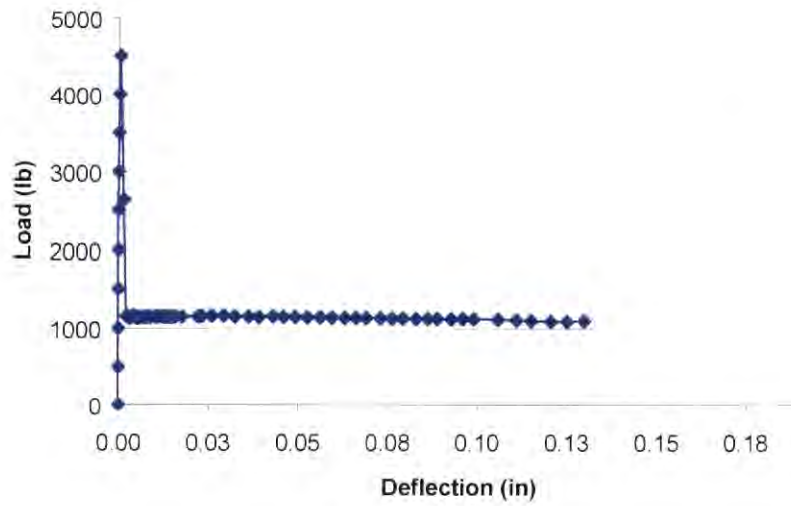


Figure B21: Load Deflection Curve (ASTM C 1018) Specimen 5G3

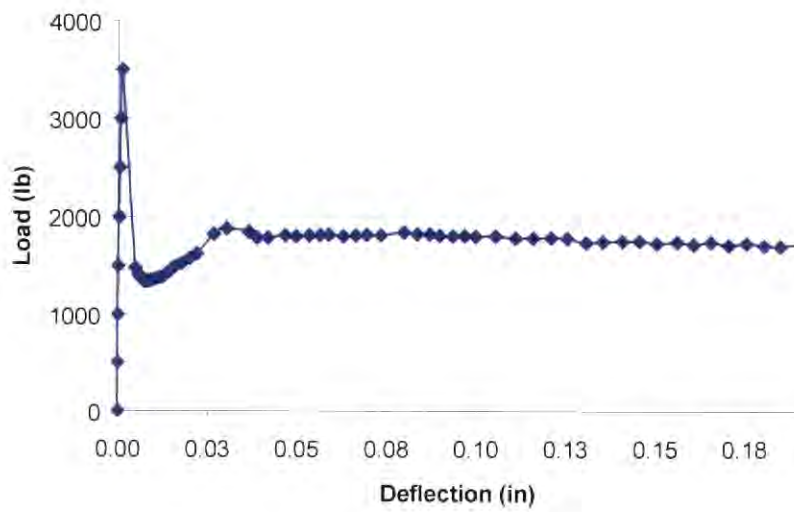


Figure B22: Load Deflection Curve (ASTM C 1018) Specimen 5G4

Appendix C

Photographs of the Field and Lab Bond Test

- Exit 32, I 90 (Sturgis)
- Exit 212, I 90 (Vivian)



The surface of the pavement was scarified, (chipped with a hammer, smoothed with a concrete carbide abrasive and cleaned with a wire brush) prior to the coring. This was done to ensure that all the surface defects like swelling, carbonation and any presence of grease, oil, etc. were removed which in turn aids in the good bonding of the surface with epoxy.



Alignment of the two legs to maintain the verticality of the core bit.



After the coring operation was completed the core bit was removed very carefully so that no lateral pressure was applied on the cores which might result in its breakage.



After the coring operation, the core location was thoroughly cleaned with compressed air. All the concrete dust, pieces of rock and moisture were removed from the core rim.



The core location was marked on the pavement and its position with respect to a permanent benchmark was measured and noted down.



Sufficient quantity of epoxy was placed on the core such that it would adequately cover the core's top.



The bond disk was placed on the core such that the hole for the pull-pin face up and was gently pressed onto the core until it was finally seated and centered.



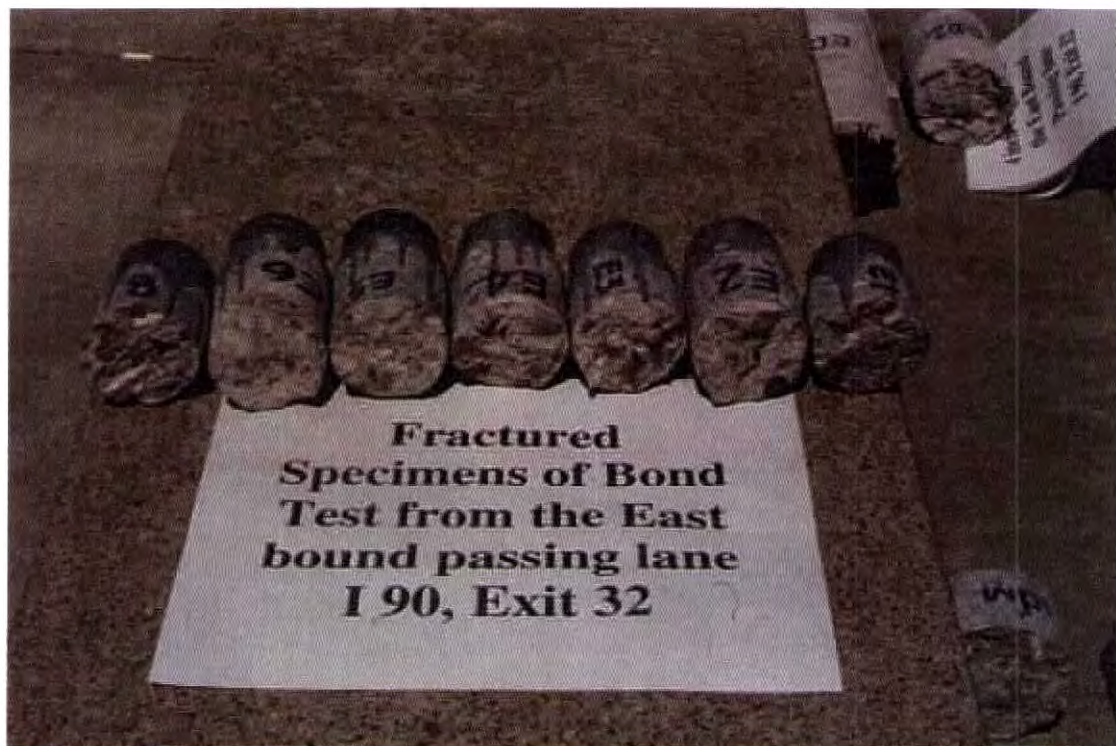
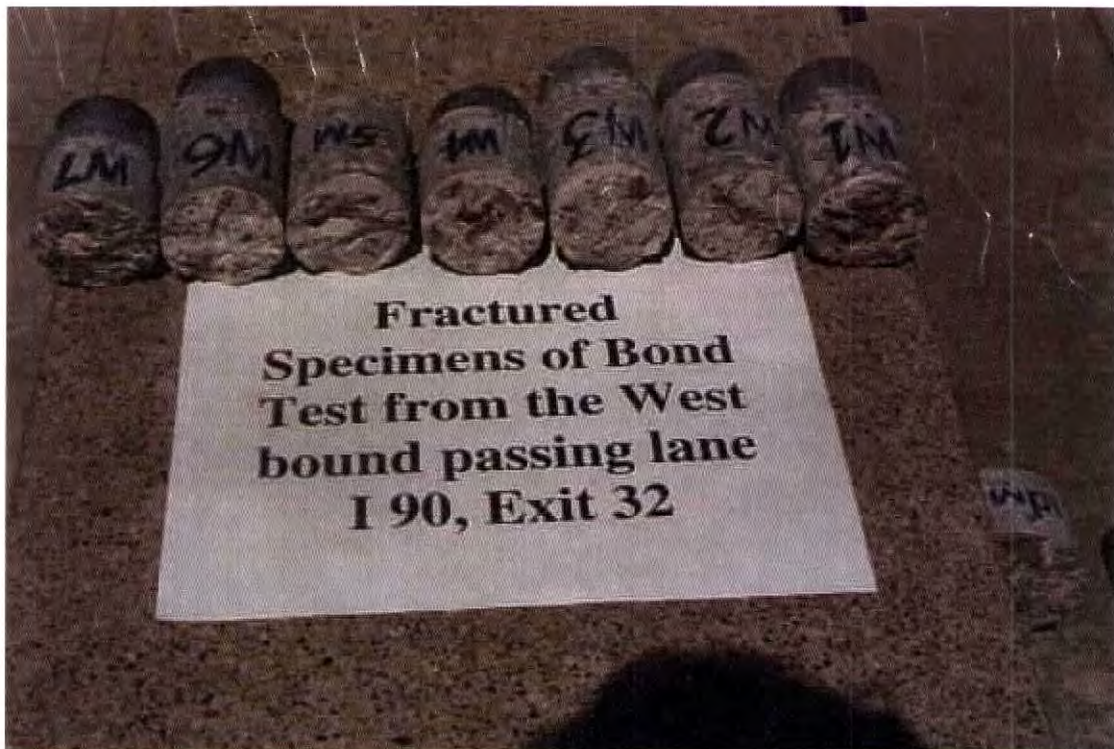
The bond test equipment was positioned on the disk.



By adjusting the notched wheel on the top, the head of the pull-pin was fixed into the socket at the base of the central axis of the equipment. The equipment was leveled by adjusting the three legs.



The pictures show fractured bond test specimens. The penny and pen are shown for size comparison.

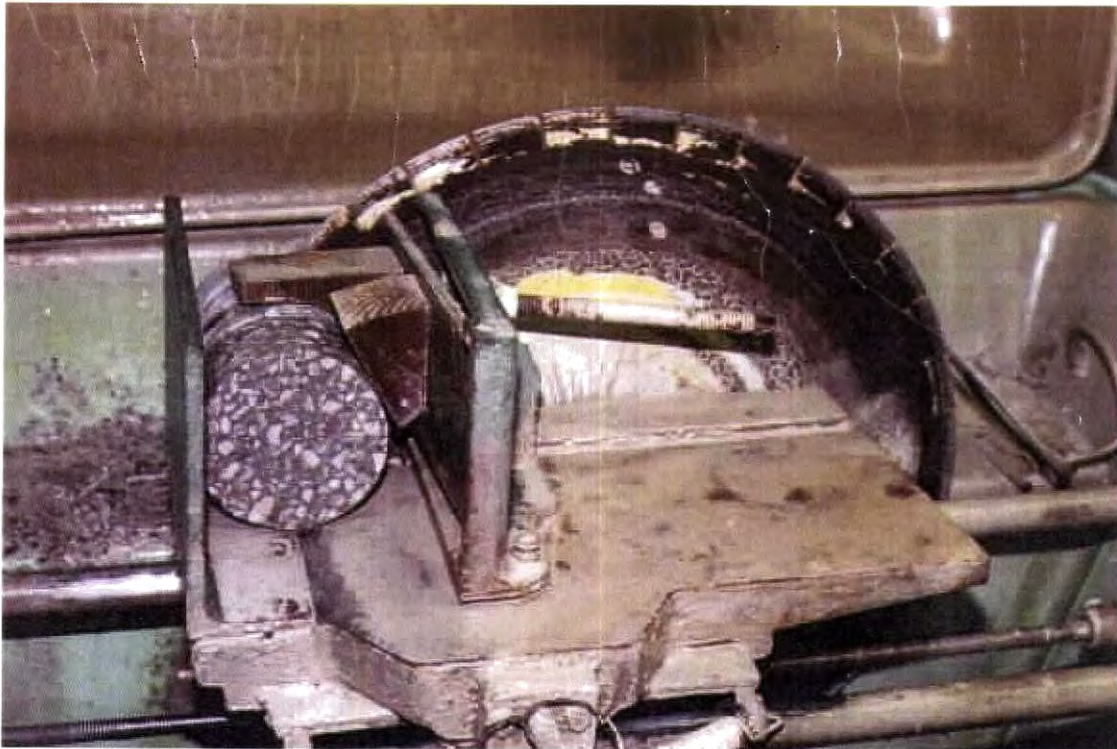












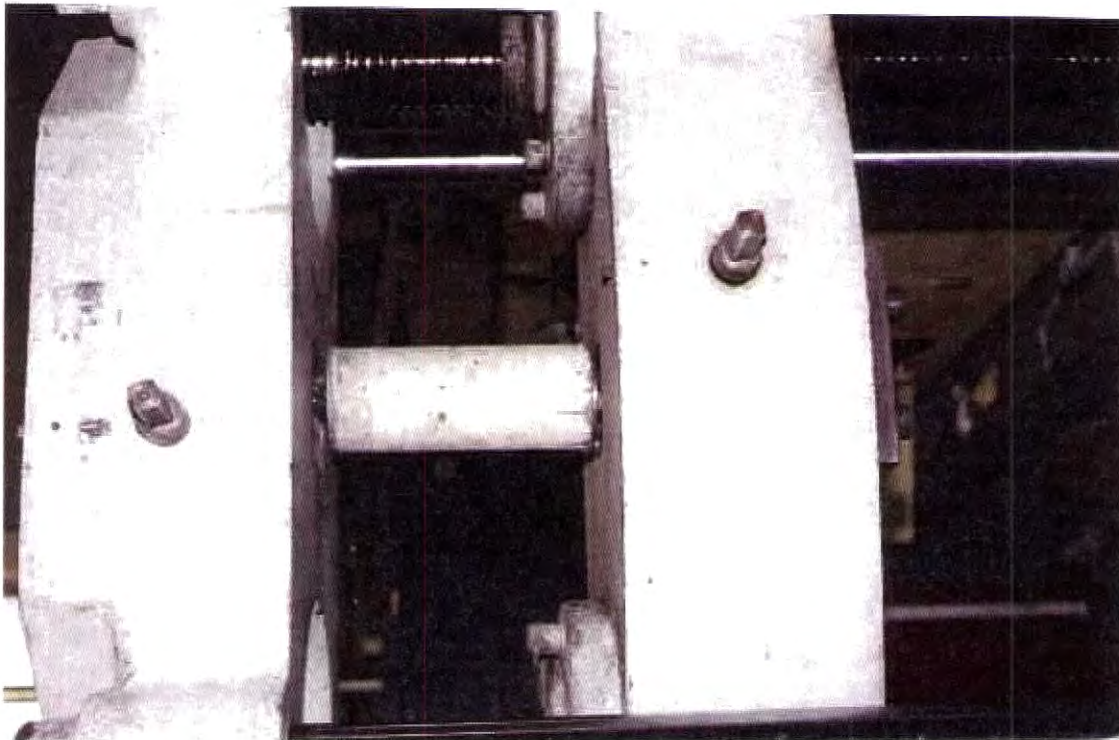
The top and bottom surfaces of the cores are cut to provide a straight surface for the lab bond test.



Specimens ready for lab bond test.



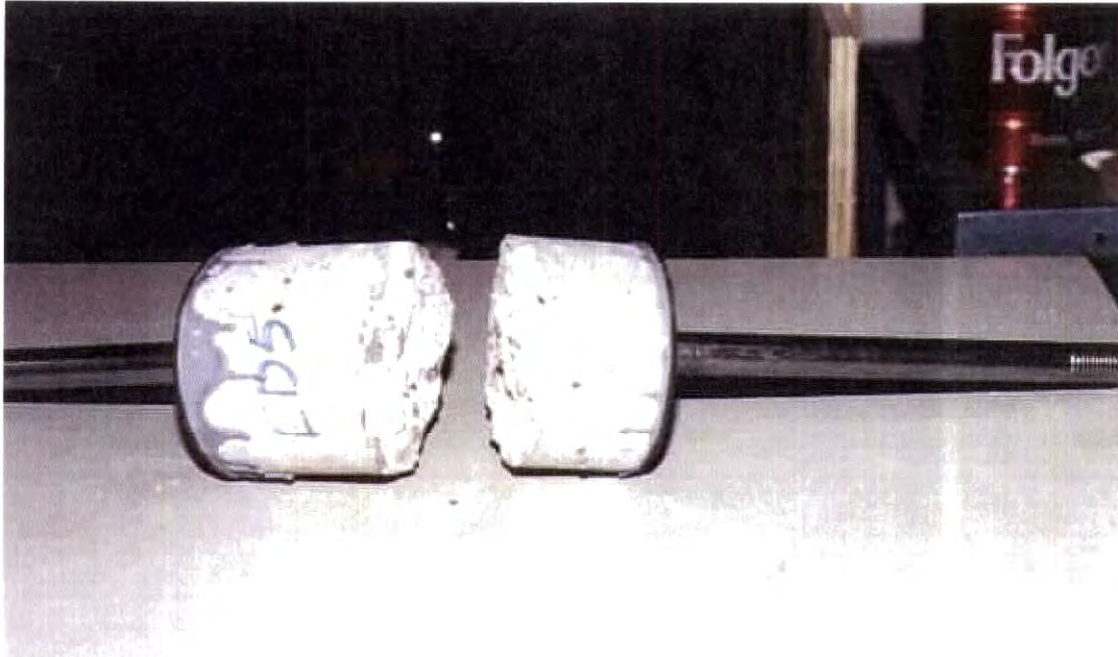
Fractured specimen immediately after lab bond test.



Lab bond test setup.



Fractured core specimens after lab bond test. The failure surface and the depth of overlay are very clearly visible. Specimens from the bridge at exit 32, I-90 (Sturgis).



Fracture very clearly in the underlying concrete due to the lack of bond between coarse aggregates and the cement mortar.



Fracture due to the failure of coarse aggregates.



Fracture due to the lack of bond between coarse aggregates and cement mortar.



Fractured specimens of lab bond test from the bridge at Exit 212, I-90 (Vivian).